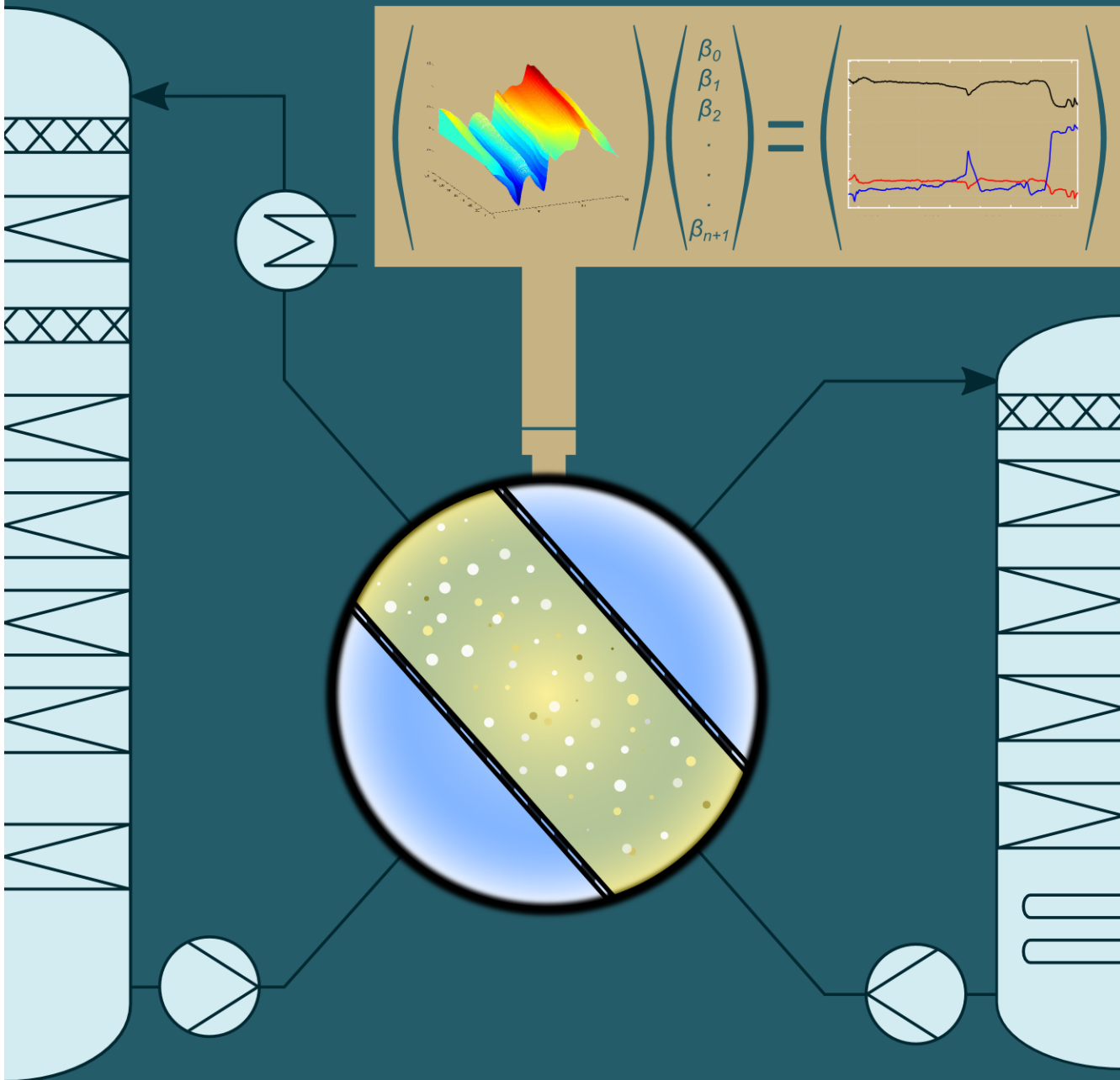


# In-line monitoring of solvents during CO<sub>2</sub> absorption using multivariate data analysis





# **In-line monitoring of solvents during CO<sub>2</sub> absorption using multivariate data analysis**

Alexandr Kachko



# In-line monitoring of solvents during CO<sub>2</sub> absorption using multivariate data analysis

Proefschrift

ter verkrijging van de graad van doctor  
aan de Technische Universiteit Delft,  
op gezag van de Rector Magnificus prof. ir. K.Ch.A.M. Luyben;  
voorzitter van het College voor Promoties,  
in het openbaar te verdedigen op  
vrijdag 23 september 2016 om 12.30 uur

door

**Alexandr KACHKO**  
Master of Science in Physics  
Novosibirsk State University  
Geboren te Chkalovsk, Tajikistan.

Dit proefschrift is goedgekeurd door de promotoren:

Prof. Dr. Ir. T. J. H. Vlugt  
Univ.-Prof. Dr.-Ing. A. Bardow

Samenstelling promotiecommissie:

Rector Magnificus,	voorzitter
Prof. Dr. Ir. T. J. H. Vlugt	Promotor, Technische Universiteit Delft
Univ.-Prof. Dr.-Ing. A. Bardow	Promotor, RWTH-Aachen University

Onafhankelijke leden:

Prof. Dr. Ir. B. J. Boersma	Technische Universiteit Delft
Prof. Dr. J. Meuldijk	Technische Universiteit Eindhoven
Prof. Dr. J. Westerweel	Technische Universiteit Delft
Dr. David Dubbeldam	Universiteit van Amsterdam
Dr. L. V. van der Ham	ASML

The research topics presented in this work have been an integral part of the Dutch national CCS project, CATO-2, and the European FP7 project, OCTAVIUS. Part of this work has been supported by ADEM Innovation Lab.



Copyright © 2016 Alexandr Kachko

ISBN: 978-94-6186-673-8

An electronic version of this thesis can be downloaded from:

<http://repository.tudelft.nl/>

*"Nothing in the world is worth having or worth doing unless it means effort, pain, difficulty . . . I have never in my life envied a human being who led an easy life. I have envied a great many people who led difficult lives and led them well."*

Theodore Roosevelt

*"The difference between ordinary and extra-ordinary is so often just simply that little word - extra. And for me, I had always grown up with the belief that if someone succeeds it is because they are brilliant or talented or just better than me . . . and the more of these words I heard the smaller I always felt! But the truth is often very different . . . and for me to learn that ordinary me can achieve something extra-ordinary by giving that little bit extra, when everyone else gives up, meant the world to me and I really clung to it . . ."*

Bear Grylls





# Contents

<b>1</b>	<b>Introduction</b>	<b>1</b>
1.1	Demand for CO <sub>2</sub> capture . . . . .	1
1.2	Amine-based CO <sub>2</sub> absorption . . . . .	2
1.3	Process monitoring and control . . . . .	4
1.4	PCC process monitoring . . . . .	5
1.5	Scope of this thesis . . . . .	7
<b>2</b>	<b>Real-time process monitoring of CO<sub>2</sub> capture by aqueous AMP-PZ using chemometrics: pilot plant demonstration</b>	<b>9</b>
2.1	Introduction . . . . .	10
2.2	Approach . . . . .	12
2.3	Materials and experimental procedure . . . . .	14
2.3.1	Chemicals . . . . .	14
2.3.2	Measurement instrumentation . . . . .	14
2.3.3	LC-MS measurements . . . . .	16
2.3.4	Installation at a pilot plant . . . . .	17
2.4	Data processing . . . . .	19
2.4.1	Analytical model calibration and validation . . . . .	19
2.4.2	NIR spectral data pretreatment . . . . .	20
2.4.3	NIR sensitivity assessment . . . . .	21
2.5	Results and discussion . . . . .	22
2.5.1	Chemometric model test and trial . . . . .	22
2.5.2	Pilot plant in-line monitoring . . . . .	28
2.6	Conclusions . . . . .	30

---

<b>3</b>	<b>In-line monitoring of the CO<sub>2</sub>, MDEA, PZ concentrations in the liquid phase during high pressure CO<sub>2</sub> capture</b>	<b>33</b>
3.1	Introduction . . . . .	34
3.1.1	Removal of CO <sub>2</sub> from natural gas . . . . .	34
3.1.2	In-line multivariate data analysis . . . . .	34
3.2	Approach . . . . .	36
3.2.1	High-pressure CO <sub>2</sub> separation mini-plant . . . . .	36
3.2.2	Design of experiments . . . . .	38
3.2.3	Sample preparation . . . . .	39
3.2.4	Simulation of the solvent properties during the CO <sub>2</sub> capture process . . . . .	40
3.3	Materials and instrumentation . . . . .	41
3.3.1	Chemicals . . . . .	41
3.3.2	Measurement instrumentation . . . . .	41
3.4	Calibration and validation . . . . .	43
3.4.1	Data processing . . . . .	43
3.5	Results and discussion . . . . .	44
3.5.1	In-line measurements . . . . .	44
3.5.2	Approach validation . . . . .	45
3.6	Conclusions . . . . .	50
<b>4</b>	<b>Comparison of Raman, NIR, and ATR FTIR spectroscopy as analytical tools for in-line monitoring of CO<sub>2</sub> concentration in an amine gas treating process</b>	<b>51</b>
4.1	Introduction . . . . .	52
4.2	Materials and equipment . . . . .	54
4.2.1	Chemicals and samples . . . . .	54
4.2.2	Raman spectroscopy . . . . .	55
4.3	Data processing . . . . .	57
4.3.1	Method performance assessment . . . . .	59
4.4	Results and discussion . . . . .	60
4.5	Conclusions . . . . .	66

---

<b>Appendix A Linear transformations for the screening procedure of samples</b>	<b>67</b>
<b>Appendix B Calibration measurements</b>	<b>73</b>
B.1 The AMP-PZ-H <sub>2</sub> O-CO <sub>2</sub> system . . . . .	75
B.1.1 Concentrations of chemicals in calibration samples .	75
B.1.2 Laboratory measurements of calibration samples . .	76
B.2 The MDEA-PZ-H <sub>2</sub> O-CO <sub>2</sub> system . . . . .	79
B.2.1 Concentrations of components in calibration samples	79
B.2.2 Laboratory measurements of calibration samples . .	80
B.3 Input and output of Aspen Plus modeling . . . . .	82
<b>References</b>	<b>87</b>
<b>Summary</b>	<b>107</b>
<b>Samenvatting</b>	<b>111</b>
<b>Curriculum Vitae</b>	<b>115</b>
<b>Publications by the Author</b>	<b>117</b>
<b>Acknowledgement</b>	<b>119</b>



# Chapter 1

## Introduction

### 1.1 Demand for CO<sub>2</sub> capture

In the modern world, emissions of greenhouse gases originate from various anthropogenic sectors. Among them are fossil fuel combustion for power generation and delivery, agriculture, waste disposal, and other industrial processes not related to energy production [1–3]. Carbon dioxide (CO<sub>2</sub>) is considered to be the main anthropogenic greenhouse gas responsible for global warming [4]. In addition, the process of deforestation leads to depletion of the natural drains of CO<sub>2</sub> from the atmosphere [5]. Many activities, aimed to alleviate the CO<sub>2</sub> emissions, are initiated by governments all over the world [6–9].

Carbon dioxide Capture and Storage (CCS) technologies have been developed intensely and tested since the late 1970s [10]. CCS technologies are aimed to limit anthropogenic CO<sub>2</sub> venting into the Earth's atmosphere [11]. The large potential of CCS lies in its ability to assist the energy industry to transfer from fossil fuels to renewable energy. Meanwhile, the conversion efficiency of non-fossil energy sources is approaching its theoretical limits. There are several state-of-the-art technologies being developed to capture CO<sub>2</sub> from flue gas emissions from stationary point sources (coal and natural gas-fired power plants, oil refineries, steel producing plants). The most promising solutions are Chemical Looping Combustion (CLC), pre-combustion carbon capture, oxy-fuel combustion, and post-combustion carbon capture [12–16].

## 1.2 Amine-based CO<sub>2</sub> absorption

In perspective of the predicted global warming up to 2 °C over the next four decades, the aforementioned Post-combustion Carbon Capture (PCC) technology is the most suitable for retrofitting on existing fossil-fuel power stations [17–24]. The most common method used in PCC processes is chemical absorption using aqueous alkanolamine solutions [17, 25, 26], which has been studied and applied for purifying gas streams from acid gases and supplying pure CO<sub>2</sub> since the 1930s [27]. Amine based aqueous solutions are used for CO<sub>2</sub> absorption from the flue gas of power plants, in cement industry, and in natural gas processing [28–34]. A solution of 30 wt. % of aqueous monoethanolamine (MEA) is the most widely used solvent to absorb CO<sub>2</sub> in industrial pilot plants. This solution has been investigated on a laboratory table, at mini-scale absorber-stripper units, and even at pilot plants operating on full size power stations [35–38]. It is also a common rule of thumb in the CCS industry to use the MEA process as a benchmark to modify properties of modern solvents and improve the configuration of CO<sub>2</sub> absorption processes [34]. Blended solutions of amines are also experimentally studied for their application to CO<sub>2</sub> absorption. For instance, adding piperazine (PZ) to sterically hindered amine 2-amino-2-methyl-1-propanol (AMP) or tertiary amine methyldiethanolamine (MDEA) accelerates reaction rate and increases the capture capacity in addition to lowering the regeneration energy requirements [39, 40]. MDEA on its own is applied for selective removal of H<sub>2</sub>S and CO<sub>2</sub> at relatively high pressures and it has been used as a component in blended alkanolamine solutions with primary and secondary amines. It has been shown that MDEA has a high capacity for removal of carbon dioxide, although this tertiary amine does not form carbamates when it reacts with CO<sub>2</sub> [41, 42]. A simple schematic flow diagram of a PCC absorption plant is shown in Figure 1.1. The flue gas from a smokestack is supplied to the absorber column, where CO<sub>2</sub> is captured by the amine-based solvent in a counter-current configuration. After absorption, the CO<sub>2</sub>-rich solvent is fed to the stripper column, where the solvent is thermally regenerated via heating. The desorbed gaseous CO<sub>2</sub> is released from the stripper column and the regenerated solvent flows back to the absorber. The working pressure is typically 1.0 bar in the absorber and up to 2.0 bars in the stripper and the temperatures of the gas-liquid mixture in the absorber

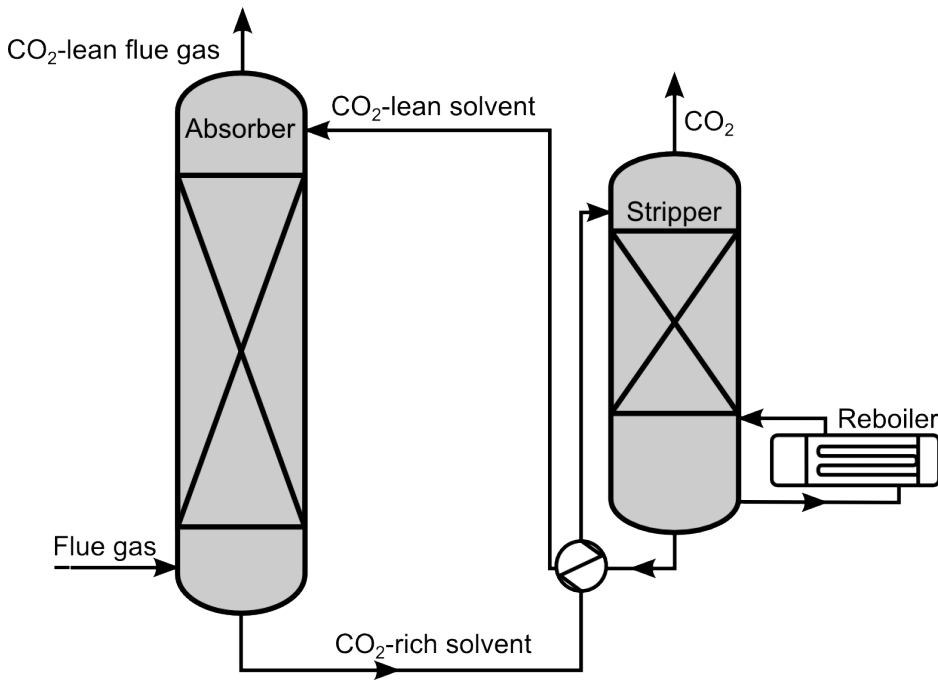


Figure 1.1. Schematic representation of a PCC plant. Absorption of CO<sub>2</sub> takes place in the absorber column of the plant. The solvent, saturated with CO<sub>2</sub>, is pumped through a heat exchanger into the stripper, where thermal regeneration takes place. The lean solvent is pumped back to the top section of the absorber for cyclic use. A more detailed scheme and description may be found elsewhere, for example in work of Cousins et al. [28]

and stripper are around 40-60 °C and 100-120 °C, respectively. Typically, a capture plant is designed to provide a capture rate of 90 % at average CO<sub>2</sub> concentrations in the range of 10-15 vol% in the exhaust flue gas from coal-fired power plants [43].

According to the latest global CCS status update [44], the world's first post-combustion coal-fired CCS project, launched at the Boundary Dam power station in Saskatchewan, Canada, has achieved the milestone of one year of operation. Another CO<sub>2</sub> capture and enhanced oil recovery demonstration project has become operational in Saudi Arabia in July 2015. There are also 22 large-scale CCS projects in operation or under construction around the world, most of which are in the sector of power

generation, iron and steel production, and natural gas processing [45]. PCC technology using aqueous amine-based solutions is being investigated extensively and improved constantly in terms of solvent capacity, capture rate, and energy efficiency [38, 46, 47]. Chemical absorption is also often used for Natural Gas (NG) sweetening [48]. Amine-based solvents have been used for CO<sub>2</sub> absorption from raw NG streams for more than 50 years [49]. Raw high-pressure NG is a complex mixture of gases, consisting mainly of hydrocarbons and impurities such as nitrogen (N<sub>2</sub>), CO<sub>2</sub>, and H<sub>2</sub>S. NG stream contains CO<sub>2</sub> at concentrations in the range of 3-5 % by volume [50]. The composition varies greatly from source to source [51, 52]. NG processing, shipping, and pipeline transportation companies set certain standards for NG quality [53]. To adhere to these specifications and at the same time reduce CO<sub>2</sub> emissions during NG combustion, NG is sweetened by removing the acid gases (CO<sub>2</sub> and H<sub>2</sub>S) [54–56]. Compared to the PCC processes, the increased supply pressures enhance CO<sub>2</sub> absorption [57].

### 1.3 Process monitoring and control

Experimental methods for *in situ* measurements are used extensively for research in fundamental and applied science. These methods are often applied for the extraction of information in the Process Analytical Technology (PAT) and Quality by Design (QbD) concepts [58–64]. Chemical manufacturing continuously requires improvement of end-product characteristics, reducing economic losses and time delays, and minimize generation of waste product. Traditionally the processes are fixed in accordance with flow-sheet and run with no intermediate changes affecting the product production routine. Any possible failures that happened during the fabrication phase become apparent post-factum, during the product quality assurance tests. To reduce risks and improve flexibility of manufacturing processes the QbD concept was proposed [65]. QbD is an approach that introduces principles of building quality in finished product by design of the manufacturing process. It demands timely identification and monitoring of all critical process parameters, which provides important information for critical decision making leading to continuous improvement of the process performance. Thus, the QbD approach is applied to move forward from process development concept, that rely on empirical information, to more



systematic and risk-based method of the quality management [66]. PAT methods combine measurement instruments and multivariate data processing algorithms [67, 68] to extract valuable chemical information directly from the production line. The PAT approach implies in-line and on-line measurements usually involving hardly any sample preparation. In-line analytical methods provide process engineers with ability to quickly determine process conditions and vary critical process parameters in real time. Thereby, PAT helps to shorten the decision-making time, in sharp contrast to the conventional practice of off-line laboratory analysis [69, 70]. Currently, process control is typical in industries like pharmaceutical, chemical, and biotechnological. The utilization of PAT instruments allows for significant expansion of the amount of the analytical data, i.e., measurements, obtained from complex systems. Multivariate statistics analysis methods applied to recognize the relations between these data and process or experiment conditions have matured into the separate scientific field known as chemometrics [71]. Chemometrics employs statistical and mathematical data processing methods for extraction of meaningful information about a material substance or natural phenomena. To make the PAT and QbD concepts applicable in practice, chemometric analysis methods are used as a connecting link [72, 73].

## 1.4 PCC process monitoring

Nowadays, continuous monitoring of the liquid phase of PCC absorption processes is performed using temperature and pressure sensors [74, 75]. On rare occasions, additional instruments for pH, conductivity, and density measurements are installed on pilot plants. The introduction of these measurement instruments helps to control and analyse process variables like solvent-water balance or CO<sub>2</sub> loading, during tests of new process conditions, plant design and packing materials, and solvents. The analytical monitoring of gaseous emissions from top of the columns during the CO<sub>2</sub> absorption process in pilot plants is usually performed via Fourier Transform Infra-Red (FTIR) spectroscopy or Gas Chromatography (GC) [76]. The composition of the liquid phase is most commonly determined using off-line measurements. The measurement methods that are used include FTIR, Liquid Chromatography in combination with Mass Spectrometry (LC-MS),

titration, and Nuclear Magnetic Resonance (NMR) spectroscopy [77–81]. It should be noted that FTIR spectroscopy is widely used method for on-line monitoring of both liquid and gaseous phase in PCC process. Mobile FTIR spectrometers are used to carry out the online analysis of amine solvent during CO<sub>2</sub> absorption [82, 83]. Off-line methods require sample extraction and long-distance transportation. Sometimes or at some locations at the process, sampling is challenging or not possible at all when complete operation shut-down or change of a procedure flow-sheet is required to take a sample [84, 85]. Control actions during the continuous process are delayed by the time span between sample withdrawal and the acquisition of the measurement results from off-line analytical technique. If such a measurement mode is impractical for continuous process control, the number of off-line measurements might be increased leading to high financial expenses. Overcoming such obstacles would lead to an improved process flexibility. It would enable introduction of rapid alterations on the Research and Development (R&D) stage and modification of existing technologies.

Automation of analytical measurements plays remarkable role in planning and execution of informative experiments [86]. This directive was adopted in this thesis to conduct a consistent samples screening procedure. The experiments were planned in accordance with the methods of the Design of Experiments (DOE) [87] approach. Construction of the calibration database was performed via precise laboratory measurements using different analytical methods under different conditions.

A chemometrics model is calibrated within a measurement domain defined by a chemical process and includes many variables in this process. PCC processes are continuously optimized using results from various research projects carried out at pilot- and demonstration-scale plants. According to the literature [88], a wide selection of process parameters are varied by the plant operator to test their qualitative and quantitative input on the outcome of a research campaign. The modification of process configurations includes, but not limited to, testing such parameters as solvent circulation, desorber pressure, temperature of the lean solvent, location and temperature of inter-stage coolers for the lean solvent flow. Such changes in process settings may result in conditions that are outside the calibration limits of the model, which can lead to the necessity of the

chemometrics model re-calibration. Therefore it is essential to establish the feedback coupling between the real-time PCC process conditions and output results of the in-line chemometrics setup, i.e., monitor how well the process parameters correspond to the applicability boundaries of the model in use. In other circumstances the measurement equipment installed in chemometrics setup might begin providing false readings due to malfunction. In the latter case a new chemometrics model that accounts for the absence of the readings from one or more measurement channels must be used until the issue is resolved. Both cases, the variation of process conditions outside the calibration range and equipment malfunction, were encountered during the works presented in this thesis. Prior to taking measures for model re-calibration the source of out-of-boundary data should be determined. In some instances these data may indicate faults in the studied process itself [89, 90].

## 1.5 Scope of this thesis

This thesis covers the topic of in-line monitoring of the solvent composition during CO<sub>2</sub> absorption processes. This research describes work performed during screening experiments in a laboratory, tests using mini plants, and measurement campaigns performed at a pilot-plant scale CO<sub>2</sub> absorption process. The developed approach has been successfully applied to solvent monitoring at three different chemical processing plants. The plants were designed and assembled by different manufacturers for developing the CO<sub>2</sub> absorption processes. The scales of these pilot plants range from 5 litre to 9 m<sup>3</sup> of solvent inventory. The main results are described in three publications submitted to international academic journals [91–93]. Chapters 2 to 4 are based on these publications.

**In chapter 2**, the combined approach of DOE and chemometrics is presented. The complete technique is described, starting at the laboratory table and leading to a realistic case study. The research is focused on the characterization of the solvent system of aqueous 2-amino-2-methyl-1-propanol (AMP) activated by piperazine (PZ) used for CO<sub>2</sub> absorption. Five physical properties and the near infra-red (NIR) absorption spectra have been used as multivariate data input for subsequent statistical analysis and model construction. The mathematical methods used for data

processing and noise reduction are described. To correlate the concentrations of species in a liquid mixture and the measured parameters, a Partial Least Squares (PLS) regression technique was used. Temperature dependency is included in the model. Validation of the in-line measurements by off-line techniques is presented. It is shown that the NIR signal significantly improves the prediction quality of the PLS models for both amines, namely AMP and PZ.

**In chapter 3**, in-line monitoring of the solvent composition during high-pressure CO<sub>2</sub> absorption is presented. Aqueous solutions of PZ-activated methyldiethanolamine (MDEA) were used as a solvent blend in these experiments. The developed approach is suitable for real-time control of natural gas purification processes. During this research, a chemometrics setup suitable for transportation and rapid installation on a site has been assembled. The procedure for calibration of the statistical model is elaborated, similar to Chapter 2. Once the predictive model is established and the instruments of a chemometrics setup are adjusted according to the process requirements, the setup may be run semi-automatic.

**Chapter 4** deals with the comparison of three spectroscopic techniques in terms of applicability for purposes of PAT in a CO<sub>2</sub> absorption process: Raman spectroscopy, Attenuated Total Reflectance FTIR (ATR FTIR) spectroscopy, and NIR spectroscopy were compared qualitatively and quantitatively. A custom-built Raman spectroscopy setup used for observation of CO<sub>2</sub> absorption into aqueous solution of monoethanolamine (MEA) is presented. The results of the comparison have shown high potential of spectroscopic methods for application to PCC absorption process. The possible areas of improvements are addressed in terms of the spectral data processing, signal-to-noise ratio treatment, and instrumentation.

## Chapter 2

# Real-time process monitoring of CO<sub>2</sub> capture by aqueous AMP-PZ using chemometrics: pilot plant demonstration

This chapter is based on:

Kachko, A.; van der Ham, L. V.; Geers, L. F. G.; Huizinga, A.; Rieder, A.; Abu-Zahra, M. R. M.; Vlugt, T. J. H.; Goetheer, E. L. V. *Real-time process monitoring of CO<sub>2</sub> capture by aqueous AMP-PZ using chemometrics: pilot plant demonstration*. Industrial & Engineering Chemistry Research. 2015, 54, 5769-5776.

## 2.1 Introduction

The operation and monitoring of chemical processes requires reliable methods for continuous on-line control of running processes, determination of properties of liquids and gases, and determination of the response to changes in the process conditions [94–97]. One of the industrial processes that is receiving a lot of attention lately is Post-combustion CO<sub>2</sub> Capture (PCC), a technology aimed to reduce the carbon dioxide emissions to the atmosphere caused by the electric power industry, chemical industry, and heavy industry [98–100]. For PCC from power plants, chemical absorption using amine-based solvents as the chemical absorption agent is the current standard [19, 22, 101, 102]. Counter-current flows of the amine-based solvent and the exhaust stream are brought into contact inside an absorber column, thus removing carbon dioxide from the flue gas. The resulting CO<sub>2</sub>-rich liquid solvent is pumped towards the thermal desorption column, where CO<sub>2</sub> gas is released from the solvent due to increased temperature. The regenerated CO<sub>2</sub>-lean solvent is supplied back to the absorber column. The water-amine ratio is subject to change due to emissions of the solvent in the absorption-desorption system, flue gas composition, gas/liquid flow rate, and solvent degradation phenomena [103–105]. Hence, the CO<sub>2</sub> capture rate also changes in time. Continuous monitoring of the composition of the solvent stream is advantageous, since it provides fast feedback in response to changing process conditions.

It is common practice to analyse solvent streams off-line by taking a sample from the lean and rich streams of the capture plant and performing, for instance, Fourier Transform Infra-red (FTIR) spectroscopy analysis [83] or more expensive LC-MS tests [106] to determine the composition of the liquid solvent. Accurate multi-component system characterization is one of the main goals for informative process analysis [107]. A reliable analytical method is especially important when substances in a mixture are hard to distinguish from one another (mixtures of two and more amines), but their concentrations have an impact on the overall performance of the process. So called “at-line” analysis, using instruments placed close to the process line, requires sample transportation and poses risks of sample contamination during tests [108]. Direct in-line installation of monitoring tools for analysis of both the lean and rich solvent slip streams reduces the likelihood of external influences and increases flexibility of

the industrial process control. In this perspective, the combination of the multi-variate measurements with subsequent data extraction using statistical tools and computer programming (chemometrics) has proven to be a powerful approach for the construction of descriptive and predictive models for chemical systems [109–112].

Recently, a chemometrics approach, similar to described in this chapter, has been successfully implemented for in-line monitoring of monoethanolamine (MEA) and absorbed CO<sub>2</sub> concentrations [113]. Another work presented the statistical data processing of the Attenuated Total Reflection FTIR (ATR FTIR) spectral responses to analyse a solvent composed of neutralized  $\beta$ -Alanine as a capture agent for CO<sub>2</sub> absorption [82]. The models were built to predict the concentrations of the acid gas (CO<sub>2</sub>) and capture agent. The predictions were restricted to a single operational temperature, which suggests frontiers for improvements in the flexibility.

This chapter is focusing on four-component mixture analysis. A solvent blend of aqueous 2-amino-2-methyl-1-propanol (AMP) activated by piperazine (PZ) and loaded with CO<sub>2</sub> was studied in a laboratory and also monitored at an industrial pilot plant. The AMP-PZ solvent blend is reported to be an energy and material saving alternative to conventional MEA-based solvents for the PCC process [114, 115]. In the current chapter, the application of the in-line chemometrics approach for the discrimination between the two amines that make up the solvent is described. The following solvent properties were measured: density ( $\rho$ ), conductivity ( $\Omega^{-1}$ ), pH, sound velocity (SV), refractive index ( $n_D$ ), and near infra-red (NIR) absorption. A model based on partial least squares (PLS) regression algorithm was used for prediction of the concentrations from the set of measured data. The temperature dependency was included in the model by using the calibration data set of measurements conducted at three temperatures: 25, 35, 40 °C. This chapter contains a description of the screening experiments, calibration and validation measurements, and chemometric model construction. The confirmation of the applicability of the method via testing at an industrial pilot plant with subsequent validation is presented as well. The developed approach is suitable for applications at chemical processes similar to PCC, like natural-gas treatment.

Table 2.1. Levels of concentration used for the calibration set. Low and High are the lower and upper limits of concentrations that may be encountered during a PCC operation process; Base defines the desired process concentrations. Extra levels of concentrations were added to the calibration procedure in order to increase the resolution of the predictive model.

	Low		Base		High
AMP [mol/kg]	2.00	2.50	3.00	3.25	3.50
PZ [mol/kg]	1.00	1.25	1.50	1.75	2.00
CO <sub>2</sub> [mol <sub>CO<sub>2</sub>]/mol<sub>Amine</sub>]</sub>	0.00	0.10	0.20	0.35	0.50

## 2.2 Approach

The measured physical properties of the liquids (in this chapter referring to the set  $\rho$ ,  $\Omega^{-1}$ , pH, SV,  $n_D$ ) are known to be highly dependent on temperature [116, 117]. If the prediction ability of a chemometric model is restricted to one operational temperature, then its applicability will be too limited, since industrial processes may run at different conditions with various temperature fluctuations. The physical properties alone may not be sufficient for accurate model construction. Spectroscopy data of the NIR absorbance can significantly supplement the data obtained by the measurements of the physical parameters. However, the spectroscopic signal is also known to be temperature dependent, though not to such an extent as the physical parameters [118]. The calibration database for the model construction consisted of the measurements conducted at 25, 35, and 40 °C, thus containing information on the temperature dependency of every measured variable.

The range of applicability for the model was defined in accordance with the requirements of the carbon dioxide capture process. The first stage in experiment design is samples screening procedure. Five levels of concentrations were selected for every compound. Each sample in the calibration set was composed of a combination of the concentrations from Table 2.1.

Given that the total number of permutations will make up  $5^3=125$  samples, the calibration procedure would become very labour-intensive, especially taking into account the number of properties that have to be measured and repeated every time for each of the three different temperatures. Therefore, a fractional factorial design of three factors at five levels



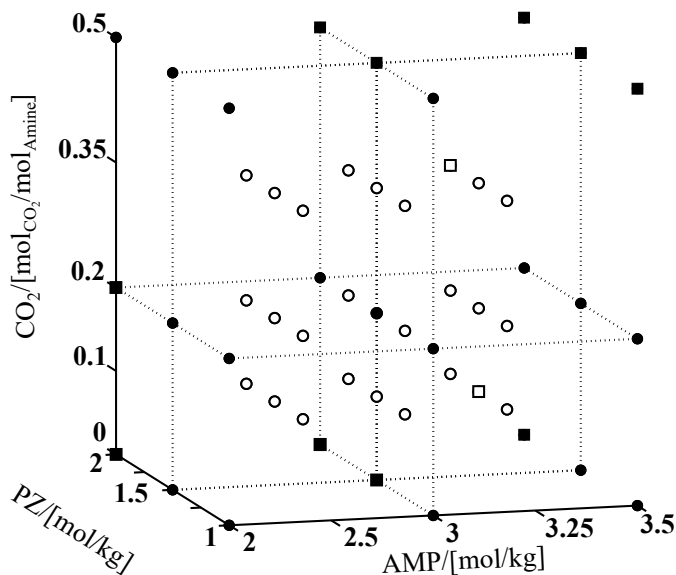


Figure 2.1. Graphical representation of the composition matrix of the calibration samples. The 27 filled symbols represent the training compositions for the PLS model and the 26 empty symbols represent the compositions that serve for model testing. The circles are the samples that were actually used for model calibrations. The squares denote those samples that have contained precipitates at the targeted temperatures. During the measurement campaign at the pilot plant, the whole set of samples, except 12 with precipitates, was used as a calibration database for the PLS model.

was generated using the so-called  $5^{**}(3-1)$  approach [119]. Additional samples (28) were mixed, in order to obtain an equally spaced array of concentrations for accurate assessment of the relations between the three compounds. Overall, 53 samples were prepared with various concentrations of both amines and  $\text{CO}_2$  (see Figure 2.1).

It turned out that 12 samples were unusable because of precipitation of amine within the selected experimental temperature range. The final calibration set of samples was subjected to analysis using measurements of six variables: density ( $\rho$ ), conductivity ( $\Omega^{-1}$ ), pH, sound velocity (SV), refractive index ( $n_D$ ), and NIR absorbance. It is convenient to sort all

of the measured values into two sets of data: physical parameters and spectroscopic data.

Two separate stock solutions of aqueous AMP and PZ with CO<sub>2</sub> contents of 0.62 and 0.86 mol<sub>CO<sub>2</sub></sub>/mol<sub>Amine</sub> were prepared. The calibration set of samples was then prepared using certain amounts of liquid from each of the stock solutions with subsequent addition of pure AMP, PZ, and water. The final total volume of every sample was 100 ml. When it is necessary to extend the applicability of the model to wider range of concentrations the described samples screening procedure can be used. Whenever the operational temperature is outside the calibration boundaries, or the composition of the liquid is not covered by the existing model, extra measurements obtained in a laboratory might be added into the calibration database. A complete list of samples with final concentrations of the constituents as well as the measurements of physical parameters at three different temperatures in a laboratory are provided in section B.1.

## 2.3 Materials and experimental procedure

### 2.3.1 Chemicals

AMP ( $\geq 99\%$ ) and PZ ( $\geq 99\%$ ) were purchased from Sigma Aldrich and used as received without further purification. Aqueous solutions of amines were prepared by mixing with deionized water at the needed proportions. Compressed CO<sub>2</sub> from a gas cylinder ( $\geq 99\%$ ) was used to load the stock solutions by feeding gaseous CO<sub>2</sub> through flasks with solutions. The CO<sub>2</sub> content in stock solutions was measured using method described in subsection 2.3.2 of this chapter.

### 2.3.2 Measurement instrumentation

The model for in-line assessment of the solvent composition was completely based on the values obtained from the calibration measurements. The construction of the in-line chemometric setup involved the measurement devices being built into the flow-through cells. The calibration measurements of pH,  $\Omega^{-1}$ , and  $\rho$  were performed using separate equipment suitable for laboratory environment. Every instrument was carefully calibrated every time before making a series of measurements with the calibration samples

in the laboratory and before starting up data logging with the chemometric setup installed at a pilot plant.

### **Near Infra-Red spectroscopy**

The NIR spectroscopy absorption signal was collected using a flow-through cell with a 5 mm path length equipped with fiber-optic cables carrying the light from the output of a tungsten halogen light source (AvaLight-HAL) to the streaming liquid and bringing the signal to the spectrometer. The same equipment was used for laboratory measurements as well as for in-line solvent monitoring at a pilot plant. A NIR256-2.0 spectrometer, light source, and software were supplied by Avantes. The wavelength range was within 1017-2044 nm with a spectral resolution of about 4 nm. The spectra acquisition time was between 3 and 4.5 ms and the averaging was done over 100-200 scans. A reference spectrum was collected from deionized water. Prior to every new measurement campaign, reference and dark spectra were recorded again to keep the instrument calibration updated.

### **Refractometry**

The refractive index of the studied solutions was measured by an in-line refractometer, CM780N manufactured by Atago, calibrated in Brix % units with an accuracy of  $\pm 0.2\%$ . The units of Brix represent the weight percentage of sucrose dissolved in pure water. The conversion of the Brix scale to the refraction index,  $n_D$ , was performed using the empirical correlation provided by Atago:

$$n_D = 1.333 + \text{Brix} \cdot 1.335 \cdot 10^{-3} + \text{Brix}^2 \cdot 7.608 \cdot 10^{-6} \quad (2.1)$$

### **Sound velocity**

An immersion sensor for sound velocity measurements, Liquisonic 40-40 from SensoTech, dipped into a custom-made flow-through cell was used to acquire values of the speed of sound in the liquid. The studied liquid fills a gap between a piezoelectric ultrasonic-sound transmitter and a receiver separated from each other at a well known distance. The measurement accuracy of the sensor is  $\pm 0.01\%$ .

### Density measurements

The density was measured by means of: (a) an Elite MicroMotion Coriolis flow meter (also capable of measuring solvent mass flow), installed inside the mobile in-line chemometrics setup, with an accuracy of  $\pm 0.05$  % and (b) a DMA 4500 Anton Paar U-tube density meter during measurements in the laboratory with an accuracy of  $\pm 0.005$  %.

### pH and conductivity sensors

For in-line measurements, the pH readings were obtained by a pH3630 device with a 2-wire pH transmitter and the conductivity was measured by a C7635 device equipped with a 7-wire transmitter with an accuracy for both devices of  $\pm 0.1$  %. Both devices were obtained from Nieuwkoop B.V. The laboratory calibrations were carried out with a portable HQ11d pH meter equipped with an IntelliCAL pH101 electrode with an accuracy of  $\pm 0.1$  % of value. The conductivity of the calibration samples was measured with an Orion Star A322 meter with an Orion 013010 MD conductivity cell (accuracy is  $\pm 0.5$  % of value), both from ThermoScientific.

### Hot phosphoric acid method

In order to determine the CO<sub>2</sub> concentration, the boiling phosphoric acid method was used. The weight percentage of CO<sub>2</sub> contained in a solvent is provided as a result of these measurements. A known amount of a CO<sub>2</sub>-loaded liquid sample was injected into a round bottom flask with a boiling aqueous solution of H<sub>3</sub>PO<sub>4</sub> ( $\geq 85$  %, Sigma Aldrich). The released CO<sub>2</sub> was dragged away from the flask with a constant rate by the flow of N<sub>2</sub>. Then, the gas flow was fed into a Binos 100 2M carbon dioxide analyser from Rosemount Analytical. The CO<sub>2</sub> amount was automatically logged. The calibration of the method was done routinely with a 1M solution of K<sub>2</sub>CO<sub>3</sub>. The accuracy of this method has been calculated to be  $\pm 4.1$  %.

### 2.3.3 LC-MS measurements

The concentrations of AMP and PZ in the validation samples from a pilot plant were also measured by a LC-MS technique. The samples were diluted to 1:10 000 in water. A deuterated internal standard was added to

the diluted samples for both of the analytes. The samples were analysed with an Agilent Infinity 1290 LC-system, combined with a 6490 Triple quadrupole MS. The samples were run in MS-MS-mode. Prior to analysis of the composition of validation samples the method calibration curves have to be build [124]. During the calibration procedure the relationship between the instrument output signal and known concentration of the analyte contained in the calibration standard is established. The standard concentrations were evenly spaced across the targeted range of concentrations of components contained in validation samples. This is performed by conducting measurements of set of standards containing a known amount of either AMP or PZ. The method calibration curves for both AMP and PZ show a  $R^2$  value  $> 0.99$ .

### 2.3.4 Installation at a pilot plant

The solvent flow was monitored at the PCC pilot plant installed at the EnBW coal-fired power plant in Heilbronn. This pilot plant has already been used for CO<sub>2</sub> capture with aqueous 30 wt. % MEA solution for almost 1600 operating hours [120]. Authors report that during the campaign with MEA as solvent CO<sub>2</sub> loadings of the solvent were above 0.5 mol CO<sub>2</sub>/mol<sub>MEA</sub>. It also has been shown that solvent degradation has happened primary due to oxidation mechanism via formation of formate and oxalate. In order to be able to reclaim degraded solvent, the electro-dialysis technology was tested at the PCC pilot plant. The effective removal of heat-stable salts anions from solvent stream has been demonstrated [121]. The PCC plant receives the flue gas and steam from the 7<sup>th</sup> unit of the power station. The flue gas flow was approximately 1500 Nm<sup>3</sup>/h and the CO<sub>2</sub> capture rate was around 90 %. The initial composition of aqueous solvent was 3.0 M of AMP and 1.5 M of PZ. The solvent circulation rate in the system of the PCC pilot plant was in the range of 3-6 m<sup>3</sup>/h. The height of the absorber and stripper column is 38 m and 30 m, respectively. The total solvent composition is constant in the closed circulation line of the PCC pilot plant. Due to the specifications of the measurement devices, high solvent temperature is the limiting factor for the chemometric setup applicability. Since temperature of the liquid in the outlet of the stripper section may reach 90 °C, it was decided to install the setup at the point where the operating temperature is lower. The solvent for in-line analysis

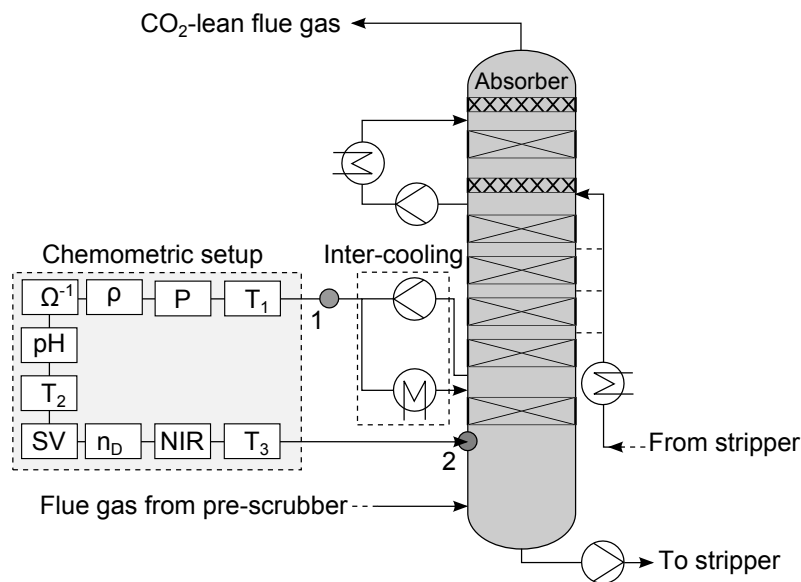


Figure 2.2. Schematic representation of the chemometric setup at the pilot plant. The solvent supply was provided via a bypass from the absorber's inter-cooling system between points 1 and 2, which are connected to the inlet and outlet of the setup. The setup consists of the following instruments: pressure sensor (P), Coriolis flow and density meter ( $\rho$ ), conductivity probe ( $\Omega^{-1}$ ), pH probe, sonic velocity sensor (SV), refractometer ( $n_D$ ), near infra-red spectrometer (NIR), thermocouples for temperature measurements at the inlet, near the center, and at the outlet of the chemometric setup ( $T_{1,2,3}$ ).

was taken via a bypass from the inter-cooling section of the absorber at a rate of around 20 l/h. After flowing through the chemometric setup, the solvent was fed back to the absorber sump (see Figure 2.2).

Approximately five weeks of in-line solvent monitoring was conducted accompanied by data collection and analysis. The PCC pilot plant was operating mostly during day time when the steam supply from the power plant was available. At night time, the solvent was only circulating, without any flue gas and without heating in the reboiler. The plant was shut down completely during weekends. The prediction of the concentrations was performed using data collected when the temperature of the solvent flow was within the calibration limits.

## 2.4 Data processing

### 2.4.1 Analytical model calibration and validation

The main functionality of chemometrics in connection with process control is its ability to provide an operator of a plant with relevant information about running chemical processes and reduce the time needed for the analysis. For this purpose, the calibration measurements were conducted in order to obtain enough experimental data points to be able to construct a correlation between two sets of data: the known composition of the mixture of interest and the physical and spectroscopic responses from the set of calibration samples.

Partial least squares (PLS) regression is a common chemometrics method [72, 122]. To develop the calibration models the PLS-1 algorithm [123] was applied. The PLS models were built for prediction of the concentration of each chemical component separately. Thus, during the model calibration procedure the matrix of the independent parameters consisted of data from one vector taken from the block with controllable factors (concentrations of chemicals) and the matrix of the dependent predictors was comprised of the measurements of all 5 physical properties and the NIR signals from the block with the output variables. The MatLab programming environment was used to build the models. The built-in PLSREGRESS function was used to compute the PLS regression models. MatLab supporting documentation contains description of this function. PLS regression models consider the correlation between the concentrations of the mixture components and the measured responses, by constructing latent variables (*LV*) that directly relate to the source data. The parameter for model quality assessment is the Root Mean Square Error of Prediction (*RMSEP*):

$$RMSEP = \sqrt{\frac{1}{N} \sum_{i=1}^N (y_{i,\text{exp}} - y_{i,\text{model}})^2} \quad (2.2)$$

where  $N$  is the number of calibration measurements used in model construction, the values of  $y_{i,\text{exp}}$  are known, and the values of  $y_{i,\text{model}}$  are predicted with the PLS model. The influence of the number of *LV*s on the

*RMSEP* was examined using the leave-one-out method for cross-validation. Following the recommendation given in works of Wise et al. [125] and Li et al. [126], the optimal number of *LVs* to be included to the PLS model was selected such that the addition of another *LV* does not significantly reduce the value of *RMSEP*. In his discussion of the optimal number of *LVs* Wise et al. [125] proposed that when the difference between *RMSEP* values of two prediction models is not greater than 2 % then the model that was build using lower number of *LVs* can be selected for further application.

Two approaches have been evaluated to include temperature dependence into the chemometric model. One option is Lagrange polynomial interpolation [127]. In this approach, we used a second-order polynomial approximation of the temperature dependence of physical parameter and the NIR peaks. Estimating the concentrations in-line by means of such an approach for every new temperature reading coming from the industrial process requires an update of the model using the established polynomial functions for every measured parameter.

The other approach, which is faster and avoids extra calculations, is to use all available measurements of the dependent variables at different temperatures as the source data for the model. This way the temperature dependence is already included as an inherent feature of the correlation between the source data and *LVs* used to build the PLS model. The final predictions represented in section 2.5 of this chapter were calculated using the second approach in order to introduce the temperature dependence.

## 2.4.2 NIR spectral data pretreatment

It is common practice to interpret NIR spectroscopy measurements using Beer's Law [128], which gives a linear functional relation between the amount of light absorbed by a studied sample, the distance of light travel through the sample, and the quantity of light-absorbing substance that is contained in that sample. Therefore, the raw NIR signal was first converted to the absorbance spectra using

$$A = -\log_{10} \left( \frac{I_{\text{sample}} - I_{\text{dark}}}{I_{\text{ref}} - I_{\text{dark}}} \right) \quad (2.3)$$

where  $A$  is the absorbance spectrum of a sample,  $I_{\text{sample}}$  is the raw NIR spectrum of a sample and  $I_{\text{ref}}$  and  $I_{\text{dark}}$  are the reference and the dark spec-



tra, respectively. Spectral signal windowing was performed to specify the region of the highest signal correlation with the change of the chemical composition. Subsequently, spectra were smoothed with the Savitzky-Golay algorithm [90, 129]. Both the 1<sup>st</sup> and 2<sup>nd</sup> derivatives of the smoothed spectra were evaluated, which results in the removal of the baseline offset differences between spectra and the differences in baseline slopes between spectra. Finally, the 1<sup>st</sup> derivative was selected for the PLS model construction. The automated mean-centering of all of the response factors was used as an inherent functionality built in the MatLab PLS regression algorithm.

### 2.4.3 NIR sensitivity assessment

The number of parameters monitored during calibration experiments and later during real case measurements was quite high, especially when considering the spectroscopy data. A spectral sensitivity analysis with respect to AMP, PZ, and CO<sub>2</sub> concentrations was performed in order to reduce the risks of overdetermination, which may happen in the case of the PLS algorithm.

It is experimentally shown that the absorption coefficient  $\alpha$  of an electromagnetic wave in a solution is proportional to the concentration  $x$  (number of molecules per unit volume) of the absorbing substance [130]. Light absorbance may thus be described as follows,

$$A(\lambda, x) = \alpha(\lambda, x) \cdot l = \sum_{j=1}^M \alpha'_j(\lambda) \cdot x_j \cdot l = \sum_{j=1}^M \beta_j(\lambda) \cdot x_j \quad (2.4)$$

where  $M$  is the number of the chemical components in a mixture;  $\alpha'$  is a constant coefficient, which depends on the nature of the media and the wavelength of the incident light  $\lambda$ ; and  $l$  is the path length of the incident light.

According to Eq. 2.4, the intensity of an absorbance peak at a certain wavelength is proportional to the concentration  $x_j$  of each solute that makes up a mixture, each with its own weighting coefficient  $\beta_j(\lambda)$ , which

in turn may be treated as a sensitivity parameter:

$$\beta_j(\lambda) = \frac{\Delta A(\lambda)}{\Delta x_j / \bar{x}_j} \quad (2.5)$$

where  $\Delta A(\lambda) = A(\lambda) - \bar{A}(\lambda)$  and  $\Delta x_j = x_j - \bar{x}_j$  are the deviation of the intensity of an absorbance peak and the deviation of the concentration of  $i$ -th mixture component from its average value, respectively.

## 2.5 Results and discussion

### 2.5.1 Chemometric model test and trial

The prediction accuracy of a model is dependent on the source measurements that are used for its construction. Individual PLS models for prediction of concentration of both amines and CO<sub>2</sub> have been calibrated using measurements of physical and NIR responses separately as well as with the entire set of the measurements. A complete summary of the calibration samples compositions as well as measurements of the physical properties at three different temperatures can be found in supporting material given in Appendix B. All measurements of NIR response taken from the calibration samples are supplied as the Supporting Information to the article by Kachko et al.[91] published in the journal *Industrial & Engineering Chemistry Research*.

#### Physical parameters

The investigation of the quality of the fit by the models built using different combinations of measured properties can be used as indication of the importance of these properties for describing the variation of the unknown variables (the concentrations of both amines and CO<sub>2</sub>). The quality of the fit was evaluated using the coefficient of determination ( $0 \leq R^2 \leq 1$ ). The  $R^2$  parameter indicates the predictive quality of the model fit [119]. Coefficient of determination is a key statistical number to explain degree of linear correlation of variables. The  $R^2$  values are calculated as the proportion between the explained variance of the observed data and the variance of these data around its mean value. Using  $R^2$  as judging parameter the

optimal combination of response parameters (columns of  $X$ ) needed for estimation of the concentrations (columns of  $Y$ ) may be defined, as given below.

$$TSS = \sum_{i=1}^N (y_{i,\text{exp}} - \bar{y}_{\text{exp}})^2 \quad (2.6)$$

$$RSS = \sum_{i=1}^N (y_{i,\text{exp}} - y_{i,\text{model}})^2 \quad (2.7)$$

$$R^2 = 1 - \frac{RSS}{TSS} \quad (2.8)$$

where Eq. 2.6 - Total Sum of Squares ( $TSS$ ), Eq. 2.7 - Residual Sum of Squares ( $RSS$ ), and Eq. 2.8 - coefficient of determination ( $R^2$ ).

Regarding the  $R^2$  parameter, three characteristic values may be pointed out: the closer the  $R^2$  value is to 1, the higher is the percentage of the variance in the response variable that can be explained from measured parameters  $X$ . This means, the model with the value of  $R^2$  closer to 1 will lead to a less error of prediction in a real application with an unknown set of concentrations. In the opposite case, if the  $R^2$  parameter is approaching 0, then the model fit is too rough and it does not explain the variation of the response data around its mean value. If  $R^2$  is negative, then it is highly probable that there are either not enough PLS components to build the model or that the response parameters  $X$  used for model calibration are not correlated with the variables in question (here, vectors of the concentrations  $Y$ ).

In this chapter the  $R^2$  values were calculated for the PLS models that were constructed based on each of the physical response factors separately, as well as using their combinations, Table 2.2. For instance, when using only the combination of conductivity and density measurements, the concentration of  $\text{CO}_2$  contained in the samples may be predicted quite accurately with a deviation of 4.5 %. The model built on the combination of  $[\Omega^{-1}, \text{pH}, \text{SV}, n_D]$  allowed for the prediction of the concentrations for

Table 2.2.  $R^2$ -based predictions assessment. Numbers in first column correspond to one of the physical properties as factor for the model: 1 – conductivity ( $\Omega^{-1}$ ), 2 – pH, 3 – refractive index ( $n_D$ ), 4 – sound velocity ( $SV$ ), 5 – density ( $\rho$ ).

$X_{\text{combinations}}$	$R_{\text{AMP}}^2$	$R_{\text{PZ}}^2$	$R_{\text{CO}_2}^2$
1	0.2454	0.0320	0.8239
2	0.0469	0.0090	0.4732
3	0.3705	0.2455	-0.1907
4	0.1579	0.3252	-0.1364
5	0.0342	0.0019	0.9346
1,2	0.3055	0.0385	0.7884
1,3	0.5887	0.2423	0.9214
1,4	0.4439	0.3598	0.9080
1,5	0.4246	0.1532	0.9705
2,3	0.4968	0.2320	0.4618
2,4	0.3438	0.3553	0.4054
2,5	0.0283	-0.2250	0.9353
3,4	0.5038	0.2947	-0.1012
3,5	0.6035	0.2625	0.9746
4,5	0.3859	0.3974	0.9602
1,2,3	0.5931	0.2353	0.8945
1,2,4	0.4474	0.2921	0.9148
1,2,5	0.4183	-0.1408	0.9860
1,3,4	0.6578	0.3225	0.9127
1,3,5	0.5899	0.2159	0.9703
1,4,5	0.2942	0.3718	0.9767
2,3,4	0.5451	0.3417	0.4345
2,3,5	0.4704	0.0770	0.9743
2,4,5	0.3322	0.1880	0.9596
3,4,5	0.6283	0.3648	0.9608
1,2,3,4	0.7060	0.2961	0.9159
1,2,3,5	0.4380	-0.0300	0.9866
1,2,4,5	0.2673	0.2277	0.9873
1,3,4,5	0.5819	0.3311	0.9804
2,3,4,5	0.5107	0.1893	0.9607
1,2,3,4,5	0.5357	0.2318	0.9879

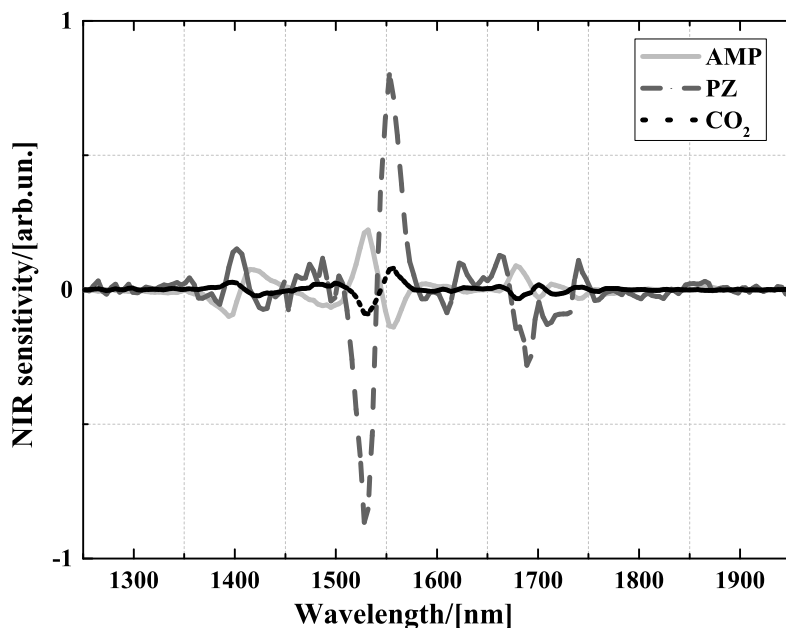


Figure 2.3. NIR absorbance sensitivity to the variation of the AMP, PZ, and CO<sub>2</sub> concentrations.

AMP and CO<sub>2</sub>, but the addition of density measurements increased the prediction quality only for CO<sub>2</sub> and decreased it for both amines. The results of the sound velocity and density measurements combined together yielded the best prediction of the PZ concentration.

### NIR spectra

Figure 2.3 shows the sensitivities  $\beta$  calculated according to the procedure described in the section 2.4.3 of this chapter.

This figure illustrates the significant role of NIR spectroscopy in the distinction between the two amines. The contribution of each component of a mixture to the absorption of the light in near infra-red region of the electromagnetic spectrum is distributed according to the wavelength of the incident radiation. In the studied liquid mixture the NIR absorption is determined by the presence of amines. The addition of spectroscopic data

Table 2.3. Symmetric mean absolute percentage error (*SMAPE*) calculated based on different sets of PLS model predictors. The combination of the physical properties and NIR spectra into the matrix of calibration measurements yields a predictive model with higher accuracy the model build using only physical properties.

	$SMAPE_{AMP}$	$SMAPE_{PZ}$	$SMAPE_{CO_2}$
Physical data	5.6%	7.3%	4.6%
NIR	2.1%	3.5%	7.3%
Physical and NIR data	2.1%	3.5%	4.3%

to the matrix of calibration measurements along with physical properties has greatly improved the accuracy of the model in predicting the PZ concentration, decreasing the error from 7.3 % to 3.5 %, as shown in Table 2.3. Prior to the calculations, the NIR absorbance spectra may be windowed to the wavelength range from 1350 nm to 1750 nm without losing valuable information.

### Physical and NIR data

The physical data and NIR signal were concatenated into a single vector for every sample from the calibration data set and for every measurement data point during in-line monitoring. The resulting information was used as an input for PLS model construction and subsequent prediction of the concentrations in the process flow. The symmetric mean absolute percentage error (*SMAPE*) was calculated to assess the accuracy of the model in predicting the concentrations of both of the amines and CO<sub>2</sub>. The *SMAPE* (as defined below) represents the average size of errors relative to the actual data and reduces the influence by outliers [131].

$$SMAPE = 100\% \cdot 2 \frac{\sum_{i=1}^N |y_{i,\text{exp}} - y_{i,\text{model}}|}{\underbrace{\sum_{i=1}^N (y_{i,\text{exp}} + y_{i,\text{model}})}_A} \quad (2.9)$$

Table 2.3 shows how combinations of data sets used for model calibration influence its accuracy. Obviously, the addition of the spectroscopy

Table 2.4. Symmetric Mean Absolute Percentage Error (*SMAPE*) of the predictions that show the performance of a PLS model when it is calibrated at one of the experimental temperatures and validated with the measurements obtained at two other temperatures.

$T, ^\circ\text{C}$	$SMAPE_{\text{AMP}}$	$SMAPE_{\text{PZ}}$	$SMAPE_{\text{CO}_2}$
25	3.8%	6.1%	6.7%
35	3.7%	7.3%	5.6%
40	3.7%	5.0%	10.6%

measurements improved the ability of the model in distinguishing between the two amines that compose the solvent blend. Whereas the addition of physical parameters measurements to the matrix with dependent parameters cuts down the error of prediction for  $\text{CO}_2$  concentration.

Table 2.4 provides the quality of the chemical component predictions if the temperature dependency is not included as a feature in the PLS model. Each row of Table 2.4 corresponds to the prediction models constructed using the source data measured at one of the following temperatures: 25, 35, and 40  $^\circ\text{C}$ . To obtain these *SMAPE* values the next action plan was employed. First, a PLS model is calibrated using measurements obtained at one of three temperatures. Then, the measurements of physical parameters and NIR signal of the same calibration samples but obtained at two other temperatures are used for the model validation. Finally, based on comparison of the real concentrations and predicted using the model, the error of prediction is calculated. The same sequence of actions is used to calculate errors of prediction for the models calibrated with measurements recorded at two other temperatures.

The optimal number of latent variables to be used by the PLS regression function for predictions was selected to be 3 for AMP, 2 for PZ, and 2 for  $\text{CO}_2$ . Such choice provides the lowest errors of prediction. The errors were estimated via the leave-one-out cross validation algorithm using the whole set of calibration samples. Standard error of the prediction (SEP), Eq. 2.10, is a common measure used to evaluate the errors of the statistical models such as PLS regression. The value of SEP shows that 68 % of deviations

fall within the limits of  $\pm 1 s_e$  for normally distributed variables.

$$s_e = \sqrt{\frac{\sum_{i=1}^n (y_{i,\text{exp}} - y_{i,\text{model}})^2}{(n - 2)}} \quad (2.10)$$

where  $n$  is number of validation tests,  $y_{i,\text{exp}}$  is a value, measured using validation methods, and  $y_{i,\text{model}}$  is a predicted value.

### 2.5.2 Pilot plant in-line monitoring

Real-time monitoring of a carbon capture process was carried out in-line at the PCC plant discussed in section 2.3.4 of this chapter. Continuous process data logging together with immediate remote access to the stored data has established the possibility for fast prediction of the amines and CO<sub>2</sub> concentrations in the solvent flow. To make the model applicable for industrial conditions the temperature range was selected based on the requirements from the PCC plant. Since every device in the chemometric setup has its own range of applicability, within which it is calibrated, some of the data points have to be excluded from the set of the dependent parameters. For instance, if the readings from the Coriolis-flow density meter start to fluctuate outside of the calibration region, it provides an unstable signal and, as a consequence, the error of the model prediction increases. It has been observed that during the non-operational state of the pilot plant, the readings from the chemometric setup provide source data outside the calibration range, which impairs the outcome of the model. Thus, the final predictions were made using data that were collected during those hours when the pilot plant was in operation. Every data point in Figure 2.4 represents the predicted concentration of either AMP, PZ or CO<sub>2</sub> at the corresponding moment in time. Thus, the developed measurement setup and the PLS model have demonstrated the feasibility of the chemometrics approach to in-line industrial PCC process monitoring.

Throughout the pilot plant campaign, samples were collected for subsequent validation of the constructed model by means of off-line analytical methods. The predictions of the concentrations of AMP and PZ were validated by means of the LC-MS method. The concentration of CO<sub>2</sub> was



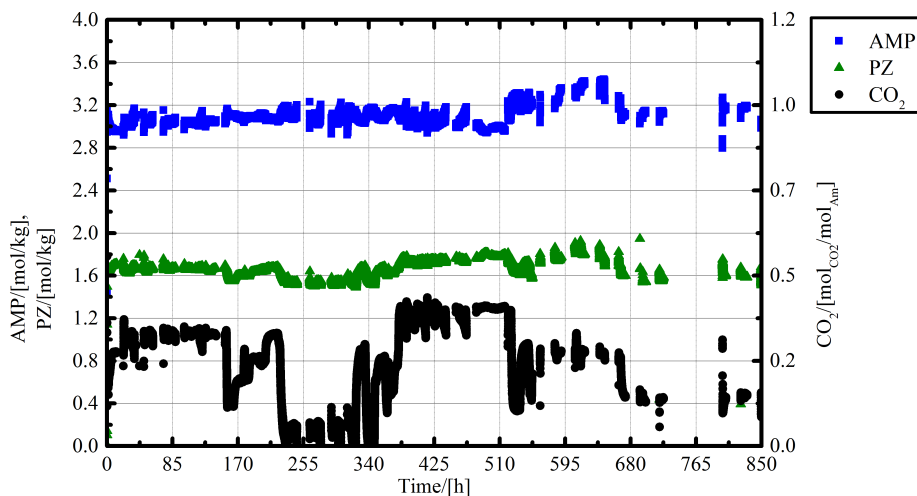


Figure 2.4. Predictions of the AMP, PZ, and  $\text{CO}_2$  concentrations in the process stream during the state of operation using the PLS model, which includes the temperature dependency. Time scale represents the hours of in-line measurements starting from the beginning of the process monitoring campaign. The complete set of the measured physical parameters and NIR spectroscopic data is used for making predictions.

measured by the hot phosphoric acid method for model validation. Demonstration of the performance of the off-line validation analytical techniques is shown in Table 2.5. On average, the bias of the results obtained using model predictions from the validation measurements is 0.05 mol/kg for the concentration of AMP and  $\text{CO}_2$ , and 0.01 mol/kg for PZ. The last row in Table 2.5 contains the average deviations between the values of the concentrations calculated using the PLS model and measured by the corresponding off-line validation technique in the samples that were withdrawn at the same date and time. The average deviations were calculated in terms of *SMAPE* and equal to  $\pm 1.8\%$ ,  $\pm 1.3\%$ , and  $\pm 3.9\%$  for the concentrations of AMP, PZ, and  $\text{CO}_2$ , respectively.

Table 2.5. Comparison of the concentrations of solvent components, calculated by the PLS model and measured by the off-line analytical validation techniques. The parameter  $s_e$  (standard error of prediction) is presented as a measure of the accuracy of the PLS models.

Time [h]	AMP <sub>PLS</sub> [mol/kg]	AMP <sub>LCMS</sub> [mol/kg]	PZ <sub>PLS</sub> [mol/kg]	PZ <sub>LCMS</sub> [mol/kg]	CO <sub>2,PLS</sub> [mol <sub>CO<sub>2</sub>]/mol<sub>Amine</sub>]</sub>	CO <sub>2,HotH<sub>3</sub>PO<sub>4</sub></sub> [mol <sub>CO<sub>2</sub>]/mol<sub>Amine</sub>]</sub>
183	3.09	2.92	1.69	1.61	0.61	0.67
225	3.24	3.02	1.57	1.59	1.30	1.14
374	3.15	3.12	1.52	1.58	0.77	0.73
564	3.14	3.07	1.63	1.64	1.33	1.30
684	3.25	3.16	1.75	1.70	1.43	1.24
754	3.11	2.90	1.55	1.55	0.63	0.61
852	3.17	2.95	1.60	1.55	0.70	0.65
$s_e$	0.19		0.06		0.12	
$SMAPE, \pm \%$	1.8		1.3		3.9	

## 2.6 Conclusions

This chapter shows the feasibility of chemometric methods for chemical process monitoring. A complex chemometric setup was constructed and tested for in-line analysis of a multiamine-based liquid solvent used for post-combustion CO<sub>2</sub> capture. The operation and control of other similar industrial processes may be improved with application of the developed approach. The PLS model was created based on the measurements of density ( $\rho$ ), conductivity ( $\Omega^{-1}$ ), sound velocity (SV), pH, refractive index ( $n_D$ ), and NIR absorbance at 25, 35, and 40 °C. The model was used to predict concentrations of AMP, PZ, and CO<sub>2</sub> within the carbon dioxide capture process at the industrial scale post combustion pilot plant. The concentrations of the chemical compounds were predicted with accuracies of  $\pm 2.1 \%$ ,  $\pm 3.5 \%$ , and  $\pm 4.3 \%$  for AMP, PZ, and CO<sub>2</sub>, respectively. The method has been validated by off-line analysis of the samples withdrawn during the measurement campaign. The deviation between the values predicted by the PLS model and the off-line technique remains untrended in time. A Raman spectroscopy analysis with more elaborated pretreatment of the spectral signal (indirect hard modeling, IHM [132]) may enhance the approach further via the introduction of chemical speciation of the solvent on a more detailed level [133]. Moreover, one of the possible future developments of the above presented setup would be its miniaturization,

rapid data treatment, and more user friendly approach of the technique. This could decrease costs of the process operation by providing fast data analysis with high accuracy.



## Chapter 3

# In-line monitoring of the CO<sub>2</sub>, MDEA, PZ concentrations in the liquid phase during high pressure CO<sub>2</sub> capture

This chapter is based on:

Kachko, A.; van der Ham, L. V.; Bakker, D.; Runstraat, A.; Nienoord, M.; Vlugt, T. J. H.; Goetheer, E. L. V. *In-line monitoring of the CO<sub>2</sub>, MDEA, PZ concentrations in liquid phase during high pressure CO<sub>2</sub> capture*. Industrial & Engineering Chemistry Research. 2016, 55, 3804-3812.

## 3.1 Introduction

### 3.1.1 Removal of CO<sub>2</sub> from natural gas

Natural gas is collected from individual wells or from a group of wells placed close to each other. Some gas wells initially produce gas at a high pressure and at a high flow rate of gas. Over time, the pressure of a gas stream decreases [134]. Gas compressors are used to raise the gas pressure for transportation. Transport companies set certain standards for the natural gas quality for feeding it through the transmission pipeline infrastructure. Special requirements should be met for the amounts of contaminant sour gases like H<sub>2</sub>S and CO<sub>2</sub> contained in natural gas streams. It is generally specified that the CO<sub>2</sub> content should not exceed 2.5 mol % [135]. Currently applied methods for CO<sub>2</sub> separation from natural gas are membrane separation and aqueous amine based absorption [136]. The chemical absorption process using aqueous MDEA solutions activated by PZ was considered in the study presented in this chapter.

The high CO<sub>2</sub> pressure in natural gas increases the solvent capacity during a CO<sub>2</sub> absorption process [137]. At a pressure of 3 MPa, micro channel experiments show that 99.94 % of CO<sub>2</sub> in the gas phase is absorbed by an aqueous MEA solution while the loading was maintained at 0.5 mol<sub>CO<sub>2</sub></sub>/mol<sub>MEA</sub> [138]. Other authors show that at a pressure of 6.5 MPa, a loading of 2.77 mol<sub>CO<sub>2</sub></sub>/mol<sub>PZ</sub> could be reached in a solution of 0.3 M PZ [139]. Nakamoto et al. [140] provide a comparative study of CO<sub>2</sub> capture at the pressures up to 7.2 MPa using an aqueous solution of MDEA, poly(ethylene glycol) dimethyl ether (DEPG), and an amine-based solvent RH-x custom-developed for high pressure conditions. In terms of capture rate and energy demand, RH-x has shown greater performance than the other two solvents, MDEA and DEPG. High pressures, up to 5 MPa, helped to increase the capture rate and the solvent capacity during the CO<sub>2</sub> absorption from natural gas by water, N-methyl-2-pyrrolidone (NMP), monoethanolamine (MEA), and MEA-NMP hybrid solutions [141].

### 3.1.2 In-line multivariate data analysis

In-line monitoring tools and methods can be introduced to improve the process quality. The discipline of extracting the qualitative and quantita-

tive information from a chemical system is known as chemometrics [71, 86]. Chemometrics combines multivariate measurements and statistical data processing. Using the methods of chemometrics to construct predictive models is a common approach in in-line process analysis [142]. The predictive model is calibrated using a set of samples with known chemical composition. The concentrations of chemical compounds in the samples are used as the matrices of independent parameters. The data set of the measurements taken from the calibration samples comprise the matrix of dependent parameters, known as predictors. Once the correlation between the two sets of data is established using statistical regression analysis, the model is ready to be used for in-line process monitoring. This approach has been proven to be suitable for in-line monitoring of a CO<sub>2</sub> absorption process by monoethanolamine (MEA) aqueous solutions in a mini-scale pilot plant [105, 113]. Geers et. al. [82] described a similar approach for characterisation of CO<sub>2</sub> absorption in neutralized  $\beta$ -alanine using Attenuated Total Reflection Fourier Transform Infra-Red Spectroscopy (ATR FTIR) as measurement method.

Chapter 2 presents application of this approach to the in-line multicomponent solvent monitoring during CO<sub>2</sub> capture at atmospheric pressure and average CO<sub>2</sub> concentrations in exhaust gases provided by power plant. The solvent used in this campaign was a blend of aqueous 2-amino-2-methyl-1-propanol (AMP) activated by PZ [91]. The method has provided predictions with accuracies of  $\pm 2.1\%$ ,  $\pm 3.5\%$ , and  $\pm 4.3\%$ , for the concentrations of AMP, PZ, and CO<sub>2</sub>, respectively. It has been reported that the degradation of MDEA-based solvents is slower than for the AMP-based solvents [143]. A solvent blend of MDEA activated by PZ is commonly used for removal of acid gases like CO<sub>2</sub> and H<sub>2</sub>S from natural gas streams [144, 145]. The importance of the Near Infra-Red spectroscopy method for differentiating between components in a mixture consisting of more than one amine has been demonstrated for real-time monitoring of CO<sub>2</sub> absorption by aqueous AMP-PZ based solvent, and is described in Chapter 2.

In this chapter provided a test case for the chemometrics approach applied to in-line monitoring of the solvent composition during a high pressure CO<sub>2</sub> capture process. The initial composition of the solvent consisted of around 35 wt. % MDEA and 5 wt. % PZ in water. Steady

states as well as transition capturing conditions were considered. The *in situ* measurements were performed using an assembled line of different analysing probes: density ( $\rho$ ), conductivity ( $\Omega$ ), pH, sound velocity (SV), refractive index ( $n_D$ ), and NIR absorption signal were recorded in the same manner as presented in Chapter 2. The obtained data were used for real-time prediction of the concentrations of both amines and CO<sub>2</sub> in a solvent stream.

## 3.2 Approach

Statistical and computational methods are used to extract important information from vast amounts of raw data generated by measurement equipment during various industrial experiments. One of the common approaches is construction of linear regression models to predict values of an unknown variable based on a matrix of measured parameters. In this study, a Partial Least Squares (PLS) regression is used to build predictive models. Prior to in-line characterisation of the solvent composition at the pilot plant, the PLS model has to be calibrated. The measurements of five physical properties ( $\rho$ , pH,  $\Omega^{-1}$ , SV,  $n_D$ ) were conducted. Monitoring of these material properties gives insight into flow conditions and helps to tailor process methodology. The matrix of dependent parameters was complemented by the NIR spectra. The temperature of the solvent flow fluctuated within the range of 21-25 °C in the lean line after heat exchanger and the cooler installed after the stripper column. According to these process conditions, all calibration measurements were performed at the minimum and maximum temperatures.

### 3.2.1 High-pressure CO<sub>2</sub> separation mini-plant

A simplified scheme of an amine treating unit is shown in Figure 3.1. The bold black lines represent high pressure pipelines and the thin green lines represent pipelines at atmospheric pressure. For this study, a small-sized version of such a process configuration was used. A mixture of CO<sub>2</sub> and N<sub>2</sub> flows was supplied to the absorber at rates of 1000 l/h and 600 l/h at steady flow conditions, respectively. The pressure and the inlet temperature of the absorber were set to 20 bar and 40 °C, respectively. In



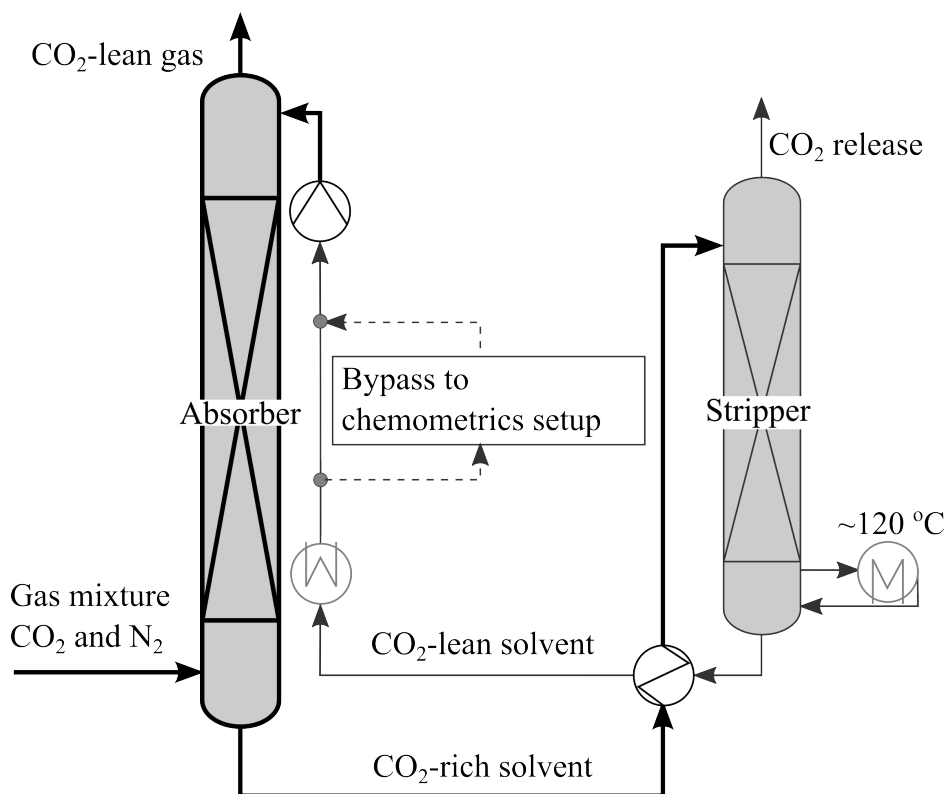


Figure 3.1. Schematic representation of a high-pressure  $\text{CO}_2$  absorption mini-plant. The thick lines denote pipelines and sections under the high pressure, up to 20 bar. The thin lines denote the low pressure, around 1.2 bar, part of the plant. The liquid solvent stream was fed to the chemometrics setup via a bypass connection from the low pressure line. The inclusion of a chemometrics setup was implemented at a location after the heat exchanger and a tube-in-tube cooler.

the stripper, the pressure and the inlet temperature were around 1.2 bar and 120 °C, respectively. Heights of the absorber column and stripper column were approximately 1.9 m and 1.3 m, respectively. The total volumes of the absorber and stripper columns were approximately 1.4 l and 0.8 l, respectively. Standard structured packing of the type DX, provided by Sulzer Chemtech, were used in both columns.

### 3.2.2 Design of experiments

In the studied experimental system the controllable factors are the concentrations of chemical reagents, temperature (T), and pressure (p). T and p are held-constant factors that influence the experiment but maintained fixed during the calibration measurements. The output variables are the measured physical parameters and the NIR signals. The mixtures under investigation are composed of three components MDEA, PZ, and CO<sub>2</sub> at 5 levels of concentrations. These 5 levels include low, base, high case plus 2 center points. This implies full factorial design of experiment  $5^{**3}$  and results in 125 experiments to perform tests that would provide information about the effects of all factors at every level even without taking into account the replication test runs. Therefore, a fractional factorial design was employed to make the sample screening procedure effective and labour saving. A description of the factorial analysis can be found in the informative textbooks by Box et al.[146] and Montgomery[147]. As it was demonstrated in Chapter 2, a  $5^{**}(3-1)$  fractional factorial scheme may be used to generate the distributions of three factors at five levels. In this case the matrix of concentrations with three columns was constructed using the *modulo* operator to compute the core combinations of the calibration samples. Assume that the columns are titled as  $M$ ,  $P$ , and  $C$ . These letters denote the levels of concentrations of MDEA, PZ, and CO<sub>2</sub> respectively (where  $M, P \in [0; 4] \cap \mathbb{N}$ ). First two columns of the matrix,  $M$  and  $P$ , are filled with unique distributions from array  $\{0, 1, 2, 3, 4\}$  over each two cells. The integers in the array span from the low to high level of concentrations through the base and both center points. The values in the third column are calculated using equation  $C = 5 - \text{mod}_5(M + P)$ . These two manipulations fill the matrix with 25 non-replicating sets of concentrations. After substitution of the integers in cells with the known concentration levels the matrix of chemical compositions for 25 calibration samples is ready, see Figure 3.2. This procedure can be done using any available spreadsheet editor by choice. The compositions of extra calibration samples were added to the matrix of samples to increase the resolution of the final PLS model in terms of concentrations. The concentrations of amines and CO<sub>2</sub> for the extra samples were obtained using the procedures of rotation and translation operators applied to the vector space of the calibration concentrations. The application of linear transformations to

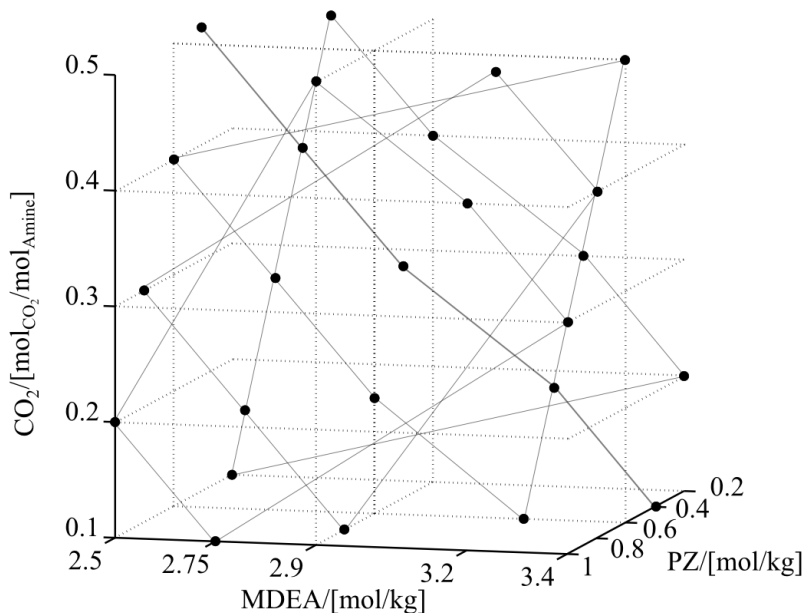


Figure 3.2. Graphical representation of the matrix of the calibration samples compositions. The three axes of the graph represent the concentrations of the three components of the studied chemical mixture. According to the fractional factorial approach, 25 samples have to be prepared to account for the first-order interactions. The symbols represent the samples. The lines are added as a guide for the eye.

construction of the matrix of concentrations for calibration samples is explained in Appendix A. These samples were used for construction of the model for prediction of the concentrations in-line.

### 3.2.3 Sample preparation

To obtain data for the PLS model construction, the measurements from calibration samples should be obtained. One part of the samples was prepared using dry ice as a source of  $\text{CO}_2$ . The other samples were prepared using stock solutions of PZ- $\text{H}_2\text{O}$  and MDEA- $\text{H}_2\text{O}$  loaded with  $\text{CO}_2$ . In case of stock solutions the loading was performed via feeding gaseous  $\text{CO}_2$

through the liquid solvent. All samples were mixed gravimetrically. The loading using dry ice was tested as an alternative method in contrary to mixing loaded stock solutions. At room temperature, CO<sub>2</sub> rapidly sublimates into the surrounding. Therefore, the gas pressure builds up fast, which could lead to the destruction of a closed container. The process of adding the dry ice pellets into the opened sample cups filled with amine solutions requires maintaining a certain dosing pace. To accelerate the sampling procedure, the required amount of amines and water were mixed in sample cups and then the dry ice pellets of needed mass were dropped into each of the solutions. Then, every sample cup was closed with a lid attached to a rubber glove. Due to elasticity the rubber gloves expanded, thus providing the necessary volume for temporary storing gaseous CO<sub>2</sub> above the solvent surface. The solution was rigorously stirred until all CO<sub>2</sub> is absorbed into the liquid. Once the samples were prepared the CO<sub>2</sub> content was checked using the boiling phosphoric acid method, as described in Chapter 2 of this thesis. A complete summary of the calibration samples compositions can be found in supporting material given in Appendix B.

### 3.2.4 Simulation of the solvent properties during the CO<sub>2</sub> capture process

An Aspen Plus model [148–150] for simulation of the CO<sub>2</sub> absorption by aqueous MDEA solutions activated by PZ was used for additional validation of the in-line predictions. The model used the unsymmetrical electrolyte NRTL (eNRTL) method and PC-SAFT equation of state to compute liquid and vapour properties, respectively. The model and equation parameters may be found in Aspen Plus rate-based MDEA+PZ model description file [151]. True species including ions were used as the components of the mixture. For liquid density, the regressions of the experimental density data of PZ-H<sub>2</sub>O [152–154], PZ-H<sub>2</sub>O-CO<sub>2</sub> [116], MDEA-H<sub>2</sub>O [155], MDEA-H<sub>2</sub>O-CO<sub>2</sub> [156] were used. The quadratic mixing rule was applied for the solvent mixtures. The Nguyen-Winter-Greiner [157] mixing rule was used for calculations of sound velocity for solvent mixtures. To obtain an additional validation method, the following procedure was elaborated: the well-known concentrations of MDEA, PZ, and CO<sub>2</sub> from calibration set of samples were used as input data for Aspen software. Based on these data, the values of  $\rho$ , pH, and SV at known  $P$  and  $T$  were calculated using

the simulation model. The concentrations of both amines and  $\text{CO}_2$  were predicted continuously in-line using the PLS model. The predicted concentrations were used as input data for Aspen Plus to calculate the values of  $\rho$ , pH, and SV for the comparison with in-line measurements. According to the correspondence between the measurements during the process and simulations, an additional indication about the validity of the PLS model can be drawn. Appendix B contains tables with all input values used for Aspen Plus calculations as well as the output results of these calculations.

### 3.3 Materials and instrumentation

#### 3.3.1 Chemicals

The amines, MDEA ( $\geq 99\%$ ) and PZ ( $\geq 99\%$ ), were purchased from Sigma Aldrich and used without further purification. The solvent for the pilot plant campaign and the calibration samples were prepared by mixing amines in the desired proportions with deionized water. The calibration samples were prepared by mixing the required portions of stock solutions of aqueous MDEA and aqueous PZ loaded with  $\text{CO}_2$ . Compressed  $\text{CO}_2$  from a gas cylinder ( $\geq 99\%$ ) and dry ice ordered from Yara in form of pellets were used to load the solutions.

#### 3.3.2 Measurement instrumentation

The measurements of five physical properties and NIR spectra comprised the matrix of dependent variables used for PLS model construction. The measurements of refractive index and sound velocity were performed using the same instruments in the laboratory environment and for the real time in-line data acquisition. The conductivity, pH, and density measurements have been performed using a different set of instruments for calibration and in-line testing campaign. All devices that took part in the in-line solvent characterisation were assembled into one compact measurement setup, see Figure 3.3.

The refractive index of the studied solutions was measured by an in-line refractometer, CM780N manufactured by Atago, calibrated in Brix % units. The NIR spectroscopy absorption signal was collected using a spectrometer (Avantes AvaSpec NIR256-2.0) and software supplied by Avantes. A

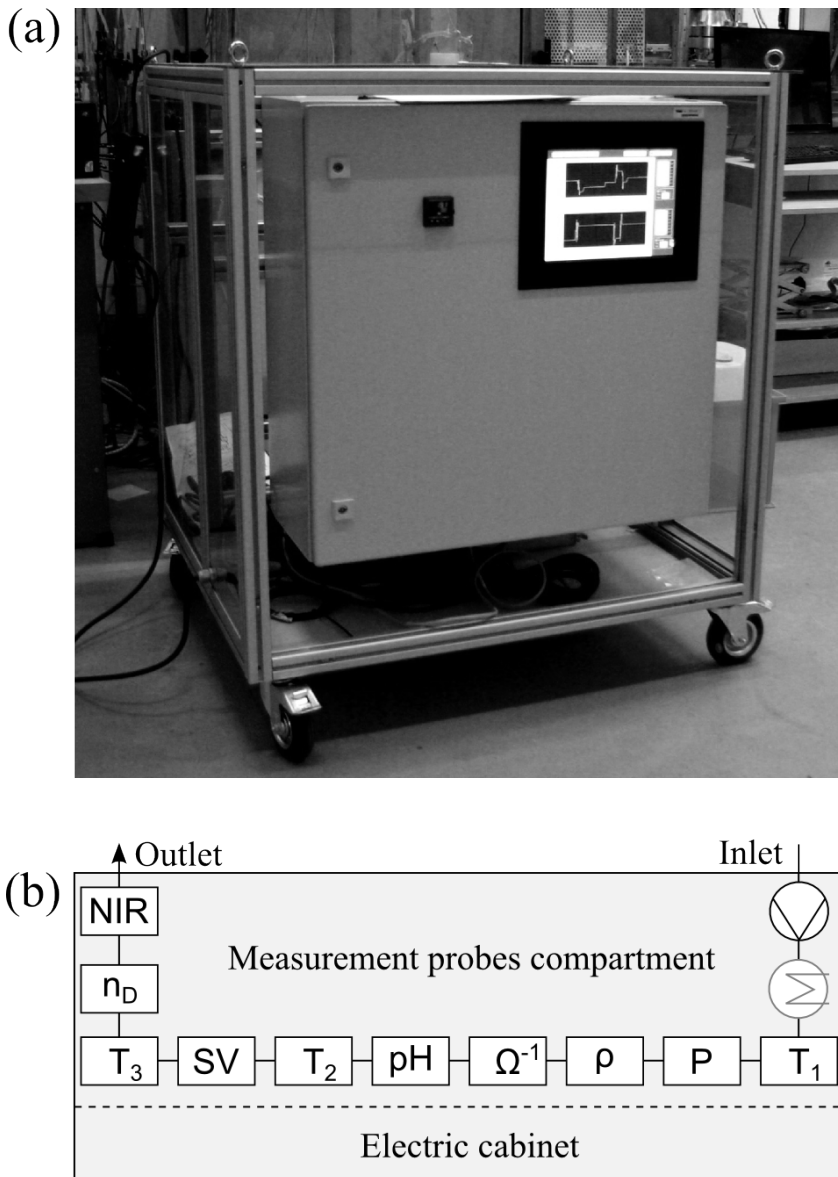


Figure 3.3. (a) Front view of the in-line chemometrics setup. The screen displays time resolved predictions of concentrations of the mixture components; (b) scheme of the instruments arrangement. The length of a frame rib is ca. 1 meter. The pump is installed on the inlet point and is used to feed the liquid to the loop. The heater is used when the temperature of the solvent has to be increased to match the calibration temperature.

tungsten halogen lamp (AvaLight-HAL) was used as an illumination light source. An immersion sensor for sound velocity measurements, Liquisonic 40-40 from SensoTech, was used to acquire measurements of the speed of sound in the liquid. The density was measured by means of: (a) an Elite MicroMotion Coriolis flow meter for in-line measurements, and (b) a DMA 4500 Anton Paar U-tube density meter during measurements in the laboratory. For in-line measurements, pH and conductivity meters from Nieuwkoop B.V were used. In the laboratory, the measurements were performed using pH and conductivity probes from Hach and ThermoScientific, respectively. A complete description of the chemometrics setup as well as specifications of the above mentioned measurement devices can be found in Chapter 2 of this thesis.

## 3.4 Calibration and validation

### 3.4.1 Data processing

The PLS regression method is a widely used tool for the multivariate data analysis [69, 122]. A PLS model explains variation in both sets of source data: independent predictors and dependent parameters, which are the concentrations of chemicals and measured solvent properties, respectively. The PLS regression model returns the vector of proportional coefficients between the concentrations and the measured physical parameters and the NIR signal. Each variable from the data matrix was mean-centered and scaled to unit variance and then used to build a predictive model. This way, the same weight is assigned to each variable (column of measured parameter), giving the equal importance before model construction. The number of latent variables (*LVs*) was selected according to the rule that adding another *LV* does not improve the quality of a constructed model. At the stage of model calibration its quality was assessed via *RMSEP*, Eq. 2.2.

Every PLS model was validated using a leave-one-out cross validation algorithm [158]. In this case, the model is being build  $n$  times, according to the number of calibration samples. One sample is excluded from a calibration matrix. This way only  $(n-1)$  samples take part in model calibration. The values of the concentrations in the omitted sample are predicted via

the constructed PLS regression model. The residuals between the predicted and experimentally measured values averaged over  $n$  runs are used for estimating the error of the predictions. Prior to the application of the PLS models to the in-line predictions the calibration samples were tested to find possible outliers. An outlier sample can be detected using method based on a comparison of the absolute difference between measured and predicted concentrations with  $4 \times \text{AAD}$  (average absolute deviation). Concentration of each component in each sample was tested using this method. In the calibration set of samples prepared in the work described in this chapter no outliers were detected. The output readings of all measurements of the physical parameters taken from the calibration samples used to build the PLS models described in this chapter are given in Appendix B. The raw NIR spectra recorded from all calibration samples are collected in tables and supplied as Supporting Information to the article by Kachko et al. [92] published in the journal *Industrial & Engineering Chemistry Research*.

NIR spectra were normalized, the baseline slope was corrected by subtraction of a line between the two ends of the spectra, also known as the ramp function. Further, a Savitzky-Golay [159] filter was applied for smoothing of the spectroscopic signal. The first order derivative was generated after smoothing to locate maxima and minima of the spectra. Two methods were used to improve the residual signal-to-noise ratio, a moving average filter and a Fast Fourier Transform (FFT) with subsequent cutting of the high frequencies. The moving average filter yielded PLS models of higher quality and was used for calibration of the models.

## 3.5 Results and discussion

### 3.5.1 In-line measurements

The chemometrics setup was hooked up to the high-pressure CO<sub>2</sub> treatment mini-plant, as shown in Figure 3.1. The solvent characterisation was performed at the lean (low pressure) stream. The monitoring of a rich stream with its especially high CO<sub>2</sub> loading is subject of the future development of the approach. The tests were run during three days. All measurement devices were calibrated before the measurement campaign.



However, some failures in operation were observed during the experiments. These failures include sudden interruption of analogue signals, receiving of impulsive or oscillatory transient signals during the data acquisition process. This leads to a deviation of the measured parameters from their calibration range. As a result, erroneous data were obtained from some devices during process monitoring, yielding wrong model predictions. Taking into account these circumstances, a new PLS model had to be constructed. Due to the established procedure, it was possible to develop a new model within short time. Changing the matrix of the calibration dataset, by removing the column with invalid measurements, leads to a different number of *LVs* and a new vector of the regression coefficients. Table 3.1 contains the parameters of the different PLS models that were eventually used for in-line concentrations prediction. The number of *LVs* and the measurement probes are the characteristic properties of each calibration model. The error of the prediction varies according to the calibration procedure. For each PLS model constructed in this work the predicted values for concentrations from the calibration data set are biased from the measured concentrations with the magnitude of -0.1 % for MDEA, 0.1 % for PZ, and -0.7 % for CO<sub>2</sub> concentration.

During the first day, the NIR signal was lost for a certain period of time due to software errors. The transition between predicted outcome values of the concentrations in Figure 3.4 is not observable due to the resolution in time. The measurements were averaged over one minute and the resulting concentrations are presented in form of continuous lines. The manipulation of the process conditions reflects on the solvent characteristics. For example, when the stripper heater was turned off at the end of the first day at 17:24 before finishing the measurements, the concentration of CO<sub>2</sub> increases in lean solvent line. On the third day of the measurement campaign the supply of CO<sub>2</sub> was started at 10:55 and then maintained in stable run, what may be seen in Figure 3.4.

### 3.5.2 Approach validation

The validation measurements were performed using ATR FTIR spectroscopy method. The method was calibrated using the same matrix of calibration samples as were used for construction of the chemometrics model. To perform the measurement was used a spectrometer, which

Table 3.1. The accuracy of the predictive models used for in-line monitoring during three days of the measurement campaign. The models are indexed in order of their application, first two correspond to first day and second and third to the other two days of measurement campaign. Sound velocity measurements were excluded from the predictive models for both amines. On the third day of the test campaign, the readings received from the conductivity probe started to interrupt and deviate from the calibration range and the model had to be recalibrated without these measurements. On the last day of the test campaign, the density probe started to supply signals oscillating at a high frequency and the sound velocity probe yielded a deformed signal, which could not be accounted for a system properties changes. This leads to the concentrations calculation based only on pH, refractive index, and NIR for the third day.

MDEA			
	<i>LVs</i>	<i>SMAPE</i> <sub>MDEA</sub> , %	Probes
Model <sub>1</sub>	4	3.0	$\rho$ , $\Omega^{-1}$ , pH, $n_D$ , NIR
Model <sub>2</sub>	4	3.1	$\rho$ , $\Omega^{-1}$ , pH, $n_D$
Model <sub>3</sub>	5	0.7	$\rho$ , pH, $n_D$ , NIR
Model <sub>4</sub>	3	1.6	pH, $n_D$ , NIR
PZ			
	<i>LVs</i>	<i>SMAPE</i> <sub>PZ</sub> , %	Probes
Model <sub>1</sub>	5	1.3	$\rho$ , $\Omega^{-1}$ , pH, $n_D$ , NIR
Model <sub>2</sub>	2	3.2	$\rho$ , $\Omega^{-1}$ , pH, $n_D$
Model <sub>3</sub>	8	0.4	$\rho$ , pH, $n_D$ , NIR
Model <sub>4</sub>	3	1.6	pH, $n_D$ , NIR
CO <sub>2</sub>			
	<i>LVs</i>	<i>SMAPE</i> <sub>CO<sub>2</sub></sub> , %	Probes
Model <sub>1</sub>	5	2.5	$\rho$ , $\Omega^{-1}$ , pH, SV, $n_D$
Model <sub>2</sub>	5	2.5	$\rho$ , $\Omega^{-1}$ , pH, SV, $n_D$
Model <sub>3</sub>	4	2.6	$\rho$ , pH, SV, $n_D$
Model <sub>4</sub>	2	3.3	pH, $n_D$ , NIR

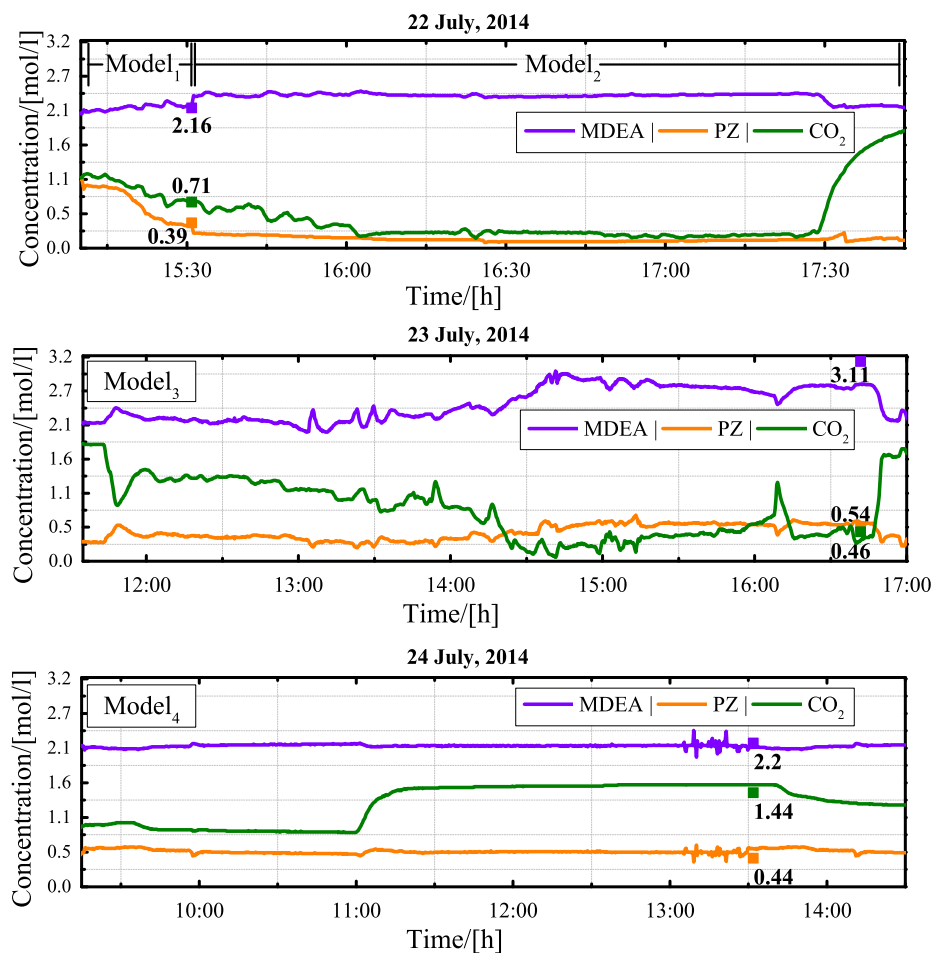


Figure 3.4. Continuous in-line predictions of the solvent composition during high pressure CO<sub>2</sub> capture process. Each figure corresponds to one day of measurements. The parameters of the models and errors are listed in Table 3.1. The points represent concentrations of the components measured using validation technique. For validation, the samples were extracted from the stream flow and analysed using ATR FTIR spectroscopy.

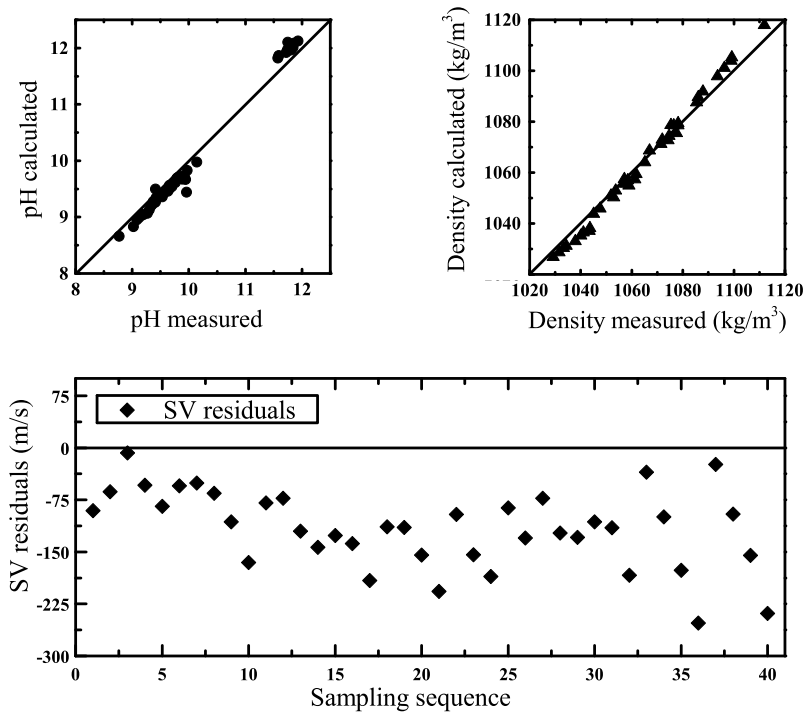


Figure 3.5. Deviation of the pH, density, and SV values calculated using Aspen Plus simulation software from measured experimentally in the laboratory. The pH, density, and SV values were measured and calculated at the temperature of 20 °C and atmospheric pressure for calibration samples. Each data point represents a sample with known content of MDEA, PZ, and CO<sub>2</sub>.

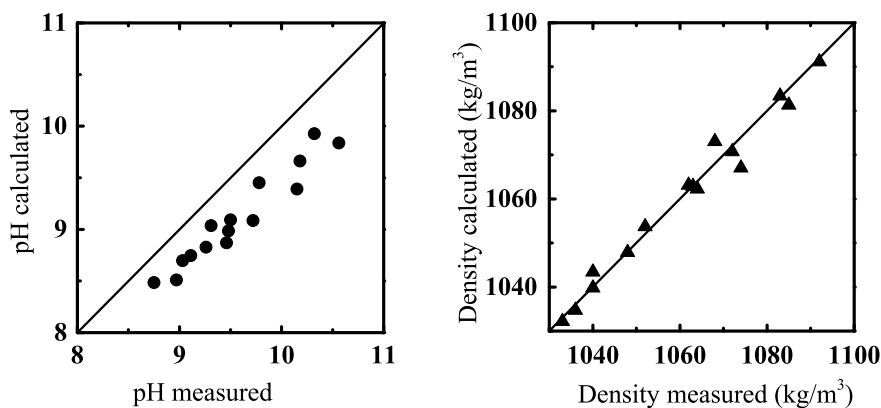


Figure 3.6. Deviation of the pH and density values calculated using Aspen Plus simulation software and measured in-line during the CO<sub>2</sub> absorption process. Each data point represents a mixture composition of a liquid solvent flowing through the chemometric measurement setup.

description is given in subsection 4.2.2 of Chapter 4. The validated concentrations are also plotted in Figure 3.4.

The accuracy of ATR FTIR method measurements are 2.9 %, 2.5 %, and 5.8 % for concentrations of MDEA, PZ, and CO<sub>2</sub>, respectively. Additional qualitative validation of the measured parameters was performed based on Aspen Plus calculations of pH, density and sound velocity of the solvents with known compositions. The calculations were performed for the same experimental pressure and temperature. In Figure 3.5, the calculated values of pH and density are plotted against the experimental measurements. In case of the SV, the residuals between calculated and measured values are presented. Both pH and density calculated using Aspen agree with the measured data. The average deviation is 0.7 % for pH and 0.1 % density. Values of the SV vary on average by 7.3 % and the deviation trend has a strong negative bias. Based on this performance the subsequent validation was carried out using only the calculations of pH and density. The differences between the measured physical properties and calculated using Aspen Plus software are larger in case of the in-line measurements due to the errors of the prediction model, Figure 3.6.

### 3.6 Conclusions

A chemometrics approach was applied to the in-line characterisation of the solvent flow during a high-pressure CO<sub>2</sub> capture process. The concentrations of MDEA, PZ, and CO<sub>2</sub> were predicted using real-time measurements of solvent properties. It was shown that once the procedure of the PLS regression construction is elaborated, it is easy to recalibrate the model with respect to the incoming data stream. The eNRTL model and PC-SAFT equation of state provide calculations of pH, density, and sound velocity of the MDEA-PZ-H<sub>2</sub>O-CO<sub>2</sub> mixture for a wide range of concentrations. These results of Aspen modelling are in agreement with experimental measurements performed in a laboratory, except for the sound velocity values.

## Chapter 4

# Comparison of Raman, NIR, and ATR FTIR spectroscopy as analytical tools for in-line monitoring of CO<sub>2</sub> concentration in an amine gas treating process

This chapter is based on:

Kachko, A.; van der Ham, L. V.; Bardow, A.; Goetheer, E. L. V.; Vlugt, T. J. H. *Comparison of Raman, NIR, and ATR FTIR spectroscopy as analytical tools for in-line monitoring of CO<sub>2</sub> concentration in an amine gas treating process*. International Journal of Greenhouse Gas Control. 2016, 47, 17-24.

## 4.1 Introduction

Scaling up PCC processes requires a detailed understanding of the problems related to industrial operation. To improve the overall process performance, process intensification is intensively investigated involving changes in the operating conditions, the use of various absorber packing material, the performance testing of different types of solvent blends, and the installation of equipment like novel pre-scrubbers or demister filters [20, 103, 160–162]. The successful introduction of new technologies may be enhanced when complemented by fast *in situ* analytical feedback [163–165]. The solvent composition and its capacity inevitably become subject to changes during testing campaigns of a chemical process. Spectroscopic techniques are widely used for qualitative and quantitative characterisation of gas, liquid, and solid materials in equilibrium as well as in transient states [83, 166–172]. Advantages of spectroscopic methods include their non-invasive nature [173], fast response time [174], and high content of chemical and molecular information about the studied media [175]. Spectroscopic techniques are highly recommended for studying both homogeneous and multiphase mixtures.

Raman spectroscopy, near infra-red (NIR) spectroscopy, and attenuated total reflectance Fourier transform infra-red spectroscopy (ATR FTIR) are three spectroscopic PATs that can be used for monitoring both the rich and lean solvent flows of a PCC process. Although UV-Vis spectroscopy has been proposed for pipeline gas content monitoring [176], it has been shown to have low correlation when used to characterize the MEA-H<sub>2</sub>O-CO<sub>2</sub> system [105, 109]. The phase transition of citric acid in suspension was monitored *in situ* using Raman spectroscopy by Caillet et al. [177]. An *in situ* Raman spectroscopy study of the hydrolysis of CCl<sub>4</sub> in hot compressed water is presented by Chen et al. [178]. These authors quantitatively analysed the production of HCl and CO<sub>2</sub> during vapour-phase hydrolysis of CCl<sub>4</sub> in a hot compressed water cell. Raman spectroscopy on the level of chemical speciation has been used for quantitative analysis of alkanolamine aqueous solutions (monoethanolamine, diethanolamine, and N-methyldiethanolamine) loaded with CO<sub>2</sub> [168]. The concentration variations of ionic components in the system of CO<sub>2</sub>-NH<sub>3</sub>-H<sub>2</sub>O was studied as function of the ratio between carbon dioxide and ammonia using Raman spectroscopy as analytical technique [179, 180]. Several research



groups have determined Raman scattering molar intensities [168, 179–181] using the association of the characteristic wavenumbers with molecular vibrations of the chemical species [182–184]. ATR FTIR spectra acquired from aqueous DEA solutions have been used to define chemical speciation at loadings up to 0.9 mole CO<sub>2</sub> per mole of DEA [185]. The applicability of in-line ATR FTIR measurements for monitoring the concentrations of MEA and CO<sub>2</sub> has been demonstrated at a pilot plant [83, 186]. The monitoring of the CO<sub>2</sub>, SO<sub>x</sub>, and neutralized  $\beta$ -alanine was performed by Geers et al. [82] via analysis of FTIR spectra during CO<sub>2</sub> capture in a test gas absorption setup. In-line monitoring of alkanolamine CO<sub>2</sub> capture has also been realised using NIR spectroscopy data and several non-spectroscopic measurement techniques in combination with chemometrics data analysis [91, 105, 113]. An extensive review by Armenta et al. [187] of vibrational spectroscopy in flow-analysis applications confirms the large demand for in-line spectroscopic tools.

A number of research groups have presented studies, containing relative assessments of the performance of two and more spectroscopic methods in different industries. The comparison of Raman and IR spectroscopy for in-line quantification of polymer melt extrusion was reported by Coates et al. [188]. These authors show that for particular experimental conditions in-line NIR was most suitable. It was pointed out that all spectroscopy techniques are suitable for real-time monitoring. In an article on experimental evaluation of Raman, FT-NIR, and FTIR methods for detection of aflatoxins in maize, Lee et al. [189] concluded that the spectroscopic methods perform well for the selected chemical process. Using the chemometrics approach, the authors determined that Raman and FTIR methods produce higher quality models than FT-NIR. Netchacovitch et al. [190] concluded that vibrational spectroscopy methods are efficient in reducing the production of dangerous waste reagents and solvents, which is possible due to the non-contact probing operation. The authors indicate the importance of the Raman and NIR methods as a PAT tool for real-time monitoring of pharmaceutical production processes. In case of biochemical industrial processes, Sivakesava et al. [191] have shown that estimation models based on FT-MIR (mid infra-red) signal possess better quality than those based on Raman and NIR signals, when applied to lactic acid fermentation. Oxygen-delignification of softwood under acidic and alkaline

regimes has been studied by Wójciak et al. [192] using spectroscopic analytical methods. Their study confirmed the potential of NIR analysis for this particular application. Although Raman and FTIR have performed well in discriminating the process conditions, their spectra acquired from the samples of kraft pulp require more thorough investigation in order to improve the correlation between characteristic peaks and the bleaching effect. Our overall conclusion, which may be drawn from the cited references, is that spectroscopic techniques are highly recommended by many research groups due to their non-invasive, fast, and robust nature. The fact that different spectroscopic techniques were preferred in different applications proves the necessity of a comparative study of these techniques for PCC. This chapter presents comparison of Raman, NIR, and ATR FTIR spectroscopy with respect to their practical applicability for in-line analysis in PCC industry.

In this chapter three spectroscopic techniques are compared for their performance for the estimation of the molecular CO<sub>2</sub> concentration in an aqueous MEA solution across a range of loadings. A custom-built Raman spectroscopy setup is presented. Data pretreatment measures to minimise the spectroscopic noise and data pollution in the Raman, NIR, and ATR FTIR spectra are discussed. The verification of the constructed PLS models has been performed using a leave-one-out cross validation algorithm.

## 4.2 Materials and equipment

### 4.2.1 Chemicals and samples

Monoethanolamine (MEA) ( $\geq 98\%$ ) was purchased from Sigma Aldrich and used as received without further purification. Aqueous solutions of amines were prepared by mixing with LC-MS grade water from Merck (LiChrosolv®) for Raman measurements and with deionized water for NIR and FTIR measurements. Compressed CO<sub>2</sub> from a gas cylinder ( $\geq 99\%$ ) was used to load the stock solutions. The number of samples and their chemical composition is listed in Table 4.1. The temperature of the mixtures during the NIR measurements was 40 °C to match the process requirements. These samples can be used for the calibration of a PLS

Table 4.1. Characteristics of the samples used for the comparison between the three spectroscopic techniques. All spectra were recorded at a constant temperature.

	MEA, wt. %	CO <sub>2</sub> , mol <sub>CO<sub>2</sub></sub> /mol <sub>MEA</sub>	Number of samples	Temperature, °C
Raman	30	0 - 0.490 ± 0.001	6	20
NIR	28	0 - 0.517 ± 0.001	6	40
ATR FTIR	30	0 - 0.513 ± 0.001	6	20

model for estimation of the CO<sub>2</sub> concentration during absorption in a PCC plant.

The absolute experimental errors of the CO<sub>2</sub> loadings were calculated using the estimation of the relative errors for the indirect measured quantities. The measurement uncertainty of the laboratory weighing scale readings was ± 0.01 g and the molar masses were used with accuracy of ± 0.01 g/mol. Aqueous solutions of MEA loaded with CO<sub>2</sub> were studied using Raman, ATR FTIR, and NIR spectroscopy. As result, PLS models were built based on the spectral information obtained by each technique.

#### 4.2.2 Raman spectroscopy

The Raman spectroscopy setup is schematically shown in Figure 4.1. For molecular vibrations excitation, a laser was used with up to 2 W output power at 532 nm wavelength from Coherent (Verdi G-Series, OPSL). A spectrograph with 300 mm focal length (SP2300) and a CCD camera with 1340x400 pixels imaging array and 20 μm x 20 μm pixels (PIXIS 400B) from Princeton Instruments were used for spectra acquisition. The width of the spectrograph entrance slit was set to 15 μm during all experiments. A diffraction grating with 1800 groves/mm has been used for spectra acquisition with resolution of 2.8 cm<sup>-1</sup>. To minimize the effect of intensity drift during experiments, the recording of each spectrum was repeated 10 times and the averaged value was used for PLS model calibration. The acquisition time of an individual spectrum was 1 second.

#### ATR FT-IR spectroscopy

An FTIR spectrometer Nicolet 6700 from Thermo Electron with the ability to collect spectra in the near-IR, mid-IR, and far-IR spectral ranges was used to validate the estimated concentrations of CO<sub>2</sub> in MEA aqueous

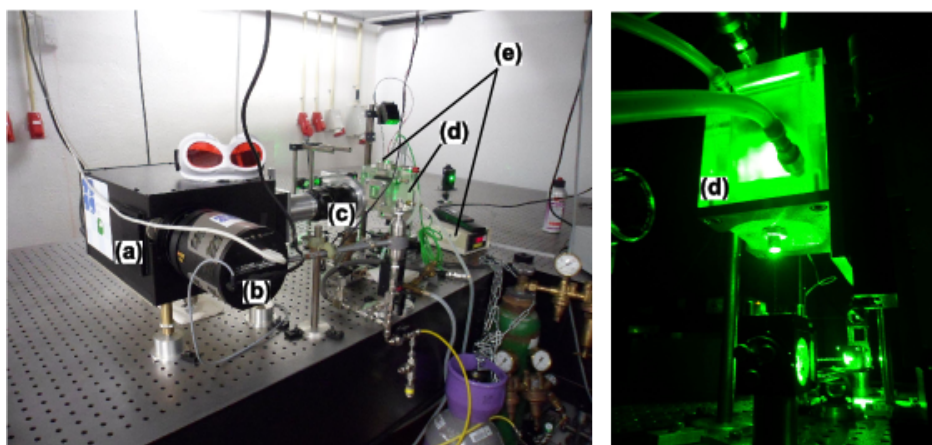
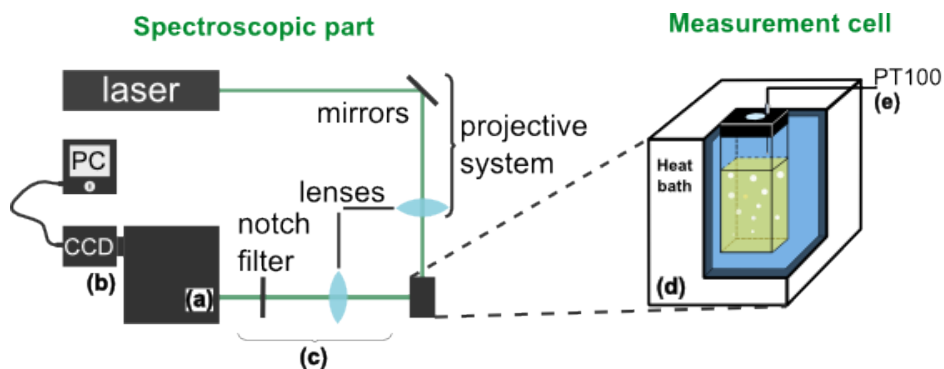


Figure 4.1. Raman spectroscopy setup. (a) - spectrograph, (b) - CCD camera, (c) - objective lens, (d) - measurement cell, (e) - PT100 resistance thermometer.

solutions. For the purposes of this study, a deuterated triglycine sulfate (DTGS) detector with a KBr protection window was used. In this combination the DTGS detectors are sensitive in the spectral region from 400 to  $6000\text{ cm}^{-1}$ , covering this way the mid-IR region [193]. The spectrometer is equipped with an MKII Golden Gate Single Reflection ATR system from Specac Ltd. The data were collected with spectral resolution of  $4\text{ cm}^{-1}$ . The FTIR spectrometer was configured to perform spectra averaging over the set of 32 scans with total collection time of 39 seconds.

### Near Infra-Red spectroscopy

The raw NIR spectroscopy signal was collected using the same equipment as described in subsection 2.3.2 of Chapter 2. The light portion from the spectral region of 1016-2044 nm was used. The spectral resolution of the spectrograph was about 3.36 nm. The spectra acquisition time was 20 ms and the averaging was performed over 10 scans. A reference spectrum was collected from deionized water. To keep the instrument calibration updated, prior to every new measurement campaign, the reference and dark spectra were freshly recorded.

## 4.3 Data processing

Each raw spectrum was subjected to data pretreatment algorithms before being used for PLS model building. Whatever spectroscopic technique is used for solvent analysis, the resulting raw data contain some parasitic components along with valuable information about the studied system. Variation of the environmental illumination, stray light, or laser intensity drift and fluorescence (in case of Raman spectroscopy) can cause signal drift, fluctuations, and background variation [194]. The intensity of the Raman spectroscopy signal is directly proportional to the concentration of the scattering species in studied media. The infra-red spectroscopy signal needs to be transformed in order to provide quantitative calculations. All spectra acquired using the ATR FTIR spectrometer were automatically displayed and stored in form of percent transmittance signal:

$$T = \frac{I}{I_0} \cdot 100\% \quad (4.1)$$

where  $I$  is the intensity of infra-red irradiation passed through the sample and  $I_0$  is the intensity of the background infra-red signal. Conventionally, published databases of the spectral libraries contain reference spectra in form of transmittance signals. According to the Beer-Lambert law [90], the absorbance scale is more useful for quantitative characterisation of the

solvent. Thus, the raw signal was converted into absorbance mode

$$A_{\text{FTIR}} = \log_{10} \left( \frac{100}{T} \right) = \log_{10} \left( \frac{I_0}{I} \right) \quad (4.2)$$

The infra-red signal recorded using the DTGS detector of the FTIR spectrometer does not require dark current correction. Both transmittance and absorbance are functions of infra-red light frequency.

Near infra-red data were converted using a similar approach. The light beam that passed through the sample and reference has been corrected for the dark signal:

$$A_{\text{NIR}} = -\log_{10} \left( \frac{I_{\text{sample}} - I_{\text{dark}}}{I_{\text{reference}} - I_{\text{dark}}} \right) \quad (4.3)$$

It is necessary to subtract accumulated dark current that originates from thermal sensitivity of the usually amorphous silicon TFT pixels of a CCD detector used to record near-IR spectra. Following the initial data collection and averaging, the acquired spectra have been subjected to background reduction via subtracting a baseline between the end points of each spectrum. Normalization of the recorded spectra has been performed using a standard normal variate method [195] applied to each spectrum after the background subtraction. Following the normalization procedure, the spectral information has been subjected to windowing by multiplication of the spectra with a rectangular function, which left the spectra untreated within the most important spectral range with respect to each spectroscopic method and set to zero the values outside the selected range. For the PLS model construction, Raman spectral signals have been taken from the region of 727-1743  $\text{cm}^{-1}$ , NIR absorbance signal contain valuable data in the region of 5280-7800  $\text{cm}^{-1}$ , and ATR FTIR transmittance data have been taken from the region of 800-1750  $\text{cm}^{-1}$ . Noise reduction using Savitzky-Golay smoothing [159] followed by taking the first derivative has provided the source data for the PLS models construction. The frame size for the smoothing filter has been selected in such a way that the choice provides the lowest error of the final outcome produced by each of the PLS model. Consequently, frame sizes were chosen to be 61, 55, and 47

for spectra from Raman, ATR FTIR, and NIR, respectively. The PLS regression models were computed using only relevant latent variables (*LVs*) for concentration estimation in case of each spectroscopic method. The selection conditions for number of *LVs* were the errors of estimation and the correlation coefficient ( $0 \leq R^2 \leq 1$ ) [119]. For each of the considered spectroscopic techniques, only 2 *LVs* were used for the models construction. The models built using 3 *LVs* produced results with *SMAPE* increased by 0.1 for Raman, 0.9 for NIR, and 0.2 for ATR FTIR data.

### 4.3.1 Method performance assessment

Regression models are a statistical method for establishing the relationships between the measured parameters and variations of independent variables, like concentration of  $\text{CO}_2$  in a solvent. Once the model is constructed, its estimation accuracy is calculated. The best performing model can be routinely applied for estimation of the concentrations of  $\text{CO}_2$ . *SMAPE*, Eq. 2.9, was calculated to assess the accuracy of the models. To provide an easily interpretable meaning to *SMAPE*, part *A* of Eq. 2.9 may be reduced to the approximated value in the following way:

$$A = \frac{\sum_{i=1}^N |y_{i,\text{exp}} - y_{i,\text{model}}|}{\sum_{i=1}^N (y_{i,\text{exp}} + y_{i,\text{model}})} \quad (4.4)$$

The value in numerator is the sum of the absolute estimation errors,  $|\Delta y_i|$ . The denominator of *A* may also be represented by  $\Delta y_i$ .

$$\begin{aligned} A &= \frac{\sum_{i=1}^N |\Delta y_i|}{\sum_{i=1}^N (y_{i,\text{exp}} + y_{i,\text{exp}} + \Delta y_i)} \\ &= \frac{\sum_{i=1}^N |\Delta y_i|}{2 \cdot \sum_{i=1}^N y_{i,\text{exp}} + \sum_{i=1}^N \Delta y_i} \end{aligned}$$

$$\begin{aligned}
&= \frac{1}{2 \cdot \frac{\sum_{i=1}^N y_{i,\text{exp}}}{\sum_{i=1}^N |\Delta y_i|} + \frac{\sum_{i=1}^N \Delta y_i}{\sum_{i=1}^N |\Delta y_i|}} \\
&= \frac{1}{2 \cdot \frac{\sum_{i=1}^N y_{i,\text{exp}}}{N} \cdot \frac{N}{\sum_{i=1}^N |\Delta y_i|} + \underbrace{\frac{\sum_{i=1}^N \Delta y_i}{N}}_{\beta} \cdot \frac{N}{\sum_{i=1}^N |\Delta y_i|}} \\
&= \frac{1}{2 \cdot \frac{1}{\langle |\Delta y_i| \rangle} \cdot \left( \langle y_{i,\text{exp}} \rangle + \frac{\beta}{2} \right)} \tag{4.5}
\end{aligned}$$

Assuming that the average absolute error of the observed parameter is a fraction of its measured value  $\langle |\Delta y_i| \rangle = \alpha \cdot \langle y_{i,\text{exp}} \rangle$  and  $\alpha \neq 0$ ,  $\beta \ll \langle y_{i,\text{exp}} \rangle$ , the following may be concluded:

$$A \sim \frac{\alpha}{2}, \tag{4.6}$$

The parameter  $\alpha$  is a mean absolute relative difference [196] for a particular PLS model. The use of *SMAPE* reduces the disturbance by outliers and its value does not depend on direction of bias between experimental measurement and its estimated value[131]. Thus, it provides an intuitive way to describe the magnitude of the errors between the estimated and measured value. Using the result of the reduction 4.6 of Eq. 2.9 helps to estimate the error of a PLS model.

## 4.4 Results and discussion

The spectra of the gradually loaded samples are shown in Figure 4.2. Each subfigure shows a set of the spectroscopic signals recorded using one of the three spectroscopy techniques. Every line corresponds to a measurement obtained from a sample with different CO<sub>2</sub> loading. The displayed spectra are normalized and windowed to the higher energetic spectroscopic



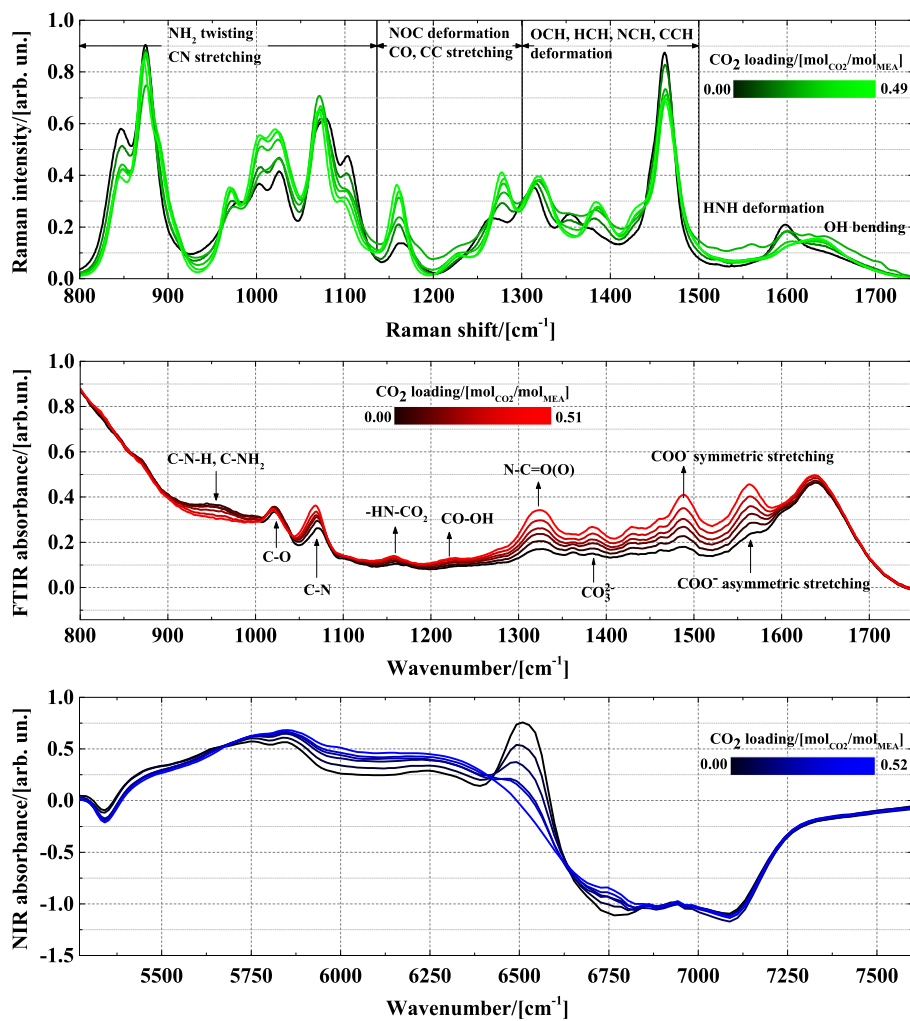


Figure 4.2. Raman, NIR, and ART FTIR spectra recorded from aqueous MEA solutions gradually loaded with CO<sub>2</sub>. The spectra were subjected to baseline correction, normalization and windowing. Every spectrum represents the solution of aqueous MEA containing CO<sub>2</sub> within the assigned range.

fingerprint region of MEA, which contains most of the information about changes in the studied chemical mixture of MEA-H<sub>2</sub>O-CO<sub>2</sub>. The positions of the characteristic scattering and absorption bands are identifiable and assigned to the vibrations of the molecular groups according to literature [168, 184, 186, 197–199]. According to Figure 4.2, Raman and ATR FTR measurements provide spectroscopic responses with rich information content about the studied media.

The robustness of a PLS estimation depends on the calibration procedure and is determined by the number of training samples and the resolution with respect to concentrations of CO<sub>2</sub>. Figure 4.3 shows the errors of the PLS models as a functions of the number of the samples used for model calibration. To obtain the first point in Figure 4.3, the matrix with the source data for the model was comprised of the measurements from three samples with different CO<sub>2</sub> loadings. One sample with maximum loading, one with minimum loading, and one from the center of calibration range were used to calibrate and validate the estimation model. Following the leave-one-out cross-validation algorithm [158], the PLS model was calibrated three times based on two out of three samples leaving out the rest. The PLS method produced regression coefficients, which then were applied to estimate the CO<sub>2</sub> concentration in the omitted sample. For the following runs, more samples were added to the calibration set of the model. The errors in terms of *SMAPE* were calculated and their averages are presented in Figure 4.3. It may be concluded that NIR absorbance signal provides estimation models of higher quality than the other two if the same number of calibration samples is available. More calibration samples lead to a better resolution in terms of the concentration, which leads to an increase in the quality of each model.

In Figure 4.4, estimated concentrations of CO<sub>2</sub> are plotted as a function of measured concentrations. The PLS regression models for each of the spectroscopic techniques were calibrated based on the measurements from maximum number of the samples.

The results of the current study reveal that for the same number of samples NIR spectroscopy provides an estimation chemometrics model with errors lower than when using Raman and ATR FTIR. The errors of the models that were built using the Raman and ATR FTIR data are comparable and are larger than that of NIR. Increasing of the number

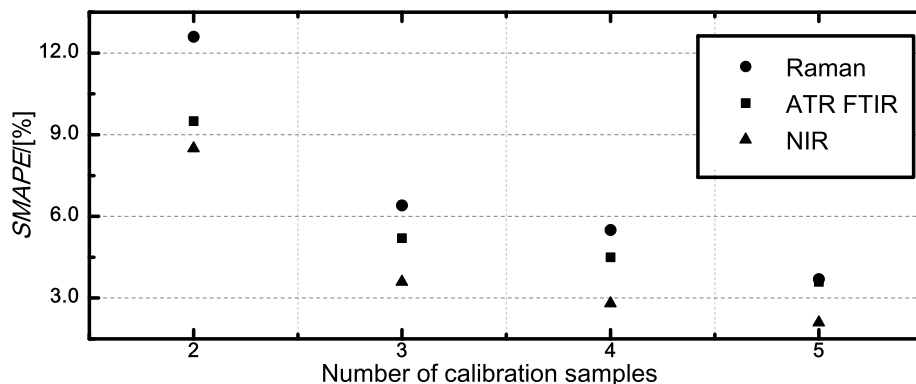


Figure 4.3. Errors of the estimation models built based on the signals of Raman, NIR, and ATR FTIR spectroscopy as functions of the number of samples used in a calibration set.

of samples included in calibration data set leads to improvement of the estimations by models constructed using spectroscopic data. Due to its linearity, the PLS regression is especially useful in the region of the  $\text{CO}_2$  loading below  $0.5 \text{ mol}_{\text{CO}_2}/\text{mol}_{\text{MEA}}$ . At these loadings,  $\text{CO}_2$  almost completely captured by a solvent as a result of the amine carbamate formation. The concentration of the carbamate increases almost linearly with the  $\text{CO}_2$  loading. At the higher loadings, the carbamate concentration decreases and  $\text{CO}_2$  transforms into bicarbonate [200]. This change of the chemical reaction equilibrium implies nonlinearity, which the PLS approach can not cover and the estimation of the  $\text{CO}_2$  concentration gets worse. This is clearly shown in Figure 4.4.

Table 4.2 shows a summary of the comparative values of the three spectroscopic techniques in application to  $\text{CO}_2$  absorption by aqueous MEA. The spectral data pre-treatment measures helped to greatly decrease the errors of estimation for models built using Raman and NIR spectra and took a small, although positive, effect on the model built using ATR FTIR spectra. In terms of  $s_e$  the estimation models built using data from all three techniques possess almost the same quality. Among three methods, NIR spectroscopy requires the shortest spectra acquisition times providing the fastest measurement response. Raman and ATR FTIR spectroscopy methods are more suitable for quantitative speciation of

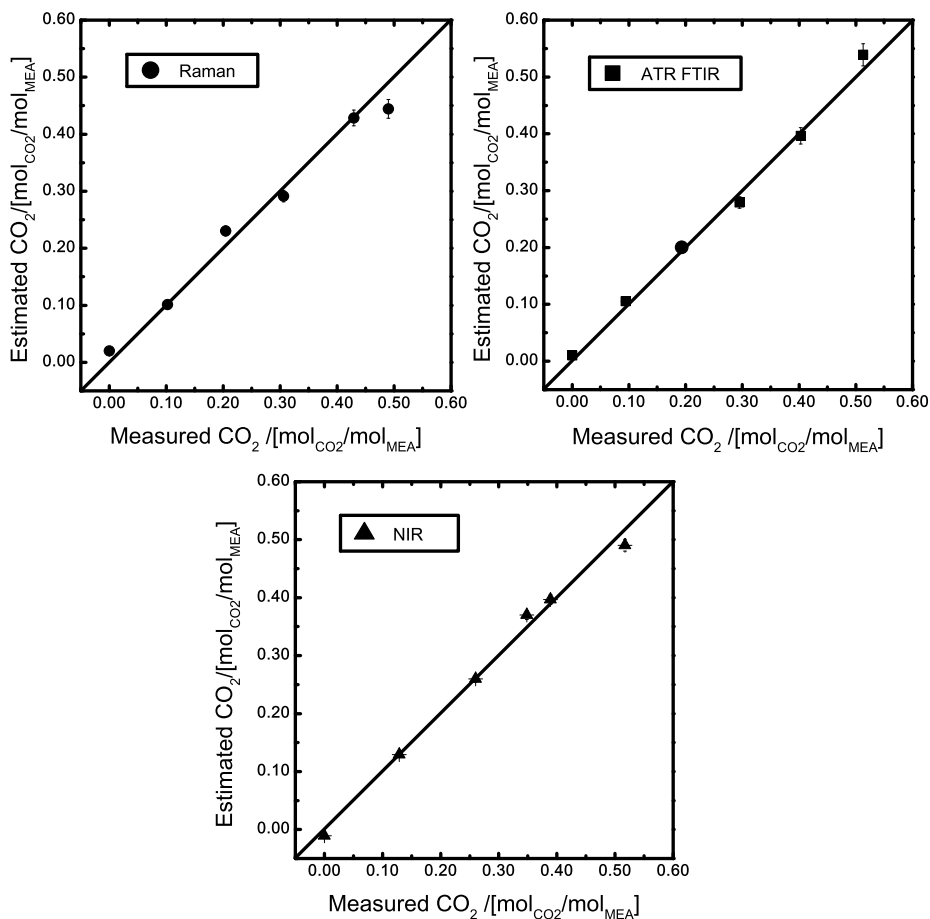


Figure 4.4. Measured versus estimated CO<sub>2</sub> concentrations using three spectroscopic methods: Raman, NIR, ATR FTIR.

chemical mixtures. The NIR spectra contain broad overlapping absorption bands and are not selective. Estimated costs for the three techniques show that NIR instrument is more favourable in terms of cost reduction. This fact in combination with accuracies of estimation of the CO<sub>2</sub> concentrations makes NIR spectroscopy most useful for the chosen application.

Modern developments of the spectroscopic instrumentation industry provide equal opportunities for all three considered methods to be used for

Table 4.2. Vibrational spectroscopy methods performance before/after spectra pretreatment (windowing, normalization, SG with 1st derivative). The table contains important qualities for assessment of all three techniques. The  $s_e$  value have been calculated using Eq. 2.10.

	Raman	ATR FTIR	NIR
$SMAPE$ , %	46.5/3.6	4.0/3.6	20.4/2.1
$s_e$ , mol <sub>CO<sub>2</sub></sub> /mol <sub>MEA</sub>	0.15/0.01	0.02/0.02	0.10/0.01
Measurement frequency	1 - 6 min <sup>-1</sup>	1 - 2 min <sup>-1</sup>	2 - 5 s <sup>-1</sup>
Chemical speciation	Possible	Possible	Difficult
Price, EUR	100,000 <sup>(this work)</sup>	100,000 [113]	20,000 [113]

both off-line laboratory applications and for on-site measurements [201–203]. However, during an industrial process solvent degradation may lead to appearance of such spectroscopic effects like fluorescence, self-absorption, weakening of the signal intensity. Eventually, the solvent turns yellow due to the operation conditions and the signal-to-noise ratio is getting worse [204]. This problem may be solved via both spectroscopy data treatment and adjusting instrumentation, for example by increasing the power of the light emitting sources or using immersion probes [205–208] suitable for real-time online diagnostics. The monitoring of the carbon dioxide concentrations in the solvent flow during PCC process may be performed effectively using NIR spectroscopy. All three spectroscopic techniques that were considered in this chapter provide rich information about the solvent. The comparative assessment may be developed further for the case of the simultaneous analysis of the concentrations of both MEA and CO<sub>2</sub>. When the CO<sub>2</sub> loading exceeds 0.5 mol<sub>CO<sub>2</sub></sub>/mol<sub>MEA</sub> the species distribution is a non-linear function with respect to the CO<sub>2</sub> loading and the PLS regression method delivers poor results due to its inherent linear origin. It might be beneficial to divide the chemical speciation into the regions of the linear behaviour and build the PLS models within the limits of these regions. During CO<sub>2</sub> absorption experiments using the Raman spectroscopy setup, the effect of the solvent thermal degradation was clearly observed. The effect has manifested itself as color change during the gradual heating of the solvent from room temperature up to 95 °C. For this particular Raman spectroscopy setup, the fluorescence background was notably observable and the transition from fresh to degraded solvent can be characterised *in situ*. This suggests that Raman spectroscopy can

be a useful technology for solvent degradation monitoring.

The CO<sub>2</sub> concentrations fluctuate within different ranges in a real industrial absorption process. The process temperature and pressure usually do not stay constant and vary according to the settings. If no reclaiming is being done to counter solvent degradation, it might also be necessary to take the impurities into account. To cope with these effects and increase accuracy of estimation, extra samples may be added to the calibration set.

## 4.5 Conclusions

Raman, ATR FTIR, and NIR spectroscopic techniques were quantitatively compared based on their predictive performance in case of aqueous MEA solutions loaded with CO<sub>2</sub>. The assessment is extended to such factors as: data pretreatment effort, acquisition time, equipment cost, and possibility for in-line installation. During the comparison, statistical models have been build to estimate CO<sub>2</sub> concentrations in the studied samples. It has been shown that the increased number of samples provides higher accuracy of estimation. The errors decrease with the trend that suggest further improvements of the approach. The NIR data has provided the estimations with the best accuracy when the same number of calibration samples are used for model construction. It is expected that the spectroscopic methods compared in this chapter are applicable for characterisation of the liquid solvents in similar gas capturing processes, like natural gas treatment.

# Appendix A

## Linear transformations for the screening procedure of samples

In general form, the system of equations for transformation of a vector with coordinates  $(x, y, z)$  to the vector  $(x^*, y^*, z^*)$  in a 3D space is presented by:

$$\begin{cases} x^* = \alpha_1 x + \beta_1 y + \gamma_1 z + \lambda \\ y^* = \alpha_2 x + \beta_2 y + \gamma_2 z + \mu \\ z^* = \alpha_3 x + \beta_3 y + \gamma_3 z + \nu \end{cases} \quad (\text{A.1})$$

where  $(\lambda, \mu, \nu)$  are the coordinates of a translation vector. For convenience, this system of equations is presented in matrix form using homogeneous coordinates ([212], pp. 35-36)

$$[x^* \ y^* \ z^* \ 1] = [x \ y \ z \ 1] [M] \quad (\text{A.2})$$

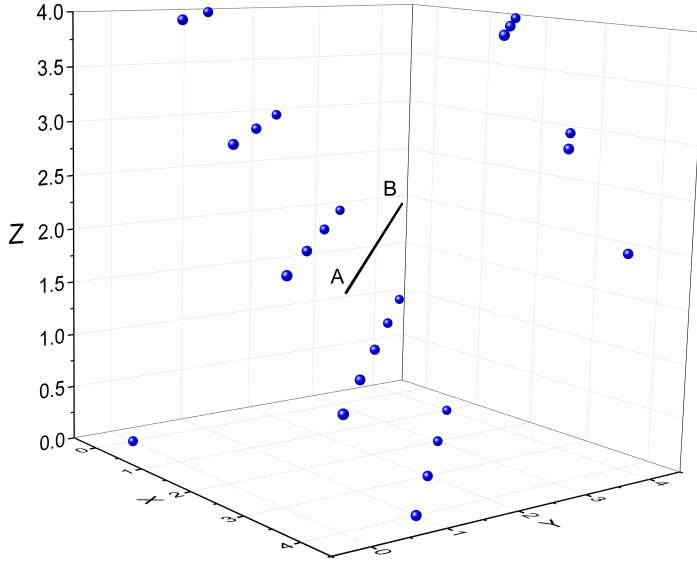


Figure A.1. The 3D representation of mixture compositions of the core set of calibration samples. Coordinate numbers 0, 1, 2, 3, and 4 correspond to low, first intermediate, base, second intermediate, and high level of concentrations of MDEA, PZ, and  $\text{CO}_2$ . Blue balls are the samples and line AB is the axis of rotation.

where  $[M]$  is the matrix of transformation coefficients

$$[M] = \begin{bmatrix} \alpha_1 & \beta_1 & \gamma_1 & 0 \\ \alpha_2 & \beta_2 & \gamma_2 & 0 \\ \alpha_3 & \beta_3 & \gamma_3 & 0 \\ \lambda & \mu & \nu & 1 \end{bmatrix} \quad (\text{A.3})$$

To obtain the new set of augmenting concentrations, the affine transformations of translation ( $[T]$ ) and rotation ( $[R]$ ) ([212], pp. 20-22) were applied to the vector space of concentrations obtained using fractional factorial design. For clarity, the core concentrations of both amines and  $\text{CO}_2$  calculated using the procedure described in subsection 3.2.2 of Chapter 3 are plotted in a 3D space using substitution of the real concentration values by numbers 0, 1, 2, 3, and 4, Figure A.1.



The rotation is performed around the line **AB** by the angle  $\theta = \pi$ . A directing vector **r** with the origin and tail in the points with coordinates  $[x_o; y_o; z_o]=[2; 2; 2]$  and  $[x_t; y_t; z_t]=[0; 4; 2]$  is selected. It is easier to rotate an object in the 3D space around one of the coordinate axis. In this work the OY axis is selected. To perform rotation around OY axis the vector **r** should be aligned with it. The alignment operation is performed in two steps: translation of the vector **r** so that its origin is nested in the origin of the coordinate system and rotation around OZ axis by angle  $\phi$  in the direction towards OY axis. Since vector **r** is parallel to the XOY plane, only one rotation is needed to align it with OY axis. When choosing the coordinates of the translation vector in this application as  $[2; 2; 2]$  for its origin and  $[0; 0; 0]$  for its tail, one can write the operator of translation as

$$[T] = \begin{bmatrix} 1 & 0 & 0 & 0 \\ 0 & 1 & 0 & 0 \\ 0 & 0 & 1 & 0 \\ -2 & -2 & -2 & 1 \end{bmatrix} \quad (\text{A.4})$$

The coordinates of the vector **r** normalized to the vector with unit length  $\hat{e}$  ([213], p. 18) are calculated by

$$\hat{e} = \frac{[(x_t - x_o); (y_t - y_o); (z_t - z_o)]}{\sqrt{(x_t - x_o)^2 + (y_t - y_o)^2 + (z_t - z_o)^2}} \quad (\text{A.5})$$

$$[e_x; e_y; e_z] = \left[ -\frac{1}{\sqrt{2}}; \frac{1}{\sqrt{2}}; 0 \right]$$

Now it is easy to determine the angle of rotation  $\phi$  around OZ axis

$$\cos \phi = \frac{e_y}{\|\hat{e}\|} = \frac{1}{\sqrt{2}} \quad \Rightarrow \quad \phi = \frac{\pi}{4} \quad (\text{A.6})$$

Thus, the operator of rotation around OZ axis is

$$[R_Z] = \begin{bmatrix} \cos \phi & -\sin \phi & 0 & 0 \\ \sin \phi & \cos \phi & 0 & 0 \\ 0 & 0 & 1 & 0 \\ 0 & 0 & 0 & 1 \end{bmatrix} = \begin{bmatrix} \frac{\sqrt{2}}{2} & -\frac{\sqrt{2}}{2} & 0 & 0 \\ \frac{\sqrt{2}}{2} & \frac{\sqrt{2}}{2} & 0 & 0 \\ 0 & 0 & 1 & 0 \\ 0 & 0 & 0 & 1 \end{bmatrix} \quad (\text{A.7})$$

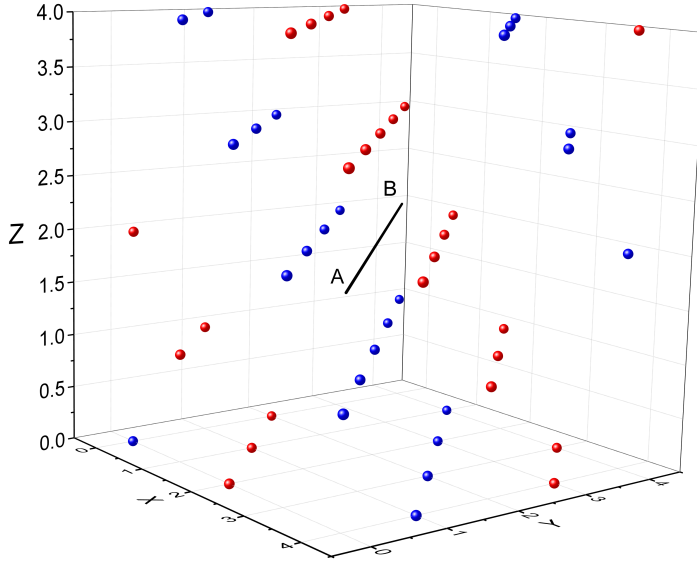


Figure A.2. The complete set of calibration samples. Every ball represents a mixture of three chemical components: MDEA, PZ, and  $\text{CO}_2$ . The coordinates are directly related to the concentrations of the chemicals that should be mixed to prepare a sample. Blue balls denote the samples from core combinations, red balls are the augmenting samples, and line AB is the axis of rotation.

Once these operations have been performed the object can be rotated around OY axis by the angle  $\theta$  using the rotation operator  $[R_Y]$

$$[R_Y] = \begin{bmatrix} \cos \theta & 0 & \sin \theta & 0 \\ 0 & 1 & 0 & 0 \\ -\sin \theta & 0 & \cos \theta & 0 \\ 0 & 0 & 0 & 1 \end{bmatrix} = \begin{bmatrix} -1 & 0 & 0 & 0 \\ 0 & 1 & 0 & 0 \\ 0 & 0 & -1 & 0 \\ 0 & 0 & 0 & 1 \end{bmatrix} \quad (\text{A.8})$$

To return back to the original coordinate space, the first two transformations should be inverted. The inverted matrices  $[R_Z]^{-1}$  and  $[T]^{-1}$  are obtained by substitution values  $-\phi$  and  $(-\lambda, -\mu, -\nu)$  in place of  $\phi$  and  $(\lambda, \mu, \nu)$  in matrices A.7 and A.4.

In the work presented in Chapter 3 the coordinate axes are the concentrations of MDEA, PZ, and  $\text{CO}_2$  for X, Y, and Z axis respectively.

Sequential execution of the described operations provides the needed rotation around the line **AB**. Thus, the matrix with transformation coefficients can be expressed as

$$[M] = [T][R_Z][R_Y][R_Z]^{-1}[T]^{-1} \quad (\text{A.9})$$

Combining the equations A.2 and A.9, the sought coordinates for extra samples can be calculated. The final set of samples is presented in Figure A.2.



## Appendix B

# Calibration measurements

In the next sections, all important data from the calibration measurements used for the models construction for the AMP-PZ-CO<sub>2</sub> and MDEA-PZ-CO<sub>2</sub> campaigns is presented. In each section, the tables are organized in the following order: the table with concentrations of chemicals in calibration samples is placed first, then the tables with values of density, conductivity, pH, sound velocity, and refractive index respectively, and NIR spectroscopy signals for each of the calibration samples is provided last.

The sample preparation procedure implies mixing amines, water, and CO<sub>2</sub> in proportions provided by the design of experiments. The stock binary solutions of each amine with H<sub>2</sub>O were loaded with CO<sub>2</sub>. This CO<sub>2</sub> was added to the solutions either by feeding it from gas bottle through the liquid solvent or using dry ice pellets. The required amounts of solvents were mixed in a sample cup and the pure chemical components were added to the cup when the concentrations of either of them has to be increased to the desired value. The mixing procedure has been conducted gravimetrically using scales with an accuracy of  $\pm 0.01$  g.

Partial Least Square (PLS) models were constructed to provide the regression lines between the concentrations of the used chemicals and readings of measurement devices. In this work, six measurement devices were employed to construct a setup for real-time in-line monitoring of solvent composition. The properties that were monitored are density, pH, conductivity, sound velocity, refractive index, and Near Infra-Red (NIR) absorbance signal. All calibration measurements were conducted in a labo-

ratory. For the system of AMP-PZ-CO<sub>2</sub> the measurements were obtained at 25°C, 35°C, and 40°C to provide a predictive model that takes into account a temperature resolution. For the same reason, the measurements were performed at 20°C and 25°C for the system of MDEA-PZ-CO<sub>2</sub>.

## B.1 The AMP-PZ-H<sub>2</sub>O-CO<sub>2</sub> system

### B.1.1 Concentrations of chemicals in calibration samples

Table B.1. Calibration samples notation and concentrations of each component - AMP, PZ, and CO<sub>2</sub>. The samples were used for PLS model construction.

Sample number	AMP, mol/kg	PZ, mol/kg	CO <sub>2</sub> , mol <sub>CO<sub>2</sub></sub> /mol <sub>Amine</sub>
s1	1.99	0.97	0.00
s2	2.01	1.47	0.00
s4	2.00	0.98	0.20
s5	1.97	1.67	0.19
s7	1.99	0.97	0.50
s8	2.00	1.46	0.50
s9	1.96	1.94	0.36
s10	2.51	1.23	0.10
s11	2.52	1.47	0.10
s12	2.51	1.72	0.10
s13	2.47	1.35	0.19
s14	2.52	1.47	0.20
s15	2.51	1.71	0.20
s16	2.50	1.24	0.35
s17	2.51	1.47	0.35
s18	2.51	1.72	0.35
s19	2.97	0.97	0.00
s20	3.01	1.47	0.00
s22	3.00	1.23	0.10
s23	3.01	1.48	0.10
s24	3.02	1.71	0.10
s25	3.10	0.98	0.19
s26	3.01	1.23	0.20
s27	3.01	1.47	0.20
s28	3.03	1.71	0.20
s29	2.93	1.91	0.20
s30	3.01	1.22	0.35
s32	3.00	1.75	0.35
s33	3.08	1.03	0.46
s36	3.26	1.23	0.10
s38	3.26	1.71	0.10
s39	3.26	1.22	0.20
s41	3.26	1.72	0.20
s42	3.25	1.25	0.35
s43	3.25	1.50	0.35
s44	3.25	1.75	0.35
s45	3.51	0.98	0.00
s46	3.51	1.47	0.00
s47	3.51	1.96	0.00
s48	3.51	0.98	0.20
s49	3.51	1.47	0.20
s50	3.50	1.97	0.20

## B.1.2 Laboratory measurements of calibration samples

Table B.2. Values of the measurements of the first five properties obtained from calibration samples of the AMP-PZ-CO<sub>2</sub> mixtures at 25°C.

Sample number	Density, kg/m <sup>3</sup>	Conductivity, mS/cm	pH	Sound velocity, m/s	Refractive index, brix
s1	1005.1	0.47	12.50	1700.4	25.8
s2	1009.0	0.32	12.54	1736.4	30.8
s4	1031.2	7.74	10.73	1711.5	29.4
s5	1039.0	5.74	10.86	1760.7	35.9
s7	1069.2	14.88	9.88	1720.6	34.7
s8	1080.0	11.58	9.95	1764.6	40.1
s9	1072.5	8.00	10.36	1795.2	42.7
s10	1023.3	3.63	11.17	1748.7	34.0
s11	1026.0	3.31	11.16	1765.3	36.1
s12	1028.6	2.98	11.21	1780.5	38.4
s13	1039.5	5.68	10.82	1764.8	36.8
s14	1042.8	5.43	10.84	1775.6	38.5
s15	1045.7	4.91	10.81	1790.9	40.7
s16	1062.1	8.91	10.40	1770.6	39.3
s17	1066.3	7.75	10.40	1789.4	41.7
s18	1070.8	6.73	10.44	1808.3	44.3
s19	1006.1	0.24	12.63	1745.2	33.6
s20	1009.4	0.25	12.82	1768.6	37.9
s22	1025.4	3.05	11.13	1770.3	37.6
s23	1028.2	2.74	11.23	1784.5	40.0
s24	1030.6	2.50	11.26	1794.4	41.9
s25	1039.2	5.40	10.83	1768.7	38.1
s26	1043.4	5.04	10.78	1780.6	39.9
s27	1046.4	4.53	10.85	1795.1	42.2
s28	1049.2	3.90	10.86	1808.6	44.5
s29	1051.6	3.73	10.93	1816.7	45.6
s30	1068.2	7.25	10.40	1796.2	43.3
s32	1062.1	4.85	10.68	1815.4	45.6
s33	1081.7	9.42	10.09	1789.0	43.9
s36	1026.6	2.85	11.20	1775.6	39.1
s38	1032.2	2.11	11.26	1800.8	44.6
s39	1044.8	4.55	10.78	1788.6	41.7
s41	1050.9	3.56	10.84	1815.0	46.2
s42	1050.7	10.47	9.14	1748.2	35.9
s43	1069.5	5.20	10.51	1818.7	46.8
s44	1086.0	8.08	10.11	1800.7	46.3
s45	1005.5	0.17	12.72	1754.1	37.0
s46	1008.6	0.11	12.74	1771.2	41.2
s47	1011.5	0.06	12.78	1783.3	45.3
s48	1043.7	4.75	10.78	1781.9	41.3
s49	1049.5	3.65	10.85	1806.3	45.6
s50	1056.1	2.72	10.90	1827.2	50.0



Table B.3. Values of the measurements of the first five properties obtained from calibration samples of the AMP-PZ-CO<sub>2</sub> mixtures at 35°C.

Sample number	Density, kg/m <sup>3</sup>	Conductivity, mS/cm	pH	Sound velocity, m/s	Refractive index, brix
s1	999.7	0.53	12.62	1689.9	26.1
s2	1003.3	0.36	12.72	1719.4	31.1
s4	1026.1	8.80	10.68	1702.8	29.7
s5	1033.3	6.70	10.73	1745.3	36.2
s7	1063.1	16.70	9.87	1718.2	35.4
s8	1074.7	13.32	9.90	1757.5	40.6
s9	1067.4	9.50	10.31	1776.7	42.6
s10	1017.8	4.22	11.10	1731.2	34.1
s11	1020.2	3.94	11.17	1742.3	36.2
s12	1022.7	3.64	11.15	1758.6	38.7
s13	1033.7	6.74	10.81	1747.6	37.0
s14	1036.9	6.48	10.80	1755.5	38.5
s15	1039.7	5.90	10.77	1770.6	41.0
s16	1056.5	10.4	10.32	1758.4	39.5
s17	1060.9	9.30	10.30	1774.7	42.1
s18	1065.4	8.17	10.41	1791.5	44.6
s19	999.7	0.28	12.73	1722.4	33.5
s20	1003.3	0.31	12.75	1737.1	38.4
s22	1019.4	3.70	11.12	1747.2	38.1
s23	1022.1	3.32	11.13	1748.9	39.0
s24	1024.0	3.07	11.20	1769.1	42.6
s25	1033.5	6.5	10.78	1749.5	38.4
s26	1037.4	6.12	10.74	1759.8	36.4
s27	1040.5	5.54	10.75	1773.0	43.1
s28	1043.5	4.87	10.80	1782.6	45.0
s29	1045.6	4.70	10.86	1788.1	45.8
s30	1062.7	8.60	10.30	1775.5	43.6
s32	1055.9	6.08	10.60	1792.8	45.6
s33	1076.8	11.36	10.00	1771.8	43.7
s36	1020.3	3.47	11.16	1752.0	39.6
s38	1025.3	2.70	11.18	1785.5	44.7
s39	1038.7	5.58	10.75	1764.6	42.8
s41	1045.1	4.51	10.84	1787.5	46.5
s42	1044.9	10.58	10.42	1734.0	35.8
s43	1063.7	6.54	10.43	1795.8	46.8
s44	1079.8	9.94	10.01	1779.6	46.4
s45	998.7	0.20	12.80	1726.0	37.4
s46	1001.2	0.13	12.93	1741.5	41.4
s47	1003.6	0.09	13.10	1733.3	45.6
s48	1037.3	5.80	10.70	1760.1	41.7
s49	1043.3	4.52	10.72	1781.5	45.9
s50	1049.2	3.62	10.83	1797.0	50.2

Table B.4. Values of the measurements of the first five properties obtained from calibration samples of the AMP-PZ-CO<sub>2</sub> mixtures at 40°C.

Sample number	Density, kg/m <sup>3</sup>	Conductivity, mS/cm	pH	Sound velocity, m/s	Refractive index, brix
s1	997.2	0.54	12.00	1684.8	26.2
s2	1000.3	0.36	12.09	1712.0	31.0
s4	1023.5	9.11	10.34	1700.7	29.5
s5	1030.7	7.14	10.48	1742.7	36.3
s7	1059.9	17.45	9.53	1717.5	34.8
s8	1071.2	13.88	9.61	1757.0	40.3
s9	1064.1	9.96	10.01	1777.6	42.7
s10	1014.8	4.48	10.71	1726.1	34.1
s11	1016.8	4.16	10.76	1737.2	36.1
s12	1019.3	3.90	10.83	1748.8	38.4
s13	1030.7	7.06	10.40	1741.4	36.9
s14	1033.5	6.90	5.35	1750.2	38.5
s15	1036.6	6.31	10.46	1762.8	40.8
s16	1052.8	11.10	9.97	1751.6	39.4
s17	1057.7	9.67	10.05	1768.2	41.7
s18	1062.3	8.80	10.07	1784.4	44.4
s19	996.6	0.28	12.10	1712.8	33.6
s20	999.1	0.33	12.48	1730.8	38.1
s22	1016.1	3.94	10.76	1736.4	37.7
s23	1018.6	3.54	10.78	1748.9	40.1
s24	1020.5	3.41	10.82	1757.4	42.1
s25	1029.9	6.85	10.38	1740.3	38.4
s26	1034.2	6.60	10.38	1754.0	40.0
s27	1037.1	5.88	10.44	1763.8	42.4
s28	1040.0	10.40	10.44	1774.5	44.8
s29	1041.6	5.11	10.05	1782.2	45.6
s30	1059.5	9.48	10.01	1788.5	43.5
s32	1051.3	6.52	10.24	1786.0	45.7
s33	1072.2	12.14	9.70	1769.0	44.1
s36	1016.7	3.76	10.73	1740.1	39.3
s38	1021.6	2.94	10.82	1762.6	44.7
s39	1034.9	6.16	10.38	1757.9	42.1
s41	1041.5	4.90	10.5	1777.4	46.4
s42	1041.9	11.15	10.07	1731.9	36.0
s43	1059.4	7.06	10.12	1788.2	46.8
s44	1075.7	10.54	9.80	1776.0	46.6
s45	995.3	0.21	12.30	1715.0	37.2
s46	997.7	0.15	12.25	1729.4	41.3
s47	1000.1	0.10	12.38	1741.6	45.5
s48	1034.1	6.30	10.38	1751.6	41.4
s49	1039.4	5.01	6.95	1773.7	45.9
s50	1045.5	3.95	10.51	1787.2	50.4

## B.2 The MDEA-PZ-H<sub>2</sub>O-CO<sub>2</sub> system

### B.2.1 Concentrations of components in calibration samples

Table B.5. Calibration samples notation and concentrations of the components: MDEA, PZ, CO<sub>2</sub>. For some of the samples within this campaign dry ice pellets were used to adjust the level of CO<sub>2</sub> content.

Sample	MDEA	PZ	CO <sub>2</sub>
	mol/l	mol/l	mol/l
m1	2.50	0.20	0.00
m2	2.50	0.40	0.52
m3	2.50	0.58	1.79
m4	2.48	0.79	0.88
m5	2.60	0.60	0.48
m6	2.74	0.20	1.12
m7	2.74	0.40	1.10
m8	2.75	0.58	0.93
m9	2.74	0.80	0.57
m10	2.75	1.00	0.00
m11	2.93	0.20	0.94
m12	2.93	0.42	1.04
m13	2.92	0.58	0.46
m15	2.94	1.00	0.71
m16	3.19	0.23	0.48
m17	3.20	0.40	0.50
m18	3.18	0.58	0.00
m19	3.20	0.80	1.20
m21	3.40	0.20	0.43
m20	3.20	1.01	1.43
m22	3.39	0.40	0.00
m23	3.40	0.58	1.83
m24	3.40	0.81	1.09
m25	3.40	1.01	1.06
m27	2.74	0.21	0.38
m28	2.93	0.20	0.00
m31	2.50	0.40	0.35
m32	2.75	0.40	0.00
m35	3.39	0.40	0.95
m36	2.49	0.58	0.00
m39	3.20	0.58	0.95
m40	3.39	0.59	0.48
m42	2.75	0.80	1.53
m43	2.92	0.80	0.93
m44	3.20	0.80	0.48
m45	3.40	0.80	0.00
m46	2.50	1.01	1.51
m47	2.74	1.00	0.94
m48	2.93	1.01	0.47
m49	3.20	1.00	0.00

## B.2.2 Laboratory measurements of calibration samples

Table B.6. Values of the measurements of the first five properties obtained from calibration samples of the MDEA-PZ-CO<sub>2</sub> mixtures at 20°C.

	Conductivity, mS/cm	pH	Density, g/cm <sup>3</sup>	SV, m/s	Refractive index, brix
m1	0.21	11.57	1.0293	1679.4	29.3
m2	5.15	9.41	1.0519	1705.4	34.0
m3	15.43	8.77	1.0992	1748.7	40.5
m4	5.97	9.53	1.0669	1741.3	39.2
m5	3.93	9.79	1.0530	1726.2	36.6
m6	11.86	9.08	1.0776	1720.0	37.3
m7	9.75	9.17	1.0782	1735.5	39.0
m8	6.62	9.37	1.0719	1744.3	39.9
m9	3.47	9.88	1.0584	1749.0	40.0
m10	0.13	11.75	1.0379	1751.6	39.3
m11	8.74	9.27	1.0714	1727.2	38.1
m12	7.32	9.3	1.0754	1746.3	40.5
m13	2.77	9.92	1.0537	1742.8	39.3
m15	2.96	9.94	1.0651	1774.1	43.9
m16	3.56	9.66	1.0567	1736.3	38.9
m17	2.92	9.76	1.0571	1747.4	40.4
m18	0.12	11.84	1.0401	1745.4	39.8
m19	4.78	9.41	1.0879	1791.5	46.9
m20	4.74	9.34	1.0989	1810.0	49.7
m21	3.06	9.70	1.0579	1745.0	40.6
m22	0.11	11.74	1.0411	1743.8	39.9
m23	8.04	9.02	1.1120	1808.6	49.0
m24	3.75	9.47	1.0860	1798.5	48.4
m25	3.02	9.96	1.0855	1806.4	49.9
m27	4.10	9.66	1.0476	1704.3	33.9
m28	0.16	11.59	1.0343	1706.8	33.7
m31	3.72	9.81	1.0450	1703.0	33.2
m32	0.18	11.72	1.0333	1710.1	33.7
m35	5.10	9.39	1.0781	1772.5	44.5
m36	0.21	11.81	1.0316	1707.2	32.8
m39	4.78	9.42	1.0765	1772.4	44.3
m40	2.29	9.85	1.0617	1769.2	43.9
m42	8.59	9.12	1.0963	1777.6	44.6
m43	4.57	9.55	1.0746	1770.3	43.6
m44	2.23	9.97	1.0612	1772.0	44.1
m45	0.08	11.86	1.0436	1768.1	43.5
m46	8.10	9.19	1.0936	1774.1	44.0
m47	4.45	9.63	1.0743	1771.5	43.6
m48	2.37	10.14	1.0589	1771.5	43.4
m49	0.09	11.93	1.0433	1772.0	43.4

Table B.7. Values of the measurements of the first five properties obtained from calibration samples of the MDEA-PZ-CO<sub>2</sub> mixtures at 25°C.

	Conductivity, mS/cm	pH	Density, g/cm <sup>3</sup>	SV, m/s	Refractive index, brix
m1	0.22	11.58	1.0277	1679.5	29.3
m2	5.50	9.55	1.0504	1705.3	34.0
m3	15.82	8.74	1.0988	1750.2	40.5
m4	6.39	9.48	1.0673	1739.5	39.2
m5	4.16	9.77	1.0517	1724.1	36.6
m6	12.29	9.05	1.0764	1721.2	37.3
m7	10.11	9.11	1.0774	1735.4	39.1
m8	6.97	9.35	1.0709	1742.6	39.9
m9	3.74	9.81	1.0571	1745.7	40.1
m10	0.14	11.89	1.0360	1746.3	39.2
m11	9.20	9.19	1.0700	1726.8	38.1
m12	7.74	9.25	1.0741	1744.5	40.5
m13	3.01	9.89	1.0521	1739.4	39.3
m15	3.23	9.88	1.0638	1769.2	44.0
m16	3.79	9.59	1.0547	1734.0	38.9
m17	3.15	9.71	1.0556	1743.3	40.3
m18	0.13	11.8	1.0379	1739.3	39.5
m19	5.16	9.34	1.0865	1787.0	47.1
m20	5.10	9.28	1.0976	1805.5	49.7
m21	3.31	9.62	1.0560	1740.4	40.6
m22	0.11	11.74	1.0390	1737.0	40.0
m23	8.50	8.98	1.1107	1805.0	49.0
m24	4.07	9.45	1.0848	1791.5	48.5
m25	3.28	9.56	1.0843	1798.6	49.9
m27	4.31	9.63	1.0462	1703.4	33.9
m28	0.17	11.55	1.0329	1704.1	33.8
m31	3.90	9.75	1.0435	1702.5	33.3
m32	0.19	11.66	1.0314	1707.2	33.7
m35	5.40	9.32	1.0768	1767.8	44.5
m36	0.22	11.74	1.0298	1704.6	32.8
m39	5.10	9.38	1.0759	1768.6	44.3
m40	2.52	9.80	1.0601	1763.0	43.9
m42	9.08	9.07	1.0958	1776.0	44.7
m43	4.92	9.48	1.0735	1766.5	43.6
m44	2.44	9.94	1.0595	1766.0	44.2
m45	0.09	11.83	1.0415	1760.0	43.5
m46	8.61	9.13	1.0930	1773.0	44.1
m47	4.78	9.57	1.0727	1768.1	43.6
m48	2.59	10.08	1.0577	1766.0	43.5
m49	0.09	11.90	1.0407	1763.2	43.5

### **B.3 Input and output of Aspen Plus modeling**

The ability of Aspen Plus model was checked to calculate physical properties for mixtures of MDEA, PZ, and CO<sub>2</sub> taken in proportions used to prepare calibration samples. The results of Aspen Plus calculations are presented in Table B.8 along with the values of pH, density, and SV that were measured in laboratory conditions. To test quality of Aspen Plus model, it was used to calculate pH, density, and SV for mixtures with chemical composition predicted in-line using PLS models, Table B.9. The results of these concentrations were compared with measurement obtained in-line, see Table B.10.

Table B.8. Input variables for Aspen Plus modeling. The calibration samples case. All measurements are taken at the temperature of sample at 20 °C and the pressure at 1 bar.

pH measured	pH Aspen Model	Density, g/cm <sup>3</sup> measured	Density, g/cm <sup>3</sup> Aspen Model	SV, m/s measured	SV, m/s Aspen Model
11.57	11.82	1029	1027	1679	1770
9.41	9.50	1052	1051	1705	1769
8.77	8.66	1099	1105	1749	1756
9.53	9.36	1067	1069	1741	1795
9.79	9.69	1053	1050	1726	1811
9.08	8.95	1078	1075	1720	1775
9.17	9.05	1078	1079	1736	1786
9.37	9.28	1072	1073	1744	1810
9.88	9.68	1058	1057	1749	1856
11.75	12.10	1038	1033	1752	1917
9.27	9.07	1071	1071	1727	1806
9.30	9.13	1075	1079	1746	1819
9.92	9.72	1054	1053	1743	1863
9.94	9.67	1065	1064	1774	1917
9.66	9.50	1057	1056	1736	1863
9.76	9.61	1057	1057	1747	1885
11.84	12.01	1040	1035	1745	1937
9.41	9.27	1088	1092	1792	1905
9.34	9.21	1099	1104	1810	1925
9.70	9.54	1058	1056	1745	1900
11.74	11.97	1041	1037	1744	1951
9.02	8.83	1112	1118	1809	1905
9.47	9.36	1086	1090	1799	1953
9.96	9.44	1086	1088	1806	1992
9.66	9.56	1048	1046	1704	1791
11.59	11.86	1034	1031	1707	1837
9.81	9.71	1045	1044	1703	1776
11.72	11.92	1033	1030	1710	1833
9.39	9.26	1078	1079	1773	1902
11.81	11.97	1032	1029	1707	1814
9.42	9.34	1077	1079	1772	1887
9.85	9.73	1062	1059	1769	1953
9.12	8.99	1096	1101	1778	1813
9.55	9.42	1075	1074	1770	1870
9.97	9.83	1061	1057	1772	1949
11.86	12.09	1044	1038	1768	2021
9.19	9.04	1094	1098	1774	1798
9.63	9.46	1074	1073	1772	1867
10.14	9.98	1059	1055	1772	1926
11.93	12.13	1043	1037	1772	2011

Table B.9. In-line predicted concentrations of the components: MDEA, PZ, CO<sub>2</sub>. Temperature and pressure readings are taken at the same time as the predictions were made.

MDEA, mol/L	PZ, mol/L	CO <sub>2</sub> , mol/L	T, °C	P, bar (absolute)
1.95	0.25	1.13	21.5	1.54
2.18	0.36	0.88	21.5	1.93
2.33	0.21	0.24	23.0	1.10
2.15	0.63	1.10	23.0	1.82
2.20	0.28	1.71	22.0	1.73
2.17	0.40	1.42	21.0	1.00
2.07	0.38	1.13	22.0	1.53
2.36	0.37	0.85	22.0	1.80
2.73	0.58	0.30	24.0	1.86
2.60	0.57	0.58	24.0	2.38
2.05	0.11	1.56	20.0	1.10
2.21	0.11	1.00	21.5	1.88
2.44	0.12	0.35	23.0	2.00
2.50	0.15	0.15	23.0	2.10
2.34	0.09	0.60	24.0	2.00



Table B.10. Results of Aspen Plus modeling for mixtures combined of MDEA, PZ, and CO<sub>2</sub> taken in proportions from Table B.9. The real time in-line measurement case. The measured values are the readings taken by the measurement equipment installed in the in-line chemometrics setup.

<b>pH</b> measured	<b>pH</b> Aspen Model	<b>Density, g/cm<sup>3</sup></b> measured	<b>Density, g/cm<sup>3</sup></b> Aspen Model	<b>SV, m/s</b> measured	<b>SV, m/s</b> Aspen Model
9.11	8.75	1074	1067	1688	1678
9.31	9.04	1064	1062	1684	1716
10.18	9.66	1036	1035	1668	1749
9.48	8.99	1068	1073	1685	1735
8.75	8.49	1092	1091	1712	1711
9.03	8.70	1083	1083	1705	1708
9.26	8.83	1072	1071	1700	1701
9.50	9.09	1062	1063	1693	1744
10.32	9.93	1040	1043	1692	1848
9.78	9.45	1052	1054	1693	1822
8.97	8.51	1085	1081	1691	1674
9.46	8.87	1063	1063	1678	1705
10.15	9.39	1040	1040	1670	1754
10.56	9.84	1033	1032	1671	1771
9.72	9.09	1048	1048	1670	1737



## References

- [1] *Inventory of U.S. greenhouse gas emissions and sinks: 1990-2013*. U.S. Environmental Protection Agency, Washington. 2015. <http://www.epa.gov/climatechange/emissions/usinventoryreport.html>
- [2] Smeets, E.; Tabeau, A.; van Berkum, S.; Moorad, J.; van Meijl, H.; Woltjer, G. *The impact of the rebound effect of the use of first generation biofuels in the EU on greenhouse gas emissions: a critical review*. Renewable and Sustainable Energy Reviews. 2014, 38, 393-403.
- [3] Holmgren, K. M.; Berntsson, T. S.; Andersson, E.; Rydberg, T. *The influence of biomass supply chains and by-products on the greenhouse gas emissions from gasification-based bio-SNG production systems*. Energy. 2015, 1-15.
- [4] Buchwitz, M.; Reuter, M.; Schneising, O.; Boesch, H.; Guerlet, S.; Dils, B.; Aben, I.; Armante, R.; Bergamaschi, P.; Blumenstock, T.; Bovensmann, H.; Brunner, D.; Buchmann, B.; Burrows, J. P.; Butz, A.; Chédin, A.; Chevallier, F.; Crevoisier, C. D.; Deutscher, N. M.; Frankenberg, C.; Hase, F.; Hasekamp, O. P.; Heymann, J.; Kaminski, T.; Laeng, A.; Lichtenberg, G.; DeMazière, M.; Noël, S.; Notholt, J.; Orphal, J.; Popp, C.; Parker, R.; Scholze, M.; Sussmann, R.; Stiller, G. P.; Warneke, T.; Zehner, C.; Bril, A.; Crisp, D.; Griffith, D. W. T.; Kuze, A.; O'Dell, C.; Oshchepkov, S.; Sherlock, V.; Suto, H.; Wennberg, P.; Wunch, D.; Yokota, T.; Yoshida, Y. *The greenhouse gas climate change initiative (GHG-CCI): comparison and quality assessment of near-surface-sensitive satellite-derived CO<sub>2</sub> and CH<sub>4</sub> global data sets*. Remote Sensing of Environment. 2015, 162, 344-362.
- [5] Denman, K. L.; Brasseur, G.; Chidthaisong, A.; Ciais, P.; Cox, P. M.; Dickinson, R. E.; Hauglustaine, D.; Heinze, C.; Holland, E.; Jacob, D.; Lohmann, U.; Ramachandran, S.; da Silva Dias, P. L.; Wofsy, S. C.; Zhang, X. *2007: Couplings between changes in the climate system and biogeochemistry*. In: *Climate change 2007: The physical science basis. Contribution of working group I to the fourth assessment report of the intergovernmental panel on climate change*, [Solomon, S., D. Qin, M. Manning, Z. Chen, M. Marquis, K. B. Averyt, M. Tignor and H. L. Miller (eds.)]. Cambridge University Press, Cambridge.
- [6] Dace, E.; Muizniece, I.; Blumberga, A.; Kaczala, F. *Searching for solutions to mitigate greenhouse gas emissions by agricultural policy decisions - application of system dynamics modeling for the case of Latvia*. Science of the Total Environment. 2015, 527-528, 80-90.
- [7] Noland, R. B.; Hanson, C. S. *Life-cycle greenhouse gas emissions associated with a highway reconstruction: a New Jersey case study*. Journal of Cleaner Production. 2015, in press, doi:10.1016/j.jclepro.2015.05.064.
- [8] Breyer, C.; Koskinen, O.; Blechinger, P. *Profitable climate change mitigation: the case of greenhouse gas emission reduction benefits enabled by solar photovoltaic systems*. Renewable and Sustainable Energy Reviews. 2015, 49, 610-628.

- [9] Hong, J.; Qiping Shen, G.; Feng, Y.; Sin-tong Lau, W.; Mao, C. *Greenhouse gas emissions during the construction phase of a building: a case study in China*. Journal of Cleaner Production. 2015, 103, 249-259.
- [10] Dooley, J. J.; Davidson, C. L.; Dahowski, R. T. *An assessment of the commercial availability of carbon dioxide capture and storage technologies as of June 2009*. Pacific Northwest National Laboratory for the U.S. Department of Energy, Richland. 2009.
- [11] Metz, B.; Davidson, O.; de Coninck, H.; Meyer, M. L. L. *IPCC special report on carbon dioxide capture and storage*. Cambridge university press, New York. 2005, ISBN: 978-0-521-68551-1.
- [12] Kapetaki, Z.; Brandani, P.; Brandani, S.; Ahn, H. *Process simulation of a dual-stage Selexol process for 95 % carbon capture efficiency at an integrated gasification combined cycle power plant*. International Journal of Greenhouse Gas Control. 2015, 39, 17-26.
- [13] Zhou, Q.; Koiwanit, J.; Piewkhaow, L.; Manuilova, A.; Chan, C. W.; Wilson, M.; Tontiwachwuthikul, P. *A comparative of life cycle assessment of post-combustion, pre-combustion and oxy-fuel CO<sub>2</sub> capture*. Energy Procedia. 2014, 63, 7452-7458.
- [14] Scheffknecht, G.; Al-Makhadmeh, L.; Schnell, U.; Maier, J. *Oxy-fuel coal combustion - a review of the current state-of-the-art*. International Journal of Greenhouse Gas Control. 2011, 5S, S16-S35.
- [15] Kobayashi, M.; Nakao, Y.; Oki, Y. *Exhaust circulation into dry gas desulfurization process to prevent carbon deposition in an Oxy-fuel IGCC power generation*. Energy Conversion and Management. 2014, 87, 1315-1323.
- [16] Babu, P.; Linga, P.; Kumar, R.; Englezos, P. *A review of the hydrate based gas separation (HBGS) process for carbon dioxide pre-combustion capture*. Energy. 2015, 85, 261-279.
- [17] Wang, M.; Lawal, A.; Stephenson, P.; Sidders, J.; Ramshaw, C. *Post-combustion CO<sub>2</sub> capture with chemical absorption: a state-of-the-art review*. Chemical Engineering Research and Design. 2011, 89, 1609-1624.
- [18] de Miguel Mercadera, F.; Magneschi, G.; Fernandez, E. S.; Gerard J. Stienstra, Goetheera, E. L. V. *Integration between a demo size post-combustion CO<sub>2</sub> capture and full size power plant. An integral approach on energy penalty for different process options*. International Journal of Greenhouse Gas Control. 2012, 11, S102-S113.
- [19] Mangalapally, H. P.; Hasse, H. *Pilot plant study of two new solvents for post combustion carbon dioxide capture by reactive absorption and comparison to monoethanolamine*. Chemical Engineering Science. 2011, 66, 5512-5522.

- [20] Olajire, A. A. *CO<sub>2</sub> capture and separation technologies for end-of-pipe applications: a review*. Energy. 2010, 35, 2610-2628.
- [21] Moser, P.; Schmidt, S.; Sieder, G.; Garcia, H.; Stoffregen, T.; Stamatov, V. *The post-combustion capture pilot plant Niederaussem – results of the first half of the testing programme*. Energy Procedia. 2011, 4, 1310-1316.
- [22] Dubois, L.; Thomas, D. *Postcombustion CO<sub>2</sub> capture by chemical absorption: screening of aqueous amine(s)-based solvents*. Energy Procedia. 2013, 37, 1648-1657.
- [23] Mathias, P. M.; Reddy, S.; O'Connell, J. P. *Quantitative evaluation of the chilled-ammonia process for CO<sub>2</sub> capture using thermodynamic analysis and process simulation*. International Journal of Greenhouse Gas Control. 2010, 4, 174-179.
- [24] Sønderby, T. L.; Carlsen, K. B.; Fosbøl, P. L.; Kiørboe, L. G.; von Solms, N. *A new pilot absorber for CO<sub>2</sub> capture from flue gases: measuring and modelling capture with MEA solution*. International Journal of Greenhouse Gas Control. 2013, 12, 181-192.
- [25] Luu, M. T.; Manaf, N. A.; Abbas, A. *Dynamic modelling and control strategies for flexible operation of amine-based post-combustion CO<sub>2</sub> capture systems*. International Journal of Greenhouse Gas Control. 2015, 39, 377-389.
- [26] Wu, X.; Yu, Y.; Qin, Z.; Zhang, Z. *The advances of post-combustion CO<sub>2</sub> capture with chemical solvents: review and guidelines*. Energy Procedia. 2014, 63, 1339-1346.
- [27] Wilcox, J.; Haghpanah, R.; Rupp, E. C.; He, J.; Lee, K. *Advancing adsorption and membrane-separation processes for the gigaton carbon capture challenge*. Annual Review of Chemical and Biomolecular Engineering. 2014, 5, 479-505.
- [28] Cousins, A.; Wardhaugh, L. T.; Feron, P. H. M. *A survey of process flow sheet modifications for energy efficient CO<sub>2</sub> capture from flue gases using chemical absorption*. International Journal of Greenhouse Gas Control. 2011, 5, 605-619.
- [29] Yang, H.; Xu, Z.; Fan, M.; Gupta, R.; Slimane, R. B.; Bland, A. E.; Wright, I. *Progress in carbon dioxide separation and capture: a review*. Journal of Environmental Sciences. 2008, 20, 14-27.
- [30] Han, K.; Ahn, C. K.; Lee, M. S. *Performance of an ammonia-based CO<sub>2</sub> capture pilot facility in iron and steel industry*. International Journal of Greenhouse Gas Control. 2014, 27, 239-246.
- [31] Johansson, D.; Franck, P. A.; Berntsson, T. *CO<sub>2</sub> capture in oil refineries: assessment of the capture avoidance costs associated with different heat supply options in a future energy market*. Energy Conversion and Management. 2013, 66, 127-142.

- [32] Fadeyi, S.; Arafat, H. A.; Abu-Zahra, M. R. M. *Life cycle assessment of natural gas combined cycle integrated with CO<sub>2</sub> post combustion capture using chemical solvent*. International Journal of Greenhouse Gas Control. 2013, 19, 441-452.
- [33] Yildirim, Ö.; Kiss, A. A.; Hüser, N.; Leßmann, K.; Kenig, E. Y. *Reactive absorption in chemical process industry: A review on current activities*. Chemical Engineering Journal. 2012, 213, 371-391.
- [34] Esmaeili, H.; Roozbehani, B. *Pilot-scale experiments for post-combustion CO<sub>2</sub> capture from gas fired power plants with a novel solvent*. International Journal of Greenhouse Gas Control. 2014, 30, 212-215.
- [35] Schäffer, A.; Brechtel, K.; Scheffknecht, G. *Comparative study on differently concentrated aqueous solutions of MEA and TETA for CO<sub>2</sub> capture from flue gases*. Fuel. 2012, 101, 148-153.
- [36] Moresa, P.; Scenna, N.; Mussati, M. *Post-combustion CO<sub>2</sub> capture process: equilibrium stage mathematical model of the chemical absorption of CO<sub>2</sub> into monoethanolamine (MEA) aqueous solution*. Chemical Engineering Research and Design. 2011, 89, 1587-1599.
- [37] Le Moullec, Y.; Kanniche, M. *Screening of flowsheet modifications for an efficient monoethanolamine (MEA) based post-combustion CO<sub>2</sub> capture*. International Journal of Greenhouse Gas Control. 2011, 5, 727-740.
- [38] Shakerian, F.; Kim, K. H.; Szulejko, J. E.; Park, J. W. *A comparative review between amines and ammonia as sorptive media for post-combustion CO<sub>2</sub> capture*. Applied Energy. 2015, 148, 10-22.
- [39] Derks, P. W. J.; Hogendoorn, J. A.; Versteeg, G. F. *Experimental and theoretical study of the solubility of carbon dioxide in aqueous blends of piperazine and N-methyldiethanolamine*. The Journal of Chemical Thermodynamics. 2010, 42, 151-163.
- [40] Dash, S. K.; Bandyopadhyay, S. S. *Carbon dioxide capture: absorption of carbon dioxide in piperazine activated concentrated aqueous 2-amino-2-methyl-1-propanol*. Journal of Clean Energy Technologies. 2013, 1, 184-188.
- [41] Closmann, F.; Nguyen, T.; Rochelle, G. T. *MDEA/Piperazine as a solvent for CO<sub>2</sub> capture*. Energy Procedia. 2009, 1, 1351-1357.
- [42] Sadegh, N.; Stenby, E. H.; Thomsen, K. *Thermodynamic modeling of CO<sub>2</sub> absorption in aqueous N-Methyldiethanolamine using Extended UNIQUAC model*. Fuel. 2015, 144, 295-306.
- [43] Yu, C. H.; Huang, C. H.; Tan, C. S. *A review of CO<sub>2</sub> capture by absorption and adsorption*. Aerosol and Air Quality Research. 2012, 12, 745-769.

- [44] *The global status of CCS: 2015*. Global CCS Institute: Melbourne, Australia. 2015,  
<http://hub.globalccsinstitute.com/sites/default/files/publications/196843/global-status-ccs-2015-summary.pdf>.
- [45] *The global status of CCS: 2014*. Global CCS Institute: Melbourne, Australia. 2014,  
<http://hub.globalccsinstitute.com/sites/default/files/publications/180923/global-status-ccs-2014.pdf>.
- [46] Liang, Z.; Rongwong, W.; Liu, H.; Fu, K.; Gao, H.; Cao, F.; Zhang, R.; Sema, T.; Henni, A.; Sumon, K.; Nath, D.; Gelowitz, D.; Srisang, W.; Saiwan, C.; Benamor, A.; Al-Marri, M.; Shi, H.; Supap, T.; Chan, C.; Zhou, Q.; Abu-Zahra, M.; Wilson, M.; Olson, W.; Idem, R.; Tontiwachwuthikul, P. *Recent progress and new developments in post-combustion carbon-capture technology with amine based solvents*. International Journal of Greenhouse Gas Control. 2015, 40, 26-54.
- [47] Muhammad, A.; GadelHak, Y. *Simulation based improvement techniques for acid gases sweetening by chemical absorption: a review*. International Journal of Greenhouse Gas Control. 2015, 37, 481-491.
- [48] Haghtalab, A.; Izadi, A. *Simultaneous measurement solubility of carbon dioxide+hydrogen sulfide into aqueous blends of alkanolamines at high pressure*. Fluid Phase Equilibria. 2014, 375, 181-190.
- [49] Harmsen, J. *Industrial process scale-up: a practical innovation guide from idea to commercial implementation*. Elsevier B. V., Oxford. 2013, ISBN: 978-0-444-62726-1.
- [50] *Carbon dioxide capture for natural gas and industrial applications*. In *Quadrennial Technology Review: an assessment of energy technologies and research opportunities*. U.S. Department of Energy. September 2015.
- [51] Farzaneh-Gord, M.; Niazmand, A.; Deymi-Dashtebayaz M.; Rahbari, H. R. *Effects of natural gas compositions on CNG (compressed natural gas) reciprocating compressors performance*. Energy. 2015, 90, 1152-1162.
- [52] Hora, T. S.; Agarwal, A. K. *Experimental study of the composition of hydrogen enriched compressed natural gas on engine performance, combustion and emission characteristics*. Fuel. 2015, 160, 470-478.
- [53] Davoudi, M.; Heidari, Y.; Safadoost, A.; Samieirad, S. *Chemical injection policy for internal corrosion prevention of South Pars sea-pipeline: a case study*. Journal of Natural Gas Science and Engineering. 2014, 21, 592-599.
- [54] He, X.; Kim, T. J.; Hägg, M. B. *Hybrid fixed-site-carrier membranes for CO<sub>2</sub> removal from high pressure natural gas: membrane optimization and process condition investigation*. Journal of Membrane Science. 2014, 470, 266-274.

- [55] Rahim, N. A.; Ghasem, N.; Al-Marzouqi, M. *Absorption of CO<sub>2</sub> from natural gas using different amino acid salt solutions and regeneration using hollow fiber membrane contactors*. Journal of Natural Gas Science and Engineering. 2015, 26, 108-117.
- [56] Jusoh, N.; Lau, K. K.; Shariff, A. M.; Yeong, Y. F. *Capture of bulk CO<sub>2</sub> from methane with the presence of heavy hydrocarbon using membrane process*. International Journal of Greenhouse Gas Control. 2014, 22, 213-222.
- [57] Shimekit, B.; Mukhtar, H. *Natural gas purification technologies - major advances for CO<sub>2</sub> separation and future directions, advances in natural gas technology*, Dr. Hamid Al-Megren (Ed.), InTech, Rijeka. 2012, ISBN: 978-953-51-0507-7.
- [58] Schaefer, C.; Clicq, D.; Lecomte, C.; Merschaert, A.; Norrant, E.; Fotiadu, F. *A Process Analytical Technology (PAT) approach to control a new API manufacturing process: development, validation and implementation*. Talanta. 2014, 120, 114-125.
- [59] Schaefer, C.; Lecomte, C.; Clicq, D.; Merschaert, A.; Norrant, E.; Fotiadu, F. *On-line near infrared spectroscopy as a Process Analytical Technology (PAT) tool to control an industrial seeded API crystallization*. Journal of Pharmaceutical and Biomedical Analysis. 2013, 83, 194-201.
- [60] Wu, H.; Khan, M. *THz spectroscopy: an emerging technology for pharmaceutical development and pharmaceutical Process Analytical Technology (PAT) applications*. Journal of Molecular Structure. 2012, 1020, 112-120.
- [61] Reis, M. M.; Araújo, P. H. H.; Sayer, C.; Giudici, R. *Spectroscopic on-line monitoring of reactions in dispersed medium: chemometric challenges*. Analytica Chimica Acta. 2007, 595, 257-265.
- [62] Fischer, D.; Sahre, K.; Abdelrhim, M.; Voit, B.; Sadhu, V. B.; Pionteck, J.; Komber, H.; Hutschenreuter, J. *Process monitoring of polymers by in-line ATR-IR, NIR and Raman spectroscopy and ultrasonic measurements*. C. R. Chimie. 2006, 9, 1419-1424.
- [63] Wu, H.; White, M.; Khan, M. A. *Quality-by-Design (QbD): An integrated process analytical technology (PAT) approach for a dynamic pharmaceutical coprecipitation process characterization and process design space development*. International Journal of Pharmaceutics. 2011, 405, 63-78.
- [64] Houson, I. *Process Understanding: For Scale-Up and Manufacture of Active Ingredients*. Wiley-VCH Verlag GmbH & Co., Weinheim. 2011, ISBN:978-3-527-32584-9.
- [65] Rathore, A. S.; Winkle, H. *Quality by design for biopharmaceuticals*. Nature Biotechnology. 2009, 27, 26-34.



- [66] Nadpara, N. P.; Thumar, R. V.; Kalola, V. N.; Patel, P. B. *Quality by design (QbD): a complete review*. Int. J. Pharm. Sci. Rev. Res. 2012, 17, 20-28.
- [67] *Guidance for industry: PAT - a framework for innovative pharmaceutical development, manufacture, and quality assurance*. FDA (Food Drug Administration), Rockville. 2004, <http://www.fda.gov/downloads/Drugs/GuidanceComplianceRegulatoryInformation/Guidances/UCM070305.pdf>.
- [68] Hopke, P. K. *The evolution of chemometrics*. Analytica Chimica Acta. 2003, 500, 365-377.
- [69] Roggo, Y.; Chalus, P.; Maurer, L.; Lema-Martinez, C.; Edmond, A.; Jent, N. *A review of near infrared spectroscopy and chemometrics in pharmaceutical technologies*. Journal of Pharmaceutical and Biomedical Analysis. 2007, 44, 683-700.
- [70] Maggio, R. M.; Calvo, N. L.; Vignaduzzo, S. E.; Kaufman, T. S. *Pharmaceutical impurities and degradation products: uses and applications of NMR techniques*. Journal of Pharmaceutical and Biomedical Analysis. 2014, 101, 102-122.
- [71] Wold, S. *Chemometrics; what do we mean with it, and what do we want from it?* Chemometrics and Intelligent Laboratory Systems. 1995, 30, 109-115.
- [72] Fülöp, A.; Hancsók, J. *Comparison of calibration models based on near-infrared spectroscopy data for the determination of plant oil properties*. Hungarian Journal of Industry and Chemistry. 2009, 37(2), 119-122.
- [73] Wang, Y.; Ni, Y. *Combination of UV-vis spectroscopy and chemometrics to understand protein-nanomaterial conjugate: A case study on human serum albumin and gold nanoparticles*. Talanta. 2014, 119, 320-330.
- [74] Arachchige, U. S. P. R.; Mohsin, M.; Melaaen, M. C. *Optimized CO<sub>2</sub>-flue gas separation model for a coal fired power plant*. International Journal of Energy and Environment. 2013, 4, 39-48.
- [75] Tobiesen, F. A.; Juliussen, O.; Svendsen, H. F. *Experimental validation of a rigorous desorber model for CO<sub>2</sub> post-combustion capture*. Chemical Engineering Science. 2008, 63, 2641-2656.
- [76] Khakharia, P.; Kvamsdal, H. M.; da Silva, E. F.; Vlugt, T. J. H.; Goetheer, E.; *Field study of a Brownian demister unit to reduce aerosol based emission from a post combustion CO<sub>2</sub> capture plant*. International Journal of Greenhouse Gas Control. 2014, 28, 57-64.
- [77] Ciftja, A. F.; Hartono, A.; Svendsen, H. F. *Experimental study on carbamate formation in the AMP-CO<sub>2</sub>-H<sub>2</sub>O system at different temperatures*. Chemical Engineering Science. 2014, 107, 317-327.

- [78] Barzagli, F.; Mani, F.; Peruzzini, M. *Efficient CO<sub>2</sub> absorption and low temperature desorption with non-aqueous solvents based on 2-amino-2-methyl-1-propanol (AMP)*. International Journal of Greenhouse Gas Control. 2013, 16, 217-223.
- [79] Bishnoi, S.; Rochelle, G. T. *Absorption of carbon dioxide into aqueous piperazine: reaction kinetics, mass transfer and solubility*. Chemical Engineering Science. 2000, 55, 5531-5543.
- [80] Zeng, Z.; Li, J.; Hugel, H. M.; Xu, G.; Marriott, P. J. *Interpretation of comprehensive two-dimensional gas chromatography data using advanced chemometrics*. Trends in Analytical Chemistry. 2014, 53, 150-166.
- [81] Wise, B. M.; Gallagher, N. B. *The process chemometrics approach to process monitoring and fault detection*. J. Proc. Cont. 1996, 6, 329-348.
- [82] Geers, L. F. G.; van de Runstraat, A.; Joh, R.; Schneider, R.; Goetheer, E. L. V. *Development of an online monitoring method of a CO<sub>2</sub> capture process*. Industrial and Engineering Chemistry Research. 2011, 50, 9175-9180.
- [83] Einbu, A.; Ciftja, A. F.; Grimstvedt, A.; Zakeri, A.; Svendsen, H. F. *Online analysis of amine concentration and CO<sub>2</sub> loading in MEA solutions by ATR-FTIR spectroscopy*. Energy Procedia. 2012, 23, 55-63.
- [84] Gadamasetti, K.; Braish, T. *Process chemistry in the pharmaceutical industry, volume 2: challenges in an ever changing climate*. CRC Press, Boca Raton. 2007, ISBN: 978-0-8493-9051-7.
- [85] O'Donnell, C. P.; Fagan, C.; Cullen, P. J. *Process analytical technology for the food industry*. Springer+Business Media, New York. 2014, ISBN: 978-1-4939-0311-5.
- [86] Rodionova, O. Ye.; Pomerantsev, A. L. *Chemometrics: achievements and prospects*. Russian Chemical Reviews. 2006, 75, 271-287.
- [87] Lundstedt, T.; Seifert, E.; Abramo, L.; Thelin, B.; Nyström, Å.; Pettersen, J.; Bergman, R. *Experimental design and optimization*. Chemometrics and Intelligent Laboratory Systems. 1998, 42, 3-40.
- [88] Idem, R.; Supap, T.; Shi, H.; Gelowitz, D.; Ball, M.; Campbell, C.; Tontiwachwuthikul, P. *Practical experience in post-combustion CO<sub>2</sub> capture using reactive solvents in large pilot and demonstration plants*. International Journal of Greenhouse Gas Control. 2015, 40, 6-25.
- [89] Russell, E. L.; Chiang, L. H.; Braatz, R. D. *Fault detection in industrial processes using canonical variate analysis and dynamic principal component analysis*. Chemometrics and Intelligent Laboratory Systems. 2000, 51, 81-93.
- [90] Bakeev, K. *Process analytical technology*. Blackwell Publishing, Oxford. 2005, ISBN: 978-1-4051-2103-3.

- [91] Kachko, A.; van der Ham, L. V.; Geers, L. F. G.; Huizinga, A.; Rieder, A.; Abu-Zahra, M. R. M.; Vlugt, T. J. H.; Goetheer, E. L. V. *Real-time process monitoring of CO<sub>2</sub> capture by aqueous AMP-PZ using chemometrics: pilot plant demonstration*. Industrial & Engineering Chemistry Research. 2015, 54, 5769-5776.
- [92] Kachko, A.; van der Ham, L. V.; Bakker, D.; Runstraat, A.; Nienoord, M.; Vlugt, T. J. H.; Goetheer, E. L. V. *In-line monitoring of the CO<sub>2</sub>, MDEA, PZ concentrations in liquid phase during high pressure CO<sub>2</sub> capture*. Ind. Eng. Chem. Res. 2015, submitted.
- [93] Kachko, A.; van der Ham, L. V.; Bardow, A.; Goetheer, E. L. V.; Vlugt, T. J. H. *Comparison of Raman, NIR, and ATR FTIR spectroscopy as analytical tools for in-line monitoring of CO<sub>2</sub> concentration in an amine gas treating process*. International Journal of Greenhouse Gas Control. 2016, 47, 17-24.
- [94] Gao, R. X.; Tang, X.; Gordon, G.; Kazmer, D. O. *On-line product monitoring through in-process measurement*. CIRP Annals-Manufacturing technology. 2014, 63, 493-496.
- [95] Kuo, C. C.; Siao, Y. T. *On-line pH value measurement of solution on the removing support material process*. Optik. 2014, 125, 3209-3213.
- [96] Mertens, J.; Lepaumier, H.; Desagher, D.; Thielens, M. L. *Understanding ethanolamine (MEA) and ammonia emissions from amine based post combustion carbon capture: Lessons learned from field tests*. International Journal of Greenhouse Gas Control. 2013, 16, 72-77.
- [97] Soons, Z. I. T. A.; Shi, J.; Stigter, J. D.; van der Pol, L. A.; van Straten, G.; van Boxtel, A. J. B. *Observer design and tuning for biomass growth and  $k_L a$  using online and offline measurements*. Journal of Process Control. 2008, 18, 621-631.
- [98] Oexmann, J.; Kather, A. *Post-combustion CO<sub>2</sub> capture in coal-fired power plants: comparison of integrated chemical absorption processes with piperazine promoted potassium carbonate and MEA*. Energy Procedia. 2009, 1, 799-806.
- [99] Kulichenko, N.; Ereira, E. *Carbon capture and storage in developing countries: a perspective on barriers to deployment*. International Bank for Reconstruction and Development, Washington. 2011, ISBN: 978-0-8213-9609-4.
- [100] Abu-Zahra, M. R. M.; Feron, P. H. M.; Jansens, P. J.; Goetheer, E. L. V. *New process concepts for CO<sub>2</sub> post-combustion capture process integrated with co-production of hydrogen*. International Journal of Hydrogen Energy. 2009, 34, 3992-4004.
- [101] Sanchez Fernandez, E.; Goetheer, E. L. V.; Manzoloni, G.; Macchi, E.; Rezvani, S.; Vlugt, T. J. H. *Thermodynamic assessment of amine based CO<sub>2</sub> capture technologies in power plants based on European Benchmarking Task Force methodology*. Fuel. 2014, 129, 318-329.

- [102] Manzolini, G.; Sanchez Fernandez, E.; Rezvani, S.; Macchi, E.; Goetheer, E. L. V.; Vlugt, T. J. H. *Economic assessment of novel amine based CO<sub>2</sub> capture technologies integrated in power plants based on European Benchmarking Task Force methodology*. Applied Energy. 2015, 138, 2015, 546-558.
- [103] Khakharia, P.; Brachert, L.; Mertens, J.; Huizinga, A.; Schallert, B.; Schaber, K.; Vlugt, T. J. H.; Goetheer, E. L. V. *Investigation of aerosol based emission of MEA due to sulphuric acid aerosol and soot in a Post Combustion CO<sub>2</sub> Capture process*. International Journal of Greenhouse Gas Control. 2013, 19, 138-144.
- [104] Wang, T.; Hovland, J.; Jens, K. J. *Amine reclaiming technologies in post-combustion carbon dioxide capture*. Journal of Environmental Sciences. 2015, 27, 276-289.
- [105] van der Ham, L. V.; van Eckveld, A. C.; Goetheer, E. L. V. *Online monitoring of dissolved CO<sub>2</sub> and MEA concentrations: effect of solvent degradation on predictive accuracy*. Energy Procedia. 2014, 63, 1223-1228.
- [106] Dye, C.; Schmidbauer, N.; Schlabach, M. *Evaluation of analytical methods for amine related emissions and degradation products in emission and ambient air*. NILU, [http://co2.nilu.no/LinkClick.aspx?fileticket=JDEy5GezzRU%\\$3D&tabid=2549&mid=5547&language=en-US](http://co2.nilu.no/LinkClick.aspx?fileticket=JDEy5GezzRU%$3D&tabid=2549&mid=5547&language=en-US). 2009, ISBN: 978-82-425-2050-0.
- [107] Rosas, J. G.; de Waard, H.; De Beer, T.; Vervaet, C.; Remon, J. P.; Hinrichs, W. L. J.; Frijlink, H. W.; Blanco, M. *NIR spectroscopy for the in-line monitoring of a multicomponent formulation during the entire freeze-drying process*. Journal of Pharmaceutical and Biomedical Analysis. 2014, 97, 39-46.
- [108] Hergeth, W. D. *Ullmann's Encyclopedia of Industrial Chemistry*. Wiley-VCH Verlag GmbH & Co. KGaA, Weinheim. 2014, ISBN: 978-82-425-2050-0.
- [109] van der Ham, L. V.; Bakker, D. E.; Geers, L. F. G.; Goetheer, E. L. V. *In-line monitoring of CO<sub>2</sub> absorption process using simple analytical techniques and multivariate modelling*. Chemical Engineering Technology. 2013, 37, 221-228.
- [110] Lavine, B. K.; Workman, J. *Chemometrics*. Analytical Chemistry. 2013, 85, 705-714.
- [111] Shashilov, V. A.; Lednev, I. K. *Advanced statistical and numerical methods for spectroscopic characterization of protein structural evolution*. Chemical Reviews. 2010, 110, 5692-5713.
- [112] González-Martínez, J. M.; Camachob, J.; Ferrera, A. *Bilinear modeling of batch processes, part III: parameter stability*. Journal of Chemometrics. 2014, 28, 10-27.
- [113] van Eckveld, A. C.; van der Ham, L. V.; Geers, L. F. G.; van den Broeke, L. J. P.; Boersma, B. J.; Goetheer, E. L. V. *Online monitoring of solvent and acid*

- gas concentration in a carbon dioxide absorption process using monoethanolamine.* Industrial and Engineering Chemistry Research. 2014, 53, 5515-5523.
- [114] Kvamsdal, H. M.; Romano, M. C.; van der Ham, L.; Bonalumi, D.; van Os, P.; Goetheer, E. *Energetic evaluation of a power plant integrated with a piperazine-based CO<sub>2</sub> capture process.* International Journal of Greenhouse Gas Control. 2014, 28, 343-355.
- [115] Artanto, Y.; Jansen, J.; Pearson, P.; Puxty, G.; Cottrell, A.; Meuleman, E.; Feron, P. *Pilot-scale evaluation of AMP/PZ to capture CO<sub>2</sub> from flue gas of an Australian brown coal-fired power station.* International Journal of Greenhouse Gas Control. 2014, 20, 189-195.
- [116] Freeman, S. A.; Rochelle, G. T. *Density and viscosity of aqueous (Piperazine + Carbon Dioxide) Solutions.* Journal of Chemical & Engineering Data. 2011, 56, 574-581.
- [117] Laesecke, A.; Fortin, T. J.; Splett, J. D. *Density, speed of sound, and viscosity measurements of reference materials for biofuels.* Journal of Chemical and Engineering Data. 2011, 56, 574-581.
- [118] Czarnik-Matuszewicz, B.; Pilorz, S. *Study of the temperature-dependent near-infrared spectra of water by two-dimensional correlation spectroscopy and principal components analysis.* Vibrational Spectroscopy. 2006, 40, 235-245.
- [119] Hill, T.; Lewicki, P. *Statistics: methods and applications.* StatSoft, Tulsa, OK. 2007, ISBN: 978-1-8842-3359-3.
- [120] Rieder, A.; Unterberger, S. *EnBW's post-combustion capture pilot plant at Heilbronn - results of the first year's testing programme.* Energy Procedia. 2013, 37, 6464-6472.
- [121] Bazhenov, S.; Vasilevsky, V.; Rieder, A.; Unterberger, S.; Grushevenko, E.; Volkov, V.; Schallert, B.; Volkov, A. *Heat stable salts (HSS) removal by electro dialysis: reclaiming of MEA used in post-combustion CO<sub>2</sub>-capture.* Energy Procedia. 2014, 63, 6349-6356.
- [122] Wold, S.; Sjöström, M.; Eriksson, L. *PLS regression: a basic tool of chemometrics.* Chemometrics and Intelligent Laboratory Systems. 2001, 58, 109-130.
- [123] Rosipal, R.; Krämer, N. *Overview and recent advances in partial least squares. In: Subspace, Latent Structure and Feature Selection,* (pp. 34-51), [Saunders, C.; Grobelnik, M.; Gunn, S.; Shawe-Taylor, J. (eds.)]. 2005, ISBN: 978-3-540-34137-6.
- [124] Sargent, M. (Ed.). *Guide to achieving reliable quantitative LC-MS measurements.* RSC Analytical Methods Committee, Teddington. 2013, ISBN: 978-0-948926-27-3.

- [125] Wise, B. M.; Gallagher, N. B.; Bro, R.; Shaver, J. M. *PLS Toolbox 3.0 for use with MatLab*. Eigenvector Research, Inc., Wenatchee. 2003, ISBN: 0-9761184-1-6.
- [126] Li, B.; Morris, J.; Martin, E. B. *Model selection for partial least squares regression*. Chemometrics and Intelligent Laboratory Systems. 2002, 64, 79-89.
- [127] White, D. R.; Saunders, P. *The propagation of uncertainty on interpolated scales, with examples from thermometry*. Metrologia. 2000, 37, 285-293.
- [128] Beer, A. *Bestimmung der Absorption des rothen Lichts in farbigen Flüssigkeiten*. Annalen der Physik und Chemie. 1852, 86, 78-88.
- [129] Rinna, Å.; van den Berg, F.; Engelsens, S. B. *Review of the most common pre-processing techniques for near-infrared spectra*. Trends in Analytical Chemistry. 2009, 28, 1201-1222.
- [130] Upstone, S. L. *Ultraviolet/visible light absorption spectrophotometry in clinical chemistry*. In: *Encyclopedia of Analytical Chemistry*, (pp. 1699-1714), [R.A. Meyers (ed.)]. John Wiley & Sons Ltd., Chichester. 2000.
- [131] Makridakis, S.; Hibon, M. *Evaluating accuracy (or error) measures*. INSEAD working papers, Fontainebleau. 1995, <http://www.insead.edu/facultyresearch/research/doc.cfm?did=46875>.
- [132] de Juan, A.; Maeder, M.; Martínez, M.; Tauler, R. *Combining hard- and soft-modelling to solve kinetic problems*. Chemometrics and Intelligent Laboratory Systems. 2000, 54, 123-141.
- [133] Beumers, P.; Brands, T.; Koss, H. J.; Bardow, A. *Model-free calibration of Raman measurements of reactive systems: Application to monoethanolamine/water/CO<sub>2</sub>*. Fluid Phase Equilibria. 2015, in press, doi:10.1016/j.fluid.2015.10.004
- [134] Abdulrahman, R. K.; Sebastine, I. M. *The studying of declining reservoir pressure on natural gas sweetening process: a case study and simulation*. Global Journal of Researches in Engineering. 2012, 12, 1-5.
- [135] Foss, M. M. *Interstate natural gas - quality specifications and interchangeability*. Center for Energy Economics, Sugar Lang. 2004.
- [136] Hedayat, M.; Soltanieh, M.; Mousavi, S. A. *Simultaneous separation of H<sub>2</sub>S and CO<sub>2</sub> from natural gas by hollow fiber membrane contactor using mixture of alkanolamines*. Journal of Membrane Science. 2011, 377, 191-197.
- [137] Kumar, S.; Cho, J. H.; Moon, I. *Ionic liquid-amine blends and CO<sub>2</sub>BOLs: prospective solvents for natural gas sweetening and CO<sub>2</sub> capture technology - a review*. International Journal of Greenhouse Gas Control. 2014, 20, 87-116.

- [138] Chunbo, Y.; Guangwen, C.; Quan, Y. *Process characteristics of CO<sub>2</sub> absorption by aqueous monoethanolamine in a microchannel reactor*. Chinese Journal of Chemical Engineering. 2012, 20, 111-119.
- [139] Kadiwala, S; Rayer, A. V.; Henni, A. *High pressure solubility of carbon dioxide (CO<sub>2</sub>) in aqueous piperazine solutions*. Fluid Phase Equilibria. 2010, 292, 20-28.
- [140] Nakamoto, T; Muraoka, T.; Yamamoto, S.; Higashii, T. *Study on high-pressure CO<sub>2</sub> capture process*. Energy Procedia. 2014, 63, 1940-1943.
- [141] Tan, L. S.; Shariff, A. M.; Lau, K. K.; Bustam, M. A. *Impact of high pressure on high concentration carbon dioxide capture from natural gas by monoethanolamine/N-methyl-2-pyrrolidone solvent in absorption packed column*. International Journal of Greenhouse Gas Control. 2015, 34, 25-30.
- [142] Camacho, J.; Picó, J.; Ferrer, A. *Bilinear modelling of batch processes. Part II: a comparison of PLS soft-sensors*. Journal of Chemometrics. 2008, 22, 533-547.
- [143] Reza, J.; Trejo, A. *Degradation of aqueous solutions of alkanolamine blends at high temperature, under the presence of CO<sub>2</sub> and H<sub>2</sub>S*. Chemical Engineering Communications. 2006, 193, 129-138.
- [144] Hoff, K. A.; Svendsen, H. F. *CO<sub>2</sub> absorption with membrane contactors vs. packed absorbers - challenges and opportunities in post combustion capture and natural gas sweetening*. Energy Procedia. 2013, 37, 952-960.
- [145] Rufford, T. E.; Smart, S.; Watson, G. C. Y.; Graham, B. F.; Boxall, J.; da Costa, J. C. D.; Maya, E. F. *The removal of CO<sub>2</sub> and N<sub>2</sub> from natural gas: A review of conventional and emerging process technologies*. Journal of Petroleum Science and Engineering. 2012, 94-95, 123-154.
- [146] Box, G. E. P.; Hunter, J. S.; Hunter, W. G. *Statistics for experimenters: design, innovation, and discovery, 2nd edition*. John Wiley & Sons, Inc., Hoboken. 2005, ISBN: 978-0-471-71813-0.
- [147] Montgomery, D. C. *Design and analysis of experiment, 5th edition*. John Wiley & Sons, Inc., New York. 2001, ISBN: 0-471-31649-0.
- [148] Liu, J.; Gao, H. C.; Peng, C. C.; Wong, D. S. H.; Jang, S. S.; Shen, J. F. *Aspen Plus rate-based modeling for reconciling laboratory scale and pilot scale CO<sub>2</sub> absorption using aqueous ammonia*. International Journal of Greenhouse Gas Control. 2015, 34, 117-128.
- [149] Moioli, S.; Pellegrini, L. A. *Improved rate-based modeling of the process of CO<sub>2</sub> capture with PZ solution*. Chemical Engineering Research and Design. 2015, 93, 611-620.

- [150] Pinto, D. D. D.; Monteiro, J. G. M.-S.; Bersås, A.; Haug-Warberg, T.; Svendsen, H. F. *eNRTL parameter fitting procedure for blended amine systems: MDEA-PZ case study*. Energy Procedia. 2013, 37, 1613-1620.
- [151] Aspen Tech. *Rate-Based Model of the CO<sub>2</sub> Capture Process by Mixed PZ and MDEA Using Aspen Plus*. Revision version 7.3.2.
- [152] Muhammad, A.; Mutalib, M. I. A.; Murugesan, T.; Shafeeq, A. *Thermophysical properties of aqueous piperazine and aqueous (N-Methyldiethanolamine + Piperazine) solutions at temperatures (298.15 to 338.15) K*. Journal of Chemical & Engineering Data. 2009, 54, 2317-2321.
- [153] Samanta, A.; Bandyopadhyay, S. S. *Density and viscosity of aqueous solutions of piperazine and (2-Amino-methyl-1-propanol + Piperazine) from 298 to 333 K*. Journal of Chemical & Engineering Data. 2006, 51, 467-470.
- [154] Murshid, G.; Shariff, A. M.; Keong, L. K.; Bustam, M. A. *Physical properties of aqueous solutions of piperazine and (2-Amino-2-methyl-1-propanol + Piperazine) from 298.15 to 333.15 K*. Journal of Chemical & Engineering Data. 2011, 56, 2660-2663.
- [155] Bernal-Garcia, J. M.; Romas-Estrada, M.; Iglesias-Silva, G. A. *Densities and excess molar volumes of aqueous solutions of N-Methyldiethanolamine (MDEA) at temperatures from 283.15 to 363.15 K*. Journal of Chemical & Engineering Data. 2003, 48, 1442-1445.
- [156] Weiland, R. H.; Dingman, J. C.; Cronin, D. B.; Browning, G. J. *Density and viscosity of some partially carbonated aqueous alkanolamine solutions and their blends*. Journal of Chemical & Engineering Data. 1998, 43, 378-382.
- [157] Nguyen, D. L.; Winter, E. R. F.; Greiner, M. *Sonic velocity in two-phase systems*. International Journal of Multiphase Flow. 1981, 7, 311-320.
- [158] Refaeilzadeh, P.; Tang, L.; Liu, H. *Cross-validation*. In: *Encyclopedia of Database Systems*, (pp. 532-538), [Liu, L. and Özsu, T. M. (eds.)]. 2009, ISBN: 978-0-387-35544-3.
- [159] Geladi, P.; Sethson, B.; Nyström, J.; Lillhonga, T.; Lestander, T.; Burger, J. *Chemometrics in spectroscopy Part 2. Examples*. Spectrochimica Acta Part B. 2004, 59, 1347-1357.
- [160] Choi, S.; Drese, J. H.; Jones, C. W. *Adsorbent materials for carbon dioxide capture from large anthropogenic point sources*. ChemSusChem. 2009, 2, 796-854.
- [161] Amann, J. M. G.; Bouallou, C. *A new aqueous solvent based on a blend of N-methyldiethanolamine and triethylene tetramine for CO<sub>2</sub> recovery in post-combustion: Kinetics study*. Energy Procedia. 2009, 1, 901-908.



- [162] Schäffer, A.; Brechtel, K.; Scheffknecht, G. *Comparative study on differently concentrated aqueous solutions of MEA and TETA for CO<sub>2</sub> capture from flue gases*. *Fuel*. 2012, 101, 148-153.
- [163] Mercier, S. M.; Diepenbroek, B.; Wijffels, R. H.; Streefland, M. *Multivariate PAT solutions for biopharmaceutical cultivation: current progress and limitations*. *Trends in Biotechnology*. 2014, 32, 329-336.
- [164] Bade, O. M.; Knudsen, J. N.; Gorset, O.; Askestad, I. *Controlling amine mist formation in CO<sub>2</sub> capture from Residual Catalytic Cracker (RCC) flue gas*. *Energy Procedia*. 2014, 63, 884-892.
- [165] Tweedie, R. J. *Process analytical instrumentation, the challenges for in-situ characterization of complex particulate materials*. *Procedia Engineering*. 2015, 102, 1714-1725.
- [166] Volodin, V. A.; Kachko, A. S. *Crystallization of hydrogenated amorphous silicon films by exposure to femtosecond pulsed laser radiation*. *Semiconductors*. 2011, 45, 265-270.
- [167] Fevotte, G. *In situ Raman spectroscopy for in-lie control of pharmaceutical crystallization and solids elaboration processes: a review*. *Chemical Engineering Research and Design*. 2007, 85, 906-920.
- [168] Souchon, V.; de Oliveira Aleixo, M.; Delpoux, O.; Sagnard, C.; Mougin, P.; Wender, A.; Raynal, L. *In situ determination of species distribution in alkanolamine-H<sub>2</sub>O-CO<sub>2</sub> systems by Raman spectroscopy*. *Energy Procedia*. 2011, 4, 554-561.
- [169] Welsh, H. L.; Stansbury, E. J.; Romanko, J.; Feldman, T. *Raman spectroscopy of gases*. *Journal of the optical society of America*. 1955, 45, 338-343.
- [170] Taquet, N.; Pironon, J.; De Donato, P.; Lucas, H.; Barres, O. *Efficiency of combined FTIR and Raman spectrometry for online quantification of soil gases: application to the monitoring of carbon dioxide storage sites*. *International Journal of Greenhouse Gas Control*. 2013, 12, 359-371.
- [171] Kneipp, K.; Kneipp, H. *Single molecule Raman scattering*. *Applied Spectroscopy*. 2006, 60, 322A-334A.
- [172] Denicourt, Th.; Hédoux, A.; Guinet, Y.; Descamps, M. *Evidence for a transient metastable state during the isothermal transformation of the quenched plastic phase of cyanoadamantane from Raman scattering investigations*. *Journal of Molecular Structure*. 2003, 651-653, 499-505.
- [173] Brody, R. H.; Edwards, H. G. M.; Pollard, A. M. *Chemometric methods applied to the differentiation of Fourier-transform Raman spectra of ivories*. *Analytica Chimica Acta*. 2001, 427, 223-232.

- [174] Kadam, S. S.; Mesbah, A.; van der Windt, E.; Kramer, H. J. M. *Rapid online calibration for ATR-FTIR spectroscopy during batch crystallization of ammonium sulphate in a semi-industrial scale crystallizer*. Chemical Engineering Research and Design. 2011, 89, 995-1005.
- [175] Hollas, J. M. *Modern spectroscopy, 4th edition*. John Wiley & Sons, Ltd., Chichester. 2004, ISBN 0-470-84416-7.
- [176] Gersen, S.; van Essen, M.; Visser, P.; Ahmad, M.; Mokhov, A.; Sepman, S.; Alberts, R.; Douma, A.; Levinsky, H. *Detection of H<sub>2</sub>S, SO<sub>2</sub> and NO<sub>2</sub> in CO<sub>2</sub> at pressures ranging from 1-40 bar by using broadband absorption spectroscopy in the UV/VIS*. Energy Procedia. 2004, 63, 2570-2582.
- [177] Caillet, A.; Puel, F.; Fevotte, G. *In-line monitoring of partial and overall solid concentration during solvent-mediated phase transition using Raman spectroscopy*. International Journal of Pharmaceutics. 2006, 307, 201-208.
- [178] Chen, Y.; Jin, Z.; Pan, Z. *In-situ Raman spectroscopic study of hydrolysis of carbon tetrachloride in hot compressed water in a fused silica capillary reactor*. Journal of Supercritical Fluids. 2012, 72, 22-27.
- [179] Kim, Y. J.; You, J. K.; Hong, W. H.; Yi, K. B.; Ko, C. H.; Kim, J. N. *Characteristics of CO<sub>2</sub> absorption into aqueous ammonia*. Separation Science and Technology. 2008, 43, 766-777.
- [180] Zhao, Q.; Wang, S.; Qin, F.; Chen, C. *Composition analysis of CO<sub>2</sub>-NH<sub>3</sub>-H<sub>2</sub>O system based on Raman spectra*. Industrial and Engineering Chemistry Research. 2011, 50, 5316-5325.
- [181] Samarakoon P. A. G. L.; Andersen, N. H.; Perinua, C.; Jens, K. J. *Equilibria of MEA, DEA and AMP with bicarbonate and carbamate: a Raman study*. Energy Procedia. 2013, 37, 2002-2010.
- [182] Wen, N.; Brooker, M. H. *Ammonia carbonate, ammonia bicarbonate, and ammonium carbamate equilibria: a Raman study*. The Journal of Physical Chemistry. 1995, 99, 359-368.
- [183] Omura, Y.; Shimanouchi, T. *Raman spectra and rotational isomerism of ethylenediammonium and monoethanolammonium ions in aqueous solution*. Journal of molecular spectroscopy. 1975, 55, 430-434.
- [184] Korolevich, M. V.; Sivchik, V. V.; Matveeva, N. A.; Zhibankov, R. G.; Lastochkina, V. A.; Frenkel, M. L.; Ladutko, A. I.; Pavlov, A. V.; Petryaev, E. P. *A study of the vibrational spectrum of monoethanolamine*. Translated from Zhurnal Prikladnoi Spektroskopii. 1987, 46, 620-624.

- [185] Diab, F.; Provost, E.; Laloué, N.; Alix, P.; Souchon, V.; Delpoux, O.; Fürst, W. *Quantitative analysis of the liquid phase by FT-IR spectroscopy in the system CO<sub>2</sub>/diethanolamine (DEA)/H<sub>2</sub>O*. *Fluid Phase Equilibria*. 2012, 325, 90-99.
- [186] Jackson, P.; Robinson, K.; Puxty, G.; Attalla. *In-situ Fourier Transform-Infrared (FT-IR) analysis of carbon dioxide absorption and desorption in amine solutions*. *Energy Procedia*. 2009, 1, 985-994.
- [187] Armenta, S.; Garrigues, S.; de la Guardia, M. *Recent developments in flow-analysis vibrational spectroscopy*. *Trends in Analytical Chemistry*. 2007, 26, 775-787.
- [188] Coates, P. D.; Barnes, S. E.; Sibley, M. G.; Brown, E. C.; Edwards, H. G. M.; Scowen, I. J. *In-process vibrational spectroscopy and ultrasound measurements in polymer melt extrusion*. *Polymer*. 2003, 44, 5937-5949.
- [189] Lee, K. M.; Davis, J.; Herrman, T. J.; Murray, S. C.; Deng, Y. *An empirical evaluation of three vibrational spectroscopic methods for detection of aflatoxins in maize*. *Food Chemistry*. 2015, 173, 629-639.
- [190] Netchacovitch, L.; Thiry, J.; De Bleye, C.; Chavez, P. F.; Krier, F.; Sacré, P. Y.; Evrard, B.; Hubert, Ph.; Ziemons, E. *Vibrational spectroscopy and microspectroscopy analyzing qualitatively and quantitatively pharmaceutical hot melt extrudates*. *Journal of Pharmaceutical and Biomedical Analysis*. (2015), in press doi: 10.1016/j.jpba.2015.01.051.
- [191] Sivakesava, S.; Irudayaraj, J.; Ali, D. *Simultaneous determination of multiple components in lactic acid fermentation using FT-MIR, NIR, and FT-Raman spectroscopic techniques*. *Process Biochemistry*. 2001, 37, 371-378.
- [192] Wójciak, A.; Kasprzyk, H.; Sikorska, E.; Krawczyk, A.; Sikorski, M.; Weselucha-Birczyńska, A. *FT-Raman, FT-infrared and NIR spectroscopic characterization of oxygen-delignified kraft pulp treated with hydrogen peroxide under acidic and alkaline conditions*. *Vibrational Spectroscopy*. 2014, 71, 62-69.
- [193] Smith, B. C. *Fundamentals of Fourier transform infra-red spectroscopy*. Taylor and Francis Group, LLC: Boca Raton. 2011, ISBN: 978-1-4200-6929-7.
- [194] Cooper, J. B. *Chemometric analysis of Raman spectroscopic data for process control applications*. *Chemometrics and Intelligent Laboratory Systems*. 1999, 46 231-247.
- [195] Sacré, P. Y.; De Bleye, C.; Chavez, P. F.; Netchacovitch, L.; Hubert, Ph.; Ziemons, E. *Data processing of vibrational chemical imaging for pharmaceutical applications*. *Journal of Pharmaceutical and Biomedical Analysis*. 2014, 101, 123-140.
- [196] Obermaier, K.; Schmelzeisen-Redeker, G.; Schoemaker, M.; Klötzer, H. M., Kirchssteiger, K.; Eikmeier, H.; del Re, L. *Performance evaluations of continuous glucose*

- monitoring systems: precision absolute relative deviation is part of the assessment.* Journal of Diabetes Science and Technology. 2013, 7, 824-832.
- [197] Carey, D. M.; Korenowski, G. M. *Measurement of the Raman spectrum of liquid water.* The Journal of Chemical Physics. 1998, 108, 2669-2675.
- [198] Richner, G.; Puxty, G. *Assessing the chemical speciation during CO<sub>2</sub> absorption by aqueous amines Using in-situ FTIR.* Industrial and Engineering Chemistry Research. 2012, 51, 14317-14324.
- [199] Nakanishi, K. *Infrared absorption spectroscopy, practical.* Holden-Day, Inc., San Francisco, and Nankondo Company, Tokyo, 1962.
- [200] Böttinger, W.; Maiwald, M.; Hasse, H. *Online NMR spectroscopic study of species distribution in MEA-H<sub>2</sub>O-CO<sub>2</sub> and DEA-H<sub>2</sub>O-CO<sub>2</sub>.* Fluid Phase Equilibria. 2008, 263, 131-143.
- [201] Zhang, X.; Young, M. A.; Lyandres, O.; Van Duyne, R. P. *Rapid Detection of an Anthrax Biomarker by Surface-Enhanced Raman Spectroscopy.* Journal of the American Chemical Society. 2005, 127, 4484-4489.
- [202] Rodriguez-Saona, L. E.; Allendorf, M. E. *Use of FTIR for rapid authentication and detection of adulteration of food.* Annual Review of Food Science and Technology. 2011, 2, 467-483.
- [203] Sorak, D.; Herberholz, L.; Iwascek, S.; Altinpinar, S.; Pfeifer, F.; Siesler, H. W. *New developments and applications of handheld Raman, mid-infrared, and near-infrared spectrometers.* Applied Spectroscopy Reviews. 2012, 47, 83-115.
- [204] Bougie, F.; Iliuta, M. C. *Stability of aqueous amine solutions to thermal and oxidative degradation in the absence and the presence of CO<sub>2</sub>.* International Journal of Greenhouse Gas Control. 2014, 29, 16-21.
- [205] Svensson, O.; Josefson, M.; Langkilde, F. W. *The synthesis of metoprolol monitored using Raman spectroscopy and chemometrics.* European Journal of Pharmaceutical Sciences. 2000, 11, 141-155.
- [206] Tumuluri, V. S.; Kemper, M. S.; Lewis, I. R.; Prodduturi, S.; Majumdar, S.; Avery, B. A.; Repka, M. A. *Off-line and on-line measurements of drug-loaded hot-melt extruded films using Raman spectroscopy.* International Journal of Pharmaceutics. 2008, 357, 77-84.
- [207] Skrdla, P. J.; Zhang, D. *Disproportionation of a crystalline citrate salt of a developmental pharmaceutical compound: Characterization of the kinetics using pH monitoring and online Raman spectroscopy plus quantitation of the crystalline free base form in binary physical mixtures using FT-Raman, XRPD and DSC.* Journal of Pharmaceutical and Biomedical Analysis. 2014, 90, 186-191.

- 
- [208] Hausman, D. S.; Cambron, R. T.; Sakr, A. *Application of Raman spectroscopy for on-line monitoring of low dose blend uniformity*. International Journal of Pharmaceutics. 2005, 298, 80-90.
- [209] Hopfe, V.; Sheel, D. W.; Graehlert, W.; Throl, O. *NIR laser diode and FTIR based process control for industrial CVD reactors*. Surface and Coatings Technology. 2001, 142-144, 328-332.
- [210] Ghita, O. R.; Baker, D. C.; Evans, K. E. *An in-line near-infrared process control tool for monitoring the effects of speed, temperature, and polymer colour in injection moulding*. Polymer Testing. 2008, 27, 459-469.
- [211] Knop, K.; Kleinebudde, P. *PAT-tools for process control in pharmaceutical film coating applications*. International Journal of Pharmaceutics. 2013, 457, 527-536.
- [212] Buss, S. R. *3-D computer graphics: a mathematical introduction with OpenGL*. Cambridge University Press: New York. 2003, ISBN: 978-0-5218-2103-2.
- [213] Farin, G.; Hansford, D. *Practical linear algebra: a geometry toolbox*. A K Peters, Ltd.: Wellesley. 2005, ISBN: 156-881-2345.



# Summary

Improving the efficiency of an industrial process requires precise monitoring tools, tailored to the specific application. One of the promising practices is to employ real-time multivariate analysis methods for continuous control of industrial processes. The benefits of the time-resolved information extraction include the potential to quantify the composition of a process stream at any given time, and to describe the reaction progress. Fast acquisition of valuable information about the process on site can be used for automated monitoring, saving cost of operation, and reducing waste products. Therefore, in-line process analytical instrumentation is being adopted extensively and it can be considered as an important part of effective and efficient industrial manufacturing. A combination of measurement sensors and multivariate statistics is widely applied to improve in-line process monitoring. Currently, post combustion CO<sub>2</sub> capture (PCC) technology often involves the use of multi-amine based chemical solvents for carbon dioxide removal from flue gas. The CO<sub>2</sub> capture efficiency and overall process performance may be improved by introduction of the chemometrics analytical methods for flexible and reliable process monitoring. This thesis is focused on the development, improvement, and demonstration of multivariate data analysis for in-line process monitoring of PCC. The developed methods may be applied not only to the PCC process, but are also suitable to other similar industrial applications.

In chapter 2, the method of simultaneous acquisition and handling of information from six measurement devices (conductivity, pH, density, speed of sound, refractive index, and near infra-red NIR spectroscopy) is introduced. A compact data-collecting chemometric setup was constructed and installed at an industrial pilot plant for in-line testing. This setup was

applied to the characterisation of CO<sub>2</sub> absorption into aqueous 2-amino-2-methyl-1-propanol (AMP) activated by piperazine (PZ) as the absorption agent. A partial least squares (PLS) regression model was calibrated and validated based on the measurements conducted in a laboratory environment. The developed approach was applied to predict the concentrations of AMP, PZ, and CO<sub>2</sub> with accuracies of  $\pm 2.1\%$ ,  $\pm 3.5\%$ , and  $\pm 4.3\%$ , respectively. The temperature dependence was included in the model in order to make it insensitive to operational temperature fluctuations during a CO<sub>2</sub> capture process. The setup and model have been tested for almost 850 hours of in-line measurements at a post-combustion CO<sub>2</sub> capture pilot plant. To validate of the chemometrics approach, an off-line analysis of the samples has been conducted. The results of the validation techniques are consistent with the values predicted in-line, with average deviations of  $\pm 1.8\%$ ,  $\pm 1.3\%$ , and  $\pm 3.9\%$  for the concentrations of AMP, PZ, and CO<sub>2</sub>, respectively.

In chapter 3, the results of the *in-situ* monitoring of CO<sub>2</sub> removal at high pressure are provided. An aqueous solution of methyldiethanolamine (MDEA) promoted by PZ for absorption rate acceleration was used. The use of this solvent is promising for natural gas purification. The CO<sub>2</sub> capture rate ranged from 60% up to 96% at a pressure in the absorber column between 15 and 20 bar. The liquid stream composition was monitored at low pressure, downstream of the stripper column, after the lean-rich heat exchanger and a cooler. The temperature of the analysed solvent varied between 21 °C and 25 °C. The concentration of both amines and CO<sub>2</sub> were predicted in-line via the chemometric approach. The prediction model was calibrated with an accuracy of  $\pm 0.7\%$ ,  $\pm 0.4\%$ ,  $\pm 2.5\%$ , for MDEA, PZ, and CO<sub>2</sub>, respectively. Several physical properties and near infra-red absorbance were measured for *in-situ* characterization of the solvent flow. A detailed description of in-line monitoring setup is presented in this work. This setup may be used for natural gas treatment process control.

In chapter 4, a comparative qualification of three vibrational spectroscopy techniques is described, namely Raman, NIR, and attenuated total reflectance Fourier transform infra-red (ATR FTIR), in application to monitoring of CO<sub>2</sub> absorption by a chemical solvent. The spectroscopic information has been used for prediction of the concentration of the CO<sub>2</sub> captured by aqueous monoethanolamine (MEA) solutions. The study is



aimed to determine the potential applicability of the spectroscopic methods to the in-line and real-time monitoring of a post-combustion carbon capture process. PLS regression models were built based on the spectroscopic data before and after spectra pretreatment procedures. The predictive model constructed using NIR data provides the highest predictive accuracy with an average deviation of about 0.2 wt. % in comparison with the models based on Raman and ATR FTIR measurements, which show deviations of around 0.4 wt. %.

When the measurement probes are distributed along a pipe, depending on the distance between them, the speed of a fluid in that pipe, and the process dynamics, the readings of a probe at the inlet might be different from the readings at the outlet at the same moment in time. Consequently, the column of dependent parameters becomes to be comprised of the measurements obtained essentially from solvent of different compositions. To tackle this problem, a lag-time interval could be introduced to data acquisition procedure. The time interval should be based on the liquid flow rate through the measurement line. Another approach is the miniaturization of the measurement equipment.



# Samenvatting

Om de efficiëntie van een industrieel proces te verbeteren zijn precieze observatiehulpmiddelen vereist, die op maat gemaakt zijn voor een specifieke toepassing. Eén van de veelbelovende methoden is het gebruik van multivariabele analyse voor de onmiddellijke en continue regeling van industriële processen. Voordelen van deze tijdsafhankelijke methode zijn bijvoorbeeld de mogelijkheid om de samenstelling van een processtroom op elk moment te kwantificeren, en om de voortgang van reacties te beschrijven. Het snel binnenhalen van waardevolle informatie over een proces kan gebruikt worden voor geautomatiseerde procesregeling, wat operationele kosten kan besparen en afvalstromen kan verminderen. Analytische instrumenten die direct in een procesleiding (in-line) kunnen meten, kunnen beschouwd worden als een belangrijk onderdeel van effectieve en efficiënte industriële productie. Een combinatie van meetsensoren en multivariabele statistiek wordt veel toegepast om in-line procesregeling te verbeteren. Voor post-combustion CO<sub>2</sub> afvang (PCC) worden vaak mengsels van meerdere amines gebruikt als chemisch oplosmiddel om CO<sub>2</sub> van verbrandingsgas te verwijderen. De CO<sub>2</sub>-afvang efficiëntie en de algehele procesprestatie kunnen verbeterd worden door het invoeren van chemometrische methoden voor flexibele en betrouwbare procesregeling. Dit proefschrift is gericht op het ontwikkelen, verbeteren en demonstreren van multivariabele data-analyse ten behoeve van het in-line regelen van PCC processen. De methoden die ontwikkeld worden kunnen niet alleen gebruikt worden voor PCC processen, maar zijn ook geschikt voor andere vergelijkbare industriële toepassingen.

In hoofdstuk 2 wordt een methode geïntroduceerd waarmee de informatie van zes meetapparaten (elektrische geleidbaarheid, pH, dichtheid, geluidssnelheid, brekingsindex, en NIR (nabij infrarood spectroscopie) tege-

lijktijd wordt uitgelezen en verwerkt. Er is een compacte chemometrische opstelling voor data-collectie in elkaar gezet en geïnstalleerd in een industriële proeffabriek om er in-line tests mee te doen. Deze opstelling is gebuikt voor het karakteriseren van de absorptie van  $\text{CO}_2$  in een waterige oplossing van 2-amino-2-methyl-1-propanol (AMP) geactiveerd door piperazine (PZ). Een gedeelde kleinste kwadraten (PLS) regressie model is gekalibreerd en gevalideerd op basis van laboratorium experimenten. De ontwikkelde aanpak is gebuikt om de concentraties van AMP, PZ, en  $\text{CO}_2$  te voorspellen met onnauwkeurigheden van  $\pm 2.1\%$ ,  $\pm 3.5\%$ , en  $\pm 4.3\%$  respectievelijk. De temperatuurafhankelijk was onderdeel van het model om het zo ongevoelig te maken voor de operationele temperatuursveranderingen in het  $\text{CO}_2$ -afvang proces. De opstelling en het model zijn bijna 850 uur lang getest bij een PCC proeffabriek. Om de chemometrie-aanpak te valideren zijn er ook monsters in het laboratorium geanalyseerd. De resultaten van de validatie-analyses zijn consistent met de in-line voorspelde waarden, met een gemiddelde afwijken van  $\pm 1.8\%$ ,  $\pm 1.3\%$ , en  $\pm 3.9\%$  voor de concentraties van AMP, PZ, en  $\text{CO}_2$  respectievelijk.

In hoofdstuk 3 worden de resultaten gepresenteerd van het in-line karakteriseren van  $\text{CO}_2$ -verwijdering op hoge druk. Een waterige oplossing van methyldiethanolamine (MDEA) wordt gebruikt, geactiveerd door PZ ter verhoging van de absorptiesnelheid. Dit oplosmiddel is veelbelovend voor het zuiveren van aardgas. Ongeveer 60% tot 96% van de  $\text{CO}_2$  werd afgevangen met een druk in de absorptiekolom van 15 tot 20 bar. De samenstelling van de vloeistofstroom werd gemeten op lage druk, op een locatie na de desorptiekolom de hoofdwarmtewisselaar en de koeler. De temperatuur van het oplosmiddel varieerde tussen de 21 °C en 25 °C. De concentraties van beide amines en van  $\text{CO}_2$  werd in-line voorspeld met behulp van de chemometrische aanpak. Het voorspellingsmodel was gekalibreerd met onnauwkeurigheden van  $\pm 0.7\%$ ,  $\pm 0.4\%$ , en  $\pm 2.5\%$  voor MDEA, PZ, en  $\text{CO}_2$  respectievelijk. Meerdere fysische grootheden en de NIR-absorptie werden gemeten ten behoeve van het in-line karakteriseren van de vloeistofstroom. Een gedetailleerde beschrijving van de in-line meetopstelling is gepresenteerd. De opstelling kan gebruikt worden voor het regelen van aardgasbehandelingsprocessen.

In hoofdstuk 4 wordt een vergelijking beschreven tussen drie vibratiespectroscopietechnieken, namelijk Raman, NIR en ATR-FTIR (attenuatie

---

van de totale reflectie van Fourier-transform-infrarood). Deze technieken worden toegepast om de CO<sub>2</sub>-absorptie door een chemisch oplosmiddel te meten. De spectroscopische informatie is gebruikt om de concentratie van CO<sub>2</sub> te voorspellen die opgelost is in waterige oplossingen van monoethanolamine (MEA). Het doel van de studie is om de toepasbaarheid vast te stellen van deze spectroscopische technieken voor de in-line en onmiddellijke procesbewaking van PCC processen. PLS-regressie modellen zijn gemaakt op basis van de spectroscopische data, zowel voor als na voorbehandelingsprocedures. Het voorspellingsmodel gebaseerd op de NIR data levert de hoogste nauwkeurigheid op, met een gemiddelde afwijking van 0.2 gewichtsprocent, in vergelijking met de modellen gebaseerd op Raman en ATR-FTIR metingen, die afwijkingen van ongeveer 0.4 gewichtsprocent hebben.

Wanneer meetsensoren zijn verdeeld over de lengte van een buis, dan kan, afhankelijk van de afstand tussen de sensoren, de snelheid van het medium in de buis, en de proces dynamica, de waarde van een sensor aan het begin van de buis anders zijn dan de waarde aan het einde van de buis op datzelfde moment. Als gevolg hiervan bevat de kolom van afhankelijke parameters meetwaarden die verkregen zijn voor oplossingen met een verschillende samenstelling. Om dit probleem aan te pakken, moet er een tijdsvertraging toegevoegd worden aan de dataverwerkingsprocedure. De tijdsvertraging moet gebaseerd worden op de stroomsnelheid van de vloeistof in de buis. Een andere aanpak is het miniaturiseren van de meetapparatuur.



# Curriculum Vitae

Alexandr Kachko was born in a little town Chkalovsk of Tajik SSR on the 2nd of June 1986. In 2003 he has been admitted to the Physics department of the Novosibirsk State University and graduated in 2007 with the BSc degree in Physics and diploma titled “Study of the initial stages of monoatomic steps echelon formation on the surface of Si(111) during the crystal annealing using the direct electric current”. Two years later he had defended his MSc degree at the NSU with the main specialization in Physics of Semiconductors and Microelectronics with the theme of diploma thesis “Phase transitions in the a-Si:H films under nano- and femtosecond laser irradiation”. Following his masters education the author was working at the Institute of Semiconductor Physics SB RAS for a year where he was continuing research of the low-temperature polycrystalline silicon technology. In 2011, the Process and Energy department of Delft University of Technology has appointed the author as a PhD candidate. He started working on the topic of “In-line monitoring of solvents during CO<sub>2</sub> absorption using multivariate data analysis” combined of studies performed as part of the national and European projects such as CATO-2 and OCTAVIUS.





# Publications by the Author

1. KACHKO, A.; VAN DER HAM, L. V.; GEERS, L. F. G.; HUIZINGA, A.; RIEDER, A.; ABU-ZAHRA, M. R. M.; VLUGT, T. J. H.; GOETHEER, E. L. V. *Real-time process monitoring of CO<sub>2</sub> capture by aqueous AMP-PZ using chemometrics: pilot plant demonstration. Industrial & Engineering Chemistry Research*, 2015, 54, 5769-5776.
2. KACHKO, A.; VAN DER HAM, L. V.; BAKKER, D.; RUNSTRAAT, A.; NIENOORD, M.; VLUGT, T. J. H.; GOETHEER, E. L. V. *In-line monitoring of the CO<sub>2</sub>, MDEA, PZ concentrations in liquid phase during high pressure CO<sub>2</sub> capture. Industrial & Engineering Chemistry Research*, 2016, 55, 3804-3812.
3. KACHKO, A.; VAN DER HAM, L. V.; BARDOW, A.; GOETHEER, E. L. V.; VLUGT, T. J. H. *Comparison of Raman, NIR, and ATR FTIR spectroscopy as analytical tools for in-line monitoring of CO<sub>2</sub> concentration in an amine gas treating process. International Journal of Greenhouse Gas Control*, 2016, 47, 17-24.



# Acknowledgement

Inherently I was always trying to notice people who were supportive of me and I am extremely thankful for their influence and participation in my life. For a proper help, especially when it is most needed, is a gift a person can get with the value among the top prizes along the route to his or her achievement. These people become special; they assist in a mindset formation and encourage to move forward, thus reaffirming that I have chosen the right direction. When being promoted like that I am getting recharged and receive a boost of motivation. This thesis writing process was not an exception. It would be impossible to bring this work to a conclusion without a help from such people. I would like to express my great appreciation to these people.

First of all, I would like to express my deep gratitude to Thijs Vlugt for being a promotor for my PhD. I am thankful for his way of positive motivation; for his habitual feature of letting me know not only the parts of my work that could be improved, but also for pointing out where I managed to succeed, which gives a huge incentive. It is as if he is capable to connect to a computer remotely avoiding the mediators to access the displayed information; he was proofreading my research scripts with an amazing speed while keeping focus on all important details. As result, the suggestions received from Thijs have always lead to improved versions of a document. During the PhD time heaps of documents have to be filled out, signed, scanned and sent here or there. Thanks to the *modus operandi* of Thijs of how to deal with the bureaucracy mechanism I have learned not to lose my bearings in view of another incoming paperwork tide-wave; these matters might be exigent, or it may be better not to rush things, sometimes it even helps not to take notice.

I would like to offer my special thanks to my promotor André Bardow who has given me an opportunity to enter the doctoral school and has been providing me with his guidance at the very beginning of my PhD track. Conduction of scientific research is an exciting career due to foremost the infinite number of interesting problems to solve; the more time a researcher is spending in a laboratory, brain storming with colleagues, or conducting literature research, the longer becomes the list of potentially fruitful ideas each of which may become a topic for a separate project. André has helped me not to become overwhelmed by the amount of work this steadily growing pool of ideas represent and stick to the subject of research. I am thankful for the opportunity to conduct my research within the walls of the Chair of Technical Thermodynamics of RWTH-Aachen University. The time I spent in Aachen will always stay on my mind and this city has become one of my favorite in Europe.

I would like to thank Earl Goetheer, principal scientist at TNO. He has given me an opportunity to finish my PhD project using the hospitable environment of the PID department and the well equipped laboratories of TNO. He has got an inexhaustible energy source that seems to be powered by candies. He is always looking for research valuable ideas with application of fundamental approach to a problem solving. Always on the go, he is a walking and talking representation of an idea that if you stop moving you are lacking behind. His idea that the work has to be enjoyable and contain a certain amount of fun is inspiring. I absolutely share his opinion that a borrel-room at 6 p.m. on Friday night serves nicely for discussion of the latest progress on project. One can even leave it to go on right away with the new experiments in a laboratory, only if you are authorized to and there is enough EHS-trained personnel in the building. And if not, then the PC on your office desk was not put there just for the interior design.

During the last year and a half of my PhD work Leen van der Ham, a research scientist at TNO, was a person of expertise with whom I have regularly been discussing every little aspect of the ongoing work. I am genuinely thankful for his attention to details when we were polishing my manuscripts. Due to his natural talent in counseling and almost Nordic patience I have been able to develop further my paper writing strategy and provide improved manuscripts, which are among the main outputs of

a scientific research.

I am thankful to Marcus Oetker and Christoph Pauls for assisting me with adjustment, alignment, and fine tuning of the home-made Raman spectroscopy setups in the beginning of my PhD project. My special thanks goes to all LTT technical-administrative staff, in particular to Iris, Willibert, Ton, Thomas, Djuro, Gregor, Waltraud, and Bernhard.

For his indispensable help on the laboratory floor of TNO as well as during installation/utilization of the chemometrics setup at a power plant in Germany I am grateful to Arjen Huizinga. Everything in a laboratory starts to clip-on, run-through, connect and hold, count and measure, blow and flow, boil or freeze once he is around.

My sincere thanks to all my former colleagues from TNO for creating an atmosphere of professional willingness to help, for sharing whatever a fresh idea comes around, and for being interested in my progress.

I would like to acknowledge my family for the support and for maintaining a perpetual faith in a positive outcome. I am also grateful to my best friend Suhrob from Khujand and the whole his family for cheering me up and for their truly sincere hospitality.

**Alexandr Kachko**  
**May 2016.**

The first part of the document discusses the importance of maintaining accurate records of all transactions and activities. It emphasizes that proper record-keeping is essential for ensuring transparency and accountability in financial management. This section also outlines the various methods and tools used to collect and analyze data, highlighting the need for consistency and precision in data collection.

The second part of the document focuses on the analysis of the collected data. It describes the various statistical techniques and models used to interpret the data, including regression analysis, time series analysis, and hypothesis testing. This section also discusses the challenges associated with data analysis, such as missing data and outliers, and provides strategies to address these issues.

The third part of the document discusses the application of the analyzed data to various fields and industries. It highlights the practical implications of the findings and provides examples of how the data can be used to inform decision-making and improve operational efficiency. This section also discusses the limitations of the current study and suggests areas for future research.

The final part of the document provides a conclusion and summarizes the key findings of the study. It reiterates the importance of accurate record-keeping and data analysis in financial management and emphasizes the need for continued research and innovation in this field.